PEOPLE'S DEMOCRATIC REPUBLIC OF ALGERIA

MINISTRY OF HIGHER EDUCATION AND SCIENTIFIC RESEARCH

Larbi Ben M'Hidi University of Oum El-Bouaghi

Faculty of Science and Applied Sciences

Electrical Engineering & Automatic Laboratory (LGEA)

Thesis

Submitted in Partial Fulfillment of the Requirements of the Doctorate Degree in Electrical Engineering & Automatics

CONTRIBUTION TO FRACTIONAL ORDER ADAPTIVE ROBUST CONTROL

By: KEZIZ Bouziane

Jury:

Pr. Barra Kamel	**University of Oum El Bouaghi**	**President**
Pr. Djouambi Abdelbaki	**University of Oum El Bouaghi**	**Supervisor**
Pr. Ladaci Samir	**Polytechnic School of Constantine**	**Co-Supervisor**
Pr. Charef Abdelfatah	**University of Constantine 1**	**Examiner**
Pr. Lashab Mohammed	**University of Oum El Bouaghi**	**Examiner**

(December 23, 2020)

PREFACE

This thesis is the result of my doctoral studies at the Department of Electrical Engineering, at the Larbi Ben M'Hidi University of Oum El Bouaghi (U-OEB), Faculty of Sciences and Applied Sciences. The work presented is undertaken from September 2016 to June 2020 for partial fulfillment of the degree of Doctorat LMD under the supervision of Professor DJOUAMBI Abdelbaki (U-OEB) and co-supervisor Professor LADACI Samir from National Polytechnic School of Constantine (NPSC). Supporting material of my studies has been provided by the LGEA Laboratory of Electrical Engineering and Automatics.

DECLARATION

I declare that this thesis was composed by myself, that the work contained herein is my own except where explicitly stated otherwise in the text, and that this work has not been submitted for any other degree or professional qualification except as specified.

Dedicated to my family

ACKNOWLEDGMENT

I sincerely thank my advisor, Prof. Djouambi Abdelbaki, for his high-quality guidance and support during my Ph.D study. He is a wise, patient supervisor and a knowledgeable person with a very rigorous attitude on research. Throughout my Ph.D study, he not only introduces the topic of the thesis to me and gives me valuable suggestions, but also provides me with many opportunities to participate in various projects and collaborate with different groups. Moreover, he is also broadening my vision in research and stimulating learning environment, thanks to him for everything else he has provided for me.

I would also like to express my thanks to my co-advisor, Prof. Samir Ladaci for his help, exchange of information and the fruitful discussions. His ideas, feedback, and encouragement are essential for this thesis to be in the form that it is. I would say that I was extremely lucky to meet him at National Polytechnic School of Constantine.

Thanks to my academic committee members, Prof. Charef Abdelfatah, Prof. Barra Kamel and Prof. Lashab Mohammed.

Thanks to my undergraduate advisor and teachers in Guelma University, for their early guidance.

I would also like to thank a number of colleagues and teachers who supported me during this work in Oum El-Boaghi University.

ABSTRACT

This work presents new ideas to improve robust control, as well as adaptive control schemes by introducing fractional order operators. Many adaptive concepts are studied, and new control algorithms are proposed using fractional order differentiator and integrator. Fundamentals definitions of the most important notions of fractional calculus are presented. Different approaches of adaptive control are also explored.

The main contribution of this work was devoted to the Model Reference Adaptive Control MRAC, with the MIT control law and lies in the following two aspects,

(1) The fractional order robust control, giving a new simple and useful tuning technique of fractional robust controllers. This technique can simply achieves user-specified gain and phase margins using the Bode's ideal transfer function as a reference model.

(2) The fractional order adaptive control, providing a novel design scheme to tune fractional order adaptive PI controller for a class of First Order Plus Time Delay (FOPTD) plants where the fractional adaptive control is improved in the two following points,

   a. The initial parameters of the adaptive algorithm can be fixed in offline first, then an online tuning is performed to achieve the robustness of the controlled plant,

   b. The second point is the new Fractional Order Model Reference tuning form which is introduced using the plant model.

Through some illustrative examples, simulation results show the effectiveness of the proposed schemes.

In the practical part of this work, we have used the fractional order calculus to develop a platform containing the necessary tools to deal with Real Time Data Acquisition and Control on both dSPACE-DS1104 Controller and a low-cost platform on Arduino microcontroller.

Key Words: Fractional Order Robust Control, Fractional Order Model Reference Adaptive Control, dSPACE-DS1104, Arduino.

RÉSUMÉ

Ce travail présente des idées nouvelles pour améliorer la commande robuste, ainsi que les schémas de la commande adaptative en introduisant des opérateurs d'ordre fractionnaire. Plusieurs concepts adaptatifs sont étudiés et de nouveaux schémas de commande sont proposés comportant des opérateurs d'ordre fractionnaire (dérivateur et intégrateur). Les définitions fondamentales des notions les plus importantes du calcul fractionnaire sont présentées. Différentes approches de commande adaptative sont également explorées.

La contribution de ce travail comporte la proposition de plusieurs schémas de commande adaptative d'ordre fractionnaire qui résident particulièrement dans les aspects suivants :

(1) -Une nouvelle technique de synthèse d'un régulateur robuste d'ordre fractionnaire basé sur l'utilisation de la boucle idéale de Bode comme modèle de référence. Le caractère le plus innovant de cette méthode réside dans sa simplicité et ses performances remarquables en termes de robustesse vis-à-vis la variation du gain statique du procédé.

(2) -Un nouveau schéma de conception et synthèse des contrôleurs PI adaptatif d'ordre fractionnaire basée sur la fonction idéale de Bode où les paramètres du contrôleur sont estimés en ligne pour une classe de systèmes de premier ordre.

À travers quelques exemples illustratifs, les résultats de simulation montrent l'efficacité des schémas proposés.

Finalement, deux plateformes numérique différentes à base de microcontrôleurs (dSPACE ds104 et low-cost microcontrôleur) sont réalisées pour l'implémentation temps réel et la validation expérimentale de quelques techniques de synthèses et contrôleurs proposés dans ce travail.

Mots clés: Commande robuste d'ordre fractionnaire, commande adaptative d'ordre fractionnaire, dSPACE-DS1104, Arduino.

مُلخـــــص:

يقدم هذا العمل أفكارًا جديدة لتحسين التحكم المتين، وكذالك مخططات التحكم المتكيف من خلال إدخال عوامل الحساب الكسري. تم دراسة العديد من المفاهيم الخاصة بالتحكم المتكيف، وتم اقتراح خوارزميات تحكم جديدة باستخدام عناصر الحساب الكسري (تفاضل ، تكامل) بالإضافة إلى دوال التحويل الكسري. تم عرض المفاهيم الأساسية مع التعاريف الاكثر أهمة ومفاهيم حساب التفاضل والتكامل الكسري. كما تم عرض مُختلف مُقاربات التحكم المتكيف.

المساهمة الرئيسية لهذا العمل تم تخصيصها للتحكم المتكيف المرجعي ذو النموذج MRAC، مع قانون التحكم MIT وهذه المساهمة تكمن في الجانبين التاليين،

(1) التحكم المتين ذو الترتيب الكسري، قدمنا في هذا الجانب تقنية ضبط جديدة بسيطة ومفيدة في التحكم المتين الكسري (FOC). يمكن لهذه التقنية ببساطة تحقيق هوامش القوة وهوامش الطور المحددة من قبل المستخدم باستعمال ما يسمى بـ "دالة التحويل المثالية لبود" (Bode) أو مُكامل ذو الترتيب الكسري كنموذج مرجعي.

(2) التحكم المتكيف ذو الترتيب الكسري، في هذا الجانب قدمنا مخطط تصميم جديد لضبط لوحدة المتحكم المتكيف ذو الترتيب الكسري (مُتحكم تناسبي تكامليPI) مع تطبيقها على فئة أنظمة الترتيب الأولي ذو تأخر زمني (FOPTD) حيث تم تحسين التحكم المتكيف ذو الترتيب الكسري في النقطتين التاليتين،

أ. يمكن اعطاء قيم ابتدائية لمعاملات خوارزمية المتكيف في وضع الفصل أولاً ، ثم يتم إجراء ضبط على الوصل لتحقيق متانة النظام الخاضع للتحكم،

ب. النقطة الثانية هي نموذج الضبط ذو الترتيب الكسري الجديد لمتحكم المتكيف المرجعي ذو النموذج أين تم تقديمه باستخدام نموذج النظام.

من خلال بعض الأمثلة التوضيحية، نتائج المحاكاة تظهر فعالية المخططات المقترحة.

في الجزء العملي من هذه الأطروحة، استخدمنا المتحكم ذو الترتيب الكسري لتطوير منصة تحتوي على الأدوات اللازمة للتعامل مع ادخال البيانات في الوقت الحقيقي والتحكم فيها في كل من وحدة تحكم (dSPACE-DS1104) وأردوينو كمنصة منخفضة التكلفة (Arduino).

الكلمات الدالة:

حساب التفاضل والتكامل الكسري، التحكم المتين ذو الترتيب الكسري، متحكم المتكيف المرجعي ذو النموذج ذو الترتيب الكسري، وحدة تحكم dSPACE-DS1104 وحدة تحكم Arduino.

TABLE OF CONTENTS

LIST OF TABLES

LIST OF FIGURES

LIST OF ACRONYMS/ABBREVIATIONS

ASPR	**A**lmost **S**trictly **P**ositive **R**eal
CRONE	**C**ommande **R**obuste d'**O**rdre **N**on **E**ntier
DAQ	**D**ata **A**Quisition
FFC	**F**eed-**F**orward **C**onfiguration
FOO	**F**ractional **O**rder **O**perator
FO-MRAC	**F**ractional **O**rder **M**odel **R**eference **A**daptive **C**ontrol
FOPDT	**F**irst **O**rder **P**lus **T**ime **D**elay
FO-PID	**F**ractional-**O**rder **PID**
GL	**G**rünwald **L**etnikov
IMC	**I**nternal **M**odel **C**ontrol
LTI	**L**inear **T**ime **I**nvariant
MIT	**M**assachusetts **I**nstitute of **T**echnology
MRAC	**M**odel **R**eference **A**daptive **C**ontrol
PD	**P**roportional **D**erivative
PI	**P**roportional **I**ntegral
PID	**P**roportional **I**ntegral **D**erivative
PRBS	**P**seudo **R**andom **B**inary **S**ignal
PWM	**P**ulse **W**idth **M**odulator
SPR	**S**trictly **P**ositive **R**eal

INTRODUCTION

This part provides the motivation of the present research work with a brief review of fractional calculus and its applications. The research contributions and key results are presented. It also highlights the organization of the thesis.

1 Motivation

Differential equations are playing a crucial role in modeling, analysis and control of dynamic systems. However, in many engineering and scientific disciplines there are a variety of phenomena and dynamics that cannot be precisely described by these ordinary differential equations. Fractional differential equations are specified by generalizing the integer order of these equations to arbitrary real or even complex order. They extend the traditional definition of integration and differentiation to non-integer order and join them into one definition where operator depends on the order sign. The popularity of this subject has increased during the last decades in several fields of science and engineering.

Fractional differential equations arise in different branches of science and engineering due to the effective memory function of their fractional derivative term. The importance of fractional derivatives for modeling phenomena is also due to their nonlocality nature which is an intrinsic property of many complex systems. Unlike the integer order derivative, fractional derivatives do not take into account only local characteristics of the dynamics but considers the global evolution of the system; for that reason, when dealing with certain phenomena, they provide more accurate models of real-world behavior than standard derivatives.

The Fractional Order Calculus (FOC) is as old as the integer one although up to recently its application was exclusively in mathematical physics. Its applications in engineering have been delayed because of its computational complexity [16, 101] and the Integer Order Calculus seems, at first sight, to be enough to solve engineering problems. In the second half of the 20th century, parallel to the development of computers and algorithms, this calculus has spread out to engineering areas and it has become very powerful and useful tool to describe many physical phenomena such as in physics [60], chemistry [128] and electrochemistry [98], aerodynamics [8], mechanics [60], electrodynamics of complex medium [41], viscoelasticity [88], electrical networks [14], biophysics [151], blood flow phenomena [127], polymer rheology [125], probability and statistics [44], control theory of dynamical systems [47, 110, 40, 112, 149, 93, 81, 157], signal and image processing [59, 138, 5, 25], [85, 119, 132], etc.

Application of fractional order calculus in Control Theory has led to the generalization of this domain for non-integer order. Thus, it can improve and generalize well-established control methods and strategies. Another generalization in the control theory known as system modelling and control using fractional-order calculus was also released. Throughout the last decades it was shown that fractional order control ensures best quality and performance for the controlled system.

The idea of using fractional-order controllers for robust control of dynamical systems belongs to A. Oustaloup, who developed the so-called CRONE controller [102] (CRONE is an abbreviation of Commande, Robuste d'Ordre Non Entier). A. Oustaloup demonstrated the advantage of the CRONE controller in comparison with the classical one. The fractional PID ($PI^{\lambda}D^{\mu}$) Controller [115], described in Chapter 2, also shows better performance than the classical PID Controller. Fractional-order derivatives and integrals in adaptive control has recently attracted considerable interest of many researchers such as, S. Ladaci, and A. Charef. [66], S. Ladaci, and Y. Bensafia [61], and especially on MRAC (Model Reference Adaptive Control) [149].

The motivation for this thesis stems from particular importance of fractional operators including practical challenges in robust and adaptive control applications. Fractional order control offers more tuning freedom, important robustness criteria, stabilizing abilities, and

superior performance compared to the existing conventional control loops. Therefore, a further set of specific research goals may be proposed: to study fractional order adaptive control models and to provide new tuning methods; to develop new fractional order techniques; to provide means for stabilizing an unstable plant.

2 Thesis Overview

2.1 Author's Contribution

Fractional control techniques provide an effective way to control dynamic behaviours, using fractional order operators. Adaptive control is an advance scheme in the field of automatic control. Regarding control techniques, the aim of this thesis is to contribute to the field by extending the classical adaptive control to the fractional case called fractional adaptive control. More specifically, it aims to generalize either existing algorithms or developing new once. This may improve the stability and increases the robustness of the closed-loop system.

Taking into account the difficulties of this task, it is necessary to provide a fundamental description and analysis of the fractional order calculus along with its mathematical preliminaries. Throughout this thesis, the mathematical aspects of the synthesis and analysis of various algorithms are also emphasized.

In the light of the description of the fractional calculus, the author has obtained some significant results on the following topics:

A. Fractional robust control

1 . A new simple and useful tuning technique of fractional robust controllers (FOC) using Bode's ideal transfer function as a reference model.

2 Design of fractional order PI$^{\lambda}$ using Bode's integrals based online estimation.

B. Fractional adaptive robust control

1 . FO-MRAC-based fractional order PI$^{\lambda}$D$^{\mu}$ Controller using MIT rule with the concept of Bode's ideal loop function.

2 . Online Fractional Order PI$^{\lambda}$ Controller Tuning Scheme by Introducing a New Fractional Order Model Reference Using the Plant Model.

3 . Robust FO-MRAC with Fractional Order Feed-Forward with Application to a DC/DC Boost Converter.

C. Implementation of fractional control

1 . Numerical Implementation of Fractional Order Controllers on dSPACE Platform.

2 . Numerical Implementation of Fractional Order Controllers on Low-Cost Platform.

The proposed fractional-order model based control design methods are verified and tested by simulation on a variety of plant models as well as real-life hardware laboratory models of certain plants.

2.2 Thesis Outline

The rest of this thesis is organized as follows.

Chapter 1 gives some fundamentals of fractional calculus that are necessary for theoretical development in this thesis. In addition, an overview of fractional order systems and most useful approximation of fractional order operators are provided with relevant comments.

Chapter 2 presents the fractional order robust control with an overview of the most popular fractional order robust controllers such as, CRONE controller and the fractional order PI$^{\lambda}$D$^{\mu}$ Controller. The well known Bode's ideal loop is also presented which is used next for the main contribution of this thesis.

Chapter 3 considers robustness criteria in plant parameter changes case by exploring the model reference adaptive control (MRAC) problem and the use of fractional operators in the adaptation algorithm.

In Chapter 4, in order to validate some results discussed in the previous chapters, some developed fractional order control is implemented on both DS1140 control board platform and Low-Cost control board based Microcontroller.

The Conclusion and Future Work part concludes the results of the above chapters, discusses some issues of the application of proposed adaptive control methods, and gives future direction of the research with respect to fractional adaptive control.

Mathematics for fractional calculus are explained in the Appendix A. Some tools for numerical implementation are presented in Appendix B. Papers published or submitted in conferences and journals are listed in the Appendix C.

Chapter 1

FUNDAMENTALS OF FRACTIONAL CALCULUS

This Chapter presents fundamentals of fractional calculus that are necessary for theoretical development of this thesis. In addition, an overview of fractional order systems and most useful approximation of fractional order operators are provided with relevant comments. A brief review of applications of fractional calculus in various scientific and engineering disciplines is also presented.

1.1 Introduction

Fractional calculus is known as a mathematical tool for generalizing conventional integrals and derivatives, the topic attracted the attention of mathematical giants such as Euler, Laplace, Fourier, Abel, Laurent, Hardy and Littlewood. In the 19^{th} cycle and thanks to the main contributions of Liouville, Grünwald, Letnikov and Riemann a whole complete theory adapted to modern mathematical developments has been formalized.

Nowadays, fractional calculus is a well-established theory with strong mathematical bases [49, 89, 100, 122, 123]. The main reason for the vast spreading of fractional calculus is that it actually provides excellent capabilities to accurately model several physical processes. In

control theory, application of fractional calculus spawned two major branches: *Fractional order modeling* and *Fractional order control*, which consequently formed three combinations in academic research and practical implementation:

1) Integer Order Control of Fractional Order Process Plants/Models;
2) Fractional Order Control of Integer Order Process Plants/Models;
3) Fractional Order Control of Fractional Order Process Plants/Models.

Regarding these topics, many existing methodologies and principles are waiting to be extended; meanwhile, dedicated new theory and methods need to be developed to deal with the sprouting circumstances.

In this section, we provide basic definitions of fractional calculus along with its mathematical preliminaries. Then, we will discuss the problem of implementing fractional operators based on the approximation of fractional operators by rational functions. At the end of this section, we provide a brief survey of the applications of fractional order calculus in science and engineering. Information of this section will be used throughout the thesis.

1.2 Mathematical Preliminaries

Fractional calculus is a generalization of integration and differentiation to the non-integer order fundamental operator ${}_{t_0}D_t^{\alpha}$, where t_0 and t are the limits of the operation. The continuous integro-differential operator is defined as,

$$ {}_{t_0}D_t^{\alpha} = \begin{cases} \frac{d^{\alpha}}{dt^{\alpha}}, & \Re(\alpha) > 0 \\ 1, & \Re(\alpha) = 0 \\ \int_{t_0}^{t} (d\tau)^{-\alpha}, & \Re(\alpha) < 0 \end{cases} \tag{1.1} $$

where α is the order of the operation, generally $\alpha \in \mathbb{R}$ but could also be a complex number [107].

1.2.1 Mathematical Definitions of Fractional Operator

Up to now, there are more than 10 types of definitions for fractional order integrals and differentiations [89]. For researchers' convenience, several commonly used definitions are briefly listed below. More details can be found in [79].

1.2.1.1 Riemann-Liouville definition of fractional order integration

The Riemann-Liouville (R-L) definition of fractional order integration is:

$$ {}_0D_t^{-\alpha}\, f(t) = \frac{1}{\Gamma(\alpha)} \int_0^t \left(\frac{f(\tau)}{(t-\tau)^{1-\alpha}} \right) d\tau \tag{1.2} $$

where, $0 < \alpha < 1$, and $\Gamma(.)$ is the Gamma function $\Gamma(x) = \int_0^\infty e^{-u} u^{x-1} du$. When the initial integral limit changes from 0 to an arbitrary point t_0, this definition is generalized to the **Weyl** definition of fractional order integral:

$$ {}_{t_0}D_t^{-\alpha}\, f(t) = \frac{1}{\Gamma(\alpha)} \int_{t_0}^t \left(\frac{f(\tau)}{(t-\tau)^{1-\alpha}} \right) d\tau \tag{1.3} $$

1.2.1.2 Riemann-Liouville definition of fractional order differentiation

The R-L definition of fractional order differentiation is based on the fractional integral and the ordinary derivatives:

$$ {}_0D_t^{\alpha}\, f(t) = \frac{d}{dt} \int_{t_0}^t \left[{}_0D_t^{-(1-\alpha)} f(t) \right] d\tau \tag{1.4} $$

More specifically, there are left R-L and right R-L definitions for fractional order differentiation by distinguishing the lower and upper limits of the integration,

$$ {}_{t_0}D_t^{\alpha}\, f(t) = \frac{1}{\Gamma(n-\alpha)} \left(\frac{d}{dt} \right)^n \int_{t_0}^t (t-\tau)^{a-\alpha-1} f(\tau) d\tau \tag{1.5a} $$

$$ {}_{t}D_{t_1}^{\alpha}\, f(t) = \frac{1}{\Gamma(n-\alpha)} \left(-\frac{d}{dt} \right)^n \int_{t}^{t_1} (t-\tau)^{a-\alpha-1} f(\tau) d\tau \tag{1.5b} $$

The complete Riemann-Liouville definition for the integration or differentiations of a fractional order α for a function $y(t)$ is given by:

$$ {}_{t_0}D_t^{\alpha}\, y(t) = \begin{cases} \frac{1}{\Gamma(-\alpha)} \int_{t_0}^{t} (t-\tau)^{-\alpha-1} y(\tau) d\tau, & \text{if } \Re(\alpha) < 0, \\ y(t), & \text{if } \Re(\alpha) = 0, \\ D^n \left[{}_{t_0}D_t^{\alpha-n} y(t) \right], \; n = \min \left\{ k \in \aleph : k > \Re(\alpha) \right\}, & \text{if } \Re(\alpha) > 0, \end{cases} \tag{1.6} $$

where $\alpha \in \mathbb{C}$, n is a positive integer and y is a locally integrable function defined on $[t_0, \infty]$.

1.2.1.3 Caputo definition of fractional order differentiation

The Caputo definition of fractional order differentiation takes the integer order differentiation of the function first and then take a fractional order integration:

$$ {}_0^C D_t^{\alpha}\, f(t) = \frac{1}{\Gamma(1-\alpha)} \int_{t_0}^{t} \left(\frac{f'(\tau)}{(t-\tau)^{\alpha}} \right) d\tau \tag{1.7} $$

Under this definition, D and ${}_0D_t^{-(1-\alpha)}$ do not commute because the initial value needs be considered:

$$ {}_0^C D_t^{\alpha}\, f(t) = {}_0D_t^{-(1-\alpha)} f(t) \left[Df(t) \right] + \frac{f(0^+)\, t^{-\alpha}}{\Gamma(1-\alpha)} \tag{1.8} $$

1.2.1.4 Grünwald-Letnikov definition

The Grünwald-Letnikov (G-L) definition defines the fractional integration and differentiation in a unified way, as positive values of α give fractional differentiation and negative values of α give fractional order integration.

$$ {}_{t_0}D_t^{\alpha}\, f(t) = \lim_{h \to 0} \left(\frac{1}{h^{\alpha}} \right) \sum_{j=0}^{\left[\frac{(t-t_0)}{h} \right]} (-1)^j \binom{\alpha}{j} f(t - jh) \tag{1.9} $$

where, $\binom{\alpha}{j}$ represents the binomial coefficient, which is described in terms of the Gamma function.

1.2.2 Properties of Fractional Order Operators

For the fractional derivative of a time function $f(t)$ exists, it is sufficient that $f(t)$ can be written in the form [89].

$$f(t) = (t - t_0)^{\lambda}\, \eta(t - t_0) \tag{1.10}$$

$$\text{with} \begin{cases} \lambda \in C, \\ \Re(\lambda), \\ \eta(t), \qquad \text{Analytic function of } C \text{ for } t \geq 0 \end{cases} \tag{1.11}$$

and so that its fractional order integral exists, it is sufficient that $f(t)$ is piecewise continuous on $]t_0, +\infty[$ and integrable on $[t_0, t]$ for any $t > t_0$.

1.2.2.1 Properties of fractional order integral

The fractional order integral operator meets the semi-group property, namely [123]:

$$I_{t_0}^{v_1} \circ I_{t_0}^{v_2} = I_{t_0}^{v_1+v_2} \text{ with } \begin{cases} \Re(v_1) > 0, \\ \Re(v_2) > 0, \end{cases} \tag{1.12}$$

and thus, the commutativity property:

$$I_{t_0}^{v_1} \circ I_{t_0}^{v_2} = I_{t_0}^{v_2} \circ I_{t_0}^{v_1} \tag{1.13}$$

1.2.2.2 Properties of fractional-order differentiation

The fractional-order differentiation has the following properties [117]:

1 . The fractional-order differentiation ${}_0D_t^{\alpha} f(t)$, with respect to t of an analytic function $f(t)$, is also analytical.

2 . The fractional-order differentiation is exactly the same with integer-order one, when $\alpha = n$ is an integer. Also ${}_0D_t^0 f(t) = f(t)$.

3 . The fractional-order differentiation is linear; *i.e.*, for any constants a, b, one has,

$${}_0D_t^{\alpha}\, D\,[af(t) + bg(t)] = a\ {}_0D_t^{\alpha}\ f(t) + b\ {}_0D_t^{\alpha}\ g(t) \tag{1.14}$$

4 . Fractional differentiation operators satisfy the commutative-law, and also satisfy,

$$ {}_0D_t^{\alpha}\left[{}_0D_t^{\beta}f(t)\right] = {}_0D_t^{\alpha}\left[{}_0D_t^{\beta}f(t)\right] = {}_0D_t^{\alpha+\beta} \tag{1.15} $$

1.2.3 Laplace Transforms of Fractional Operators

Laplace transform (denoted as $\mathcal{L}$) is one of the most mathematical tools in dynamic system and control engineering. For this reason, we will give here the equation of these transforms for the defined fractional order integrals and differentiations.

1.2.3.1 Laplace transform of fractional order integral

Writing of equation (Eq. 1.1) using the convolution product, the Laplace transform of fractional integral is [100]:

$$ \mathcal{L}\left\{{}_0D_t^{-\alpha}f(t)\right\} = \mathcal{L}\left\{\frac{t^{\alpha-1}u(t)}{\Gamma(\alpha)} * f(t)\right\} = \mathcal{L}\left\{\frac{t^{\alpha-1}u(t)}{\Gamma(\alpha)}\right\}\mathcal{L}\left\{f(t)\right\} = s^{-\alpha}\,F(s), \tag{1.16} $$

where, $u(t)$ is the unit step function, $\Re(\alpha) > 0$, $F(s) = \mathcal{L}f(t)$ and $s = (\sigma + j\omega)$ is the Laplace operator.

This is a remarkable result that generalizes the well-known formula of the integral Laplace transform in the integer case.

1.2.3.2 Laplace transform of fractional order differentiation

The Laplace transform of the fractional derivative of a causal time function is given by [100]:

$$ \mathcal{L}\left\{D^{\alpha}f(t)\right\} = s^{\alpha}\,F(s) - \left[D^{\alpha-1}f(t)\right]_{t=0} \tag{1.17} $$

This is a remarkable result that generalizes the well-known formula of the derivative Laplace transform in the integer case.

In particular, if the derivatives of the function $f(t)$ are all equal to 0 at $t = 0$, one has,

$$ \mathcal{L}\left[{}_0D_t^{\alpha}f(t)\,\right] = s^{\alpha}\,\mathcal{L}\left[f(t)\right] $$

1.3 Time and Frequency Domain Analysis of FO-Operators

From the previous sections, it can be seen that the analysis and design of the fractional-order operators are difficult tasks.

1.3.1 Frequency Domain Analysis

The computation of frequency responses of fractional-order operators plays an important role in the application of frequency domain methods for the analysis and design of control systems.

Fractional-order operators can be classified to three categories [55]: fractional-order pure differential operator, fractional derivative operator and fractional-order integral operator.

1.3.1.1 Fractional-order pure integro-differential operator

The expression of a pure differential operator is,

$$G(s) = s^{\mu}\,, \tag{1.18}$$

where μ is an arbitrary real number. It reduces to fractional derivative when $\mu > 0$ and to fractional integral when $\mu < 0$. It degrades to a constant gain, whose value equals to 1, if $\mu = 0$. If we let $-1 \leq \mu \leq 1$. Then, for a frequency $\omega \in (-\infty; +\infty)$, the frequency domain response may be obtained by substituting $s = j\omega$ in (Eq. 1.18), and we have [136],

$$\begin{aligned} G(j\omega) &= (j\omega)^{\mu} \\ &= \omega^{\mu}\left[\cos\frac{\pi}{2} + j\sin\frac{\pi}{2}\right]^{\mu} \\ &= \omega^{\mu}\left[\cos\frac{\mu\pi}{2} + j\sin\frac{\mu\pi}{2}\right] \end{aligned} \tag{1.19}$$

In addition, consider the following useful relation for the non-integer power $\mu \in \mathbb{R}$ of the imaginary unit j.

$$j^{\mu} = \cos\left(\frac{\mu\pi}{2}\right) + j\sin\left(\frac{\mu\pi}{2}\right) \tag{1.20}$$

Magnitude and phase expressions are:

$$|G(j\omega)| = A(\omega) = |\omega^{\mu}| \tag{1.21}$$

$$\angle G(j\omega) = \theta(\omega) = \frac{\pi}{2}\left[\mu - \left(1 - \frac{\omega}{|\omega|}\right)\right] \tag{1.22}$$

$$20\log A(\omega) = 20\log|\omega^{\mu}| = 20\mu\log|\omega| \tag{1.23}$$

resulting in:

- Magnitude (dB *vs* log-frequency): a beeline with a slope of $+20\mu\,dB$ when $\omega > 0$ and $-20\mu\,dB$ when $\omega < 0$ passing through $0\,dB$ for $\omega = \pm 1$ see (Fig. 1.1),
- Phase (rad *vs* log-frequency): independent with frequency. Under a certain order μ, the phase is $\mu\frac{\pi}{2}$ when $\omega > 0$ and $(-\pi + \mu\frac{\pi}{2})$ when $\omega < 0$ see (Fig. 1.1).

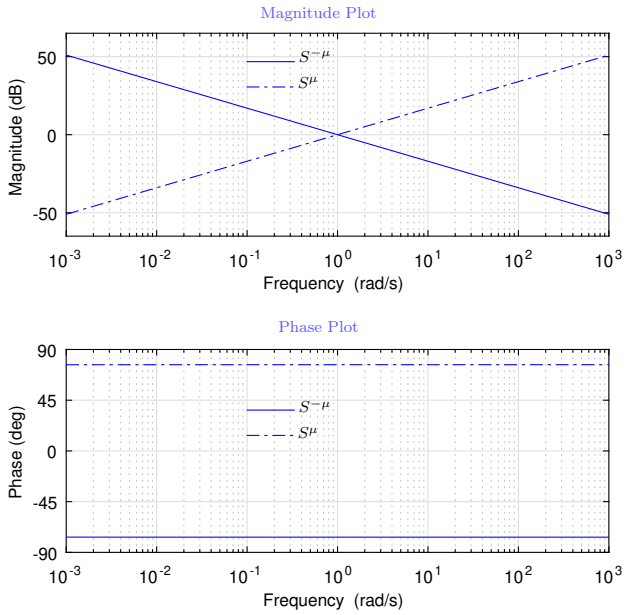

Figure 1.1 Bode diagrams of s^{μ}, with $\mu = 0.85$ and $\mu = -0.85$

1.3.1.2 Fractional-order derivative operator

The expression of a fractional-order derivative operator is:

$$G(s) = \tau_{\alpha}\, s^{\mu} + 1, \qquad \mu \in [0, 1] \tag{1.24}$$

where,

$$\begin{aligned}\tau_\alpha &= A_\alpha \angle\theta_\alpha \\ &= A_\alpha(\cos\theta_\alpha + j\sin\theta_\alpha), \quad A_\alpha > 0, \quad \theta_\alpha \in [0, 2\pi], \quad 0 < \mu \leq 1.\end{aligned}$$

Then, for a frequency $\omega \in (-\infty; +\infty)$, the frequency domain response may be obtained by substituting $s = j\omega$ in (Eq. 1.24), and we have,

$$\begin{aligned}G(j\omega) &= \tau_\alpha(j\omega)^\mu + 1 \\ &= 1 + \omega^\mu A_\alpha \cos\left(\theta_\alpha + \mu\frac{\pi}{2}\right) + j\omega^\mu A_\alpha \sin\left(\theta_\alpha + \mu\frac{\pi}{2}\right)\end{aligned} \tag{1.25}$$

Thus, the magnitude expression is,

$$A(\omega) = \sqrt{\left[1 + \omega^\mu A_\alpha \cos\left(\theta_\alpha + \mu\frac{\pi}{2}\right)\right]^2 + \left[\omega^\mu A_\alpha \sin\left(\theta_\alpha + \mu\frac{\pi}{2}\right)\right]^2} \tag{1.26}$$

and, the phase expression is,

$$\theta(\omega) = \tan^{-1}\left(\frac{\omega^\mu A_\alpha \sin\left(\theta_\alpha + \mu\frac{\pi}{2}\right)}{1 + \omega^\mu A_\alpha \cos\left(\theta_\alpha + \mu\frac{\pi}{2}\right)}\right) \tag{1.27}$$

resulting in:

- Magnitude diagram (dB *vs* log-frequency): a $0\,dB$ line when $|\omega| < A_\alpha^{\left(-\frac{1}{\mu}\right)} = \omega_b$ (break frequency), of a beeline with slope of $20\mu\,dB$ when $\omega > \omega_b$ and a beeline with its slope of -$20\mu\,dB$ when $\omega > \omega_b$, see (Fig. 1.2);

- Phase (rad *vs* log-frequency): starts from the origin and approaches to limit phase $\Theta = \left(\theta_\alpha + \mu\frac{\pi}{2}\right)$ in positive frequency domain, from $(\Theta - \pi)$ to the origin in negative frequency domain. At the break frequency ω_b, the phase values $\frac{1}{2}\left(\theta_\alpha + \mu\frac{\pi}{2}\right)$, see (Fig. 1.2). The Nyquist contour is a beeline obtained by anticlockwise rotation of real axis $\left(\theta_\alpha + \mu\frac{\pi}{2}\right)$ around the (1,0) point.

1.3.1.3 Fractional-order integral operator

The expression of a fractional-order integral operator is:

$$G(s) = \frac{1}{\tau_\alpha\, s^\mu + 1}, \quad \mu \in [0, 1] \tag{1.28}$$

Then, for a frequency $\omega \in (-\infty; +\infty)$, the frequency domain response may be obtained by substituting $s = j\omega$ in (Eq. 1.28), and we have the magnitude and phase expressions,

$$A(\omega) = \frac{1}{\sqrt{\left[1 + \omega^{\mu} A_{\alpha} \cos\left(\theta_{\alpha} + \mu\frac{\pi}{2}\right)\right]^2 + \left[\omega^{\mu} A_{\alpha} \sin\left(\theta_{\alpha} + \mu\frac{\pi}{2}\right)\right]^2}} \tag{1.29}$$

$$\theta(\omega) = tan^{-1}\left(\frac{\omega^{\mu} A_{\alpha} \sin\left(\theta_{\alpha} + \mu\frac{\pi}{2}\right)}{1 + \omega^{\mu} A_{\alpha} \cos\left(\theta_{\alpha} + \mu\frac{\pi}{2}\right)}\right) \tag{1.30}$$

Hence, the logarithm frequency properties are minus functions of those of fractional-order derivative operator resulting in:

- Magnitude diagram (dB *vs* log-frequency): a $0\,dB$ line when $|\omega| < A_{\alpha}^{\left(-\frac{1}{\mu}\right)} = \omega_b$ (break frequency), of a beeline with slope of -$20\mu\,dB$ when $\omega > \omega_b$ and a beeline with its slope of $20\mu\,dB$ when $\omega < -\omega_b$, see (Fig. 1.2).

- Phase (rad *vs* log-frequency): starts from the origin and approaches to limit phase $\Theta = -\left(\theta_{\alpha} + \mu\frac{\pi}{2}\right)$ in positive frequency domain, from $(\Theta - \pi)$ to the origin in negative frequency domain. At the break frequency ω_b, the phase values $-\frac{1}{2}\left(\theta_{\alpha} + \mu\frac{\pi}{2}\right)$, see (Fig. 1.2). The Nyquist contour starts along the asymptote with its slop $-\left(\theta_{\alpha} + \mu\frac{\pi}{2}\right)$ from the origin and approach the (1,0) point in negative frequency domain, begins at the point (1,0) and approaches to origin along the same direction of the asymptote in the positive frequency domain.

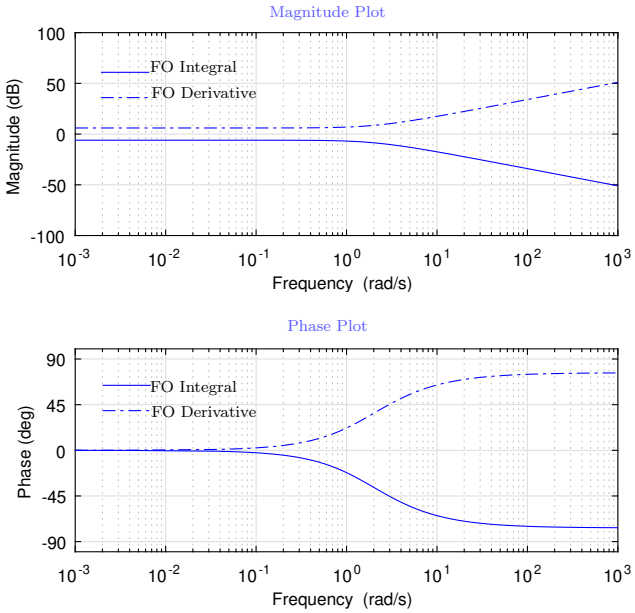

Figure 1.2 Bode diagrams of $(\tau_\alpha s^\mu + 1)$ and $1/(\tau_\alpha s^\mu + 1)$, with $\mu = 0.85$

1.3.2 Time Domain Analysis

Time domain responses of fractional-order operators can be evaluated with different methods. The impulse and step responses can be obtained by the use of the analytical solution of the inverse Laplace transform.

1.3.2.1 Impulse response

From equation (Eq. 1.6) we can write:

$$\mathcal{L}\left\{{}_0D_t^\alpha y(t)\right\} = \mathcal{L}\left\{\frac{t^{-\alpha-1}u(t)}{\Gamma(-\alpha)} * y(t)\right\} = \mathcal{L}\left\{\frac{t^{-\alpha-1}u(t)}{\Gamma(-\alpha)}\right\}\mathcal{L}\left\{y(t)\right\} = s^\alpha Y(s), \tag{1.31}$$

where $u(t)$ is the unit step function. The case $Y(s) = 1$ corresponds to the fractional-order derivative α of the Dirac function $y(t) = \delta(t)$, then, by substituting $y(t)$ in (Eq. 1.31), we can deduce the impulse response of a fractional order derivative, as,

$$\mathcal{L}\left\{{}_0D_t^\alpha \delta(t)\right\} = s^\alpha = \mathcal{L}\left\{\frac{t^{-\alpha-1}u(t)}{\Gamma(-\alpha)}\right\} \Leftrightarrow \mathcal{L}\left\{{}_0D_t^\alpha \delta(t)\right\} = \frac{t^{-\alpha-1}u(t)}{\Gamma(-\alpha)}, \tag{1.32}$$

Figure (1.3) shows the impulse response of a fractional derivative for different values of the order α.

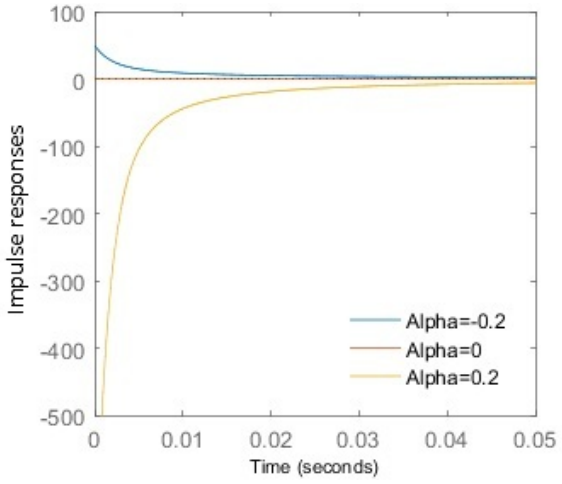

Figure 1.3 Impulse response of a fractional derivative for different values of α.

1.3.2.2 Step response

The fractional order derivative of a unit step is obtained by substituting $Y(s) = 1/s$ in the (Eq. 1.31), which gives:

$$\mathcal{L}\left\{{}_0D_t^{\alpha} y_{unit}(t)\right\} = s^{\alpha-1} \Leftrightarrow {}_0D_t^{\alpha} y_{unit}(t) = \frac{t^{-\alpha}u(t)}{\Gamma(-\alpha+1)}, \tag{1.33}$$

Figure (1.4) shows the step response of a fractional order derivative for different values of α.

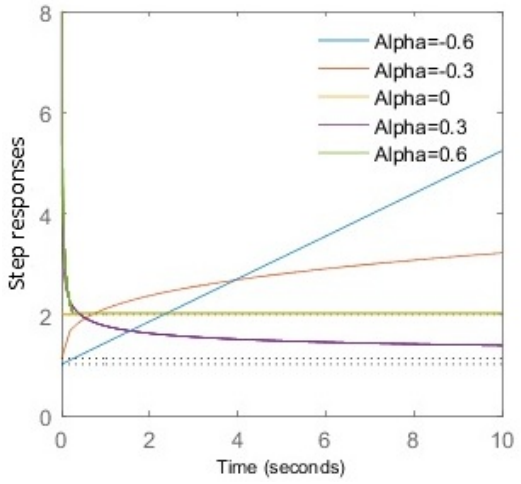

Figure 1.4 Step response of a fractional derivative for different values of α.

1.4 Approximation of Fractional-Order Operators

In the previous sections, different types of definitions for fractional-order operators as well as their analysis in frequency and time domain are addressed. The most difficult problem yet to be solved particularly in time domain is how to implement them. A feasible way to implement fractional operators is to use finite dimensional integer-order transfer functions.

Theoretically speaking, an integer-order transfer function representation of a Fractional-Order Operator (FOO) s^α is infinite-dimensional. However, it should be pointed out that the finite-dimensional approximation of the FOO should be done in a proper range of frequencies of practical interest [106, 107]. Moreover, the fractional-order can be a complex number [107].

For a single term s^α with α a real number, there are many approximation methods proposed but unfortunately it is not possible to say that one of them is the best. In general, we have analog realizations [52, 99, 133, 117] and digital realizations. A good review of these approximations can be found in [141, 117, 147].

1.4.1 Continuous-Time Approximation of Fractional Operators

Oustaloup and Charef's approximation are the well-known methods. Charef's approximation is good enough in most cases for the works presented in this thesis.

1.4.1.1 Oustaloup method

The Oustaloup recursive filter, proposed in [107] and discussed in [91, 147], gives a very good approximation of fractional operators in a specified frequency range. It is a well-established method and is often used for practical implementation of fractional-order systems and controllers. It is summarized next.

In order to approximate a fractional differentiator of order α or a fractional integrator of order $(-\alpha)$ by a conventional transfer function one may compute the zeros and poles of the latter using the following equations:

$$s^\alpha \approx K \prod_{k=1}^{N} \frac{s+\omega_k^{'}}{s+\omega_k}, \tag{1.34}$$

where,

$$\omega_k^{'} = \omega_b.\omega_u^{(2k-1-\alpha)/N}, \tag{1.35}$$

$$\omega_k = \omega_b.\omega_u^{(2k-1+\alpha)/N}, \tag{1.36}$$

$$K = \omega_h^{\alpha)}, \quad \omega_u = \sqrt{\frac{\omega_h}{\omega_b}}, \tag{1.37}$$

N is the approximation order in a valid frequency range $(\omega_b; \omega_h)$. For fractional orders $\alpha \geq 1$ we can write,

$$s^\alpha = s^n s^\gamma, \tag{1.38}$$

where $n = \alpha - \gamma$ denotes the integer part of α and s^γ is obtained by the Oustaloup approximation by using (Eq. 1.34). Thus, every operator may be approximated using (Eq. 1.38) and substituted by the obtained approximation, yielding a conventional integer-order transfer function. For digital implementations, the obtained approximation may be converted to its discrete-time equivalent using a suitable method.

1.4.1.2 Charef's method

In this method [20] the differentiator or integrator is approximated in a given frequency band $[\omega_b; \omega_h]$ by a rational function using a set of elementary first order cells of the form:

$$H(s) = \frac{1}{\left(1 + \frac{s}{pT}\right)^\alpha}, \tag{1.39}$$

by a quotient of polynomials in s in a factorized form:

$$\hat{H}(s) = \frac{\prod_{i=0}^{n-1}\left(1 + \frac{s}{z_i}\right)}{\prod_{i=0}^{n}\left(1 + \frac{s}{p_i}\right)}, \tag{1.40}$$

where the coefficients are computed for obtaining a maximum deviation from the original magnitude response in the frequency domain of $y\,dB$. Defining,

$$a = 10^{\left[\frac{y}{10(1-\alpha)}\right]}, \quad b = 10^{\left[\frac{y}{10\alpha}\right]}, \quad ab = 10^{\left[\frac{y}{10\alpha(1-\alpha)}\right]}, \tag{1.41}$$

the poles and zeros of the approximated rational function are obtained by applying the following formulae:

$$p_0 = pT\sqrt{b}, \quad p_i = p_0\,(ab)^i, \quad z_i = ap_0\,(ab)^i, \tag{1.42}$$

The number of poles and zeros is related to the desired bandwidth and the error criteria used by the expression:

$$N = Integer \left[\frac{log\left(\frac{\omega_{max}}{p_0}\right)}{log\,(ab)} \right] + 1\,, \tag{1.43}$$

1.4.2 Discrete-time Approximation of Fractional Order Operators

The key step in discrete approximation or implementation of a FOO is the discretization of the term s^α. In general, there are two classes of discretization methods: direct discretization and indirect discretization.

In indirect discretization methods [107], two steps are required, *i.e.*, frequency domain fitting in continuous time domain first and then discretizing the fit s-transfer function. The most common are Tustin's, Simpson's, or Al-Alaoui's approximations [2, 147]. Existing direct discretization methods include the application of the direct power series expansion (PSE) of the Euler operator [78, 148, 146, 147], continued fraction expansion (CFE) of the Tustin operator [23, 148, 146, 147], and numerical integration based method [23, 78].

The former discretization methods of s^α lead naturally to the DFOO (Digital Fractional Order Operator) usually in Infinite Impulse Response (IIR) form. Actually, there are some methods to directly obtain the DFOOs in infinite impulse response (FIR) form [138, 139] . However, using an FIR filter to approximate s^α may be less efficient due to the very high order of the FIR filter. Thus, discretizing fractional-order operators in IIR (Infinite Impulse Response) forms is preferred [2, 23, 26].

1.4.3 Numerical Evaluation of Fractional Order Operators

Numerical computation of fractional order derivatives and integrals for any function $y(t)$ is generally very difficult when using analytical methods. Therefore, a numerical approximation is necessary. The most simply used method is the one based on the Grünwald-Letnikov definition. Thus, the formula (1.9) can be used to approximately compute numerical evaluation of the fractional order derivatives and integrals by choosing an appropriate value of

the sampling step [89], that is to say:

$$ {}_{t_0}D_t^{\alpha}\, y(t) \approx \frac{1}{h^{\alpha}} \sum_{k=0}^{int\left[\frac{(t-t_0)}{h}\right]} (-1)^k \binom{\alpha}{k} y(t-kh) \tag{1.44} $$

For $t \gg t_0$ the number of addends in the fractional approximation (Eq. 1.44) becomes enormously large, in other words, we need unlimited memory. For a given approximation error ε, these addends can be decreased to a limited term N, fixed by using short memory principle.

Theorem 1.4.1 (Short memory principle) *[113]: if a time function y is bounded in the interval $[t_0, t]$, i.e., if there exists a value M verifying:*

$$ |y(\xi)| < M, \qquad \forall \xi \in [t_0,\, t]\,, \tag{1.45} $$

thus, the approximation:

$$ {}_{t_0}D_t^{\alpha}\, y(t) = {}_{t-L}D_t^{\alpha} y(t) \qquad with\, L < t - t_0\,, \tag{1.46} $$

gives an error ε such that:

$$ |\varepsilon| < \frac{ML^{-\alpha}}{|\Gamma(1-\varepsilon)|}\,, \tag{1.47} $$

Consequently, the formula (1.44) can be rewritten as:

$$ {}_{a}D_t^{\alpha}\, y(t) \approx \frac{1}{h^{\alpha}} \sum_{k=0}^{N} (-1)^k \binom{\alpha}{k} y(t-kh) \tag{1.48} $$

where, $N = integer(\frac{L}{h})$.

The main advantage of this approach lies in its simplicity of implementation.

1.5 Representation, Analysis and Simulation of Fractional Order Systems

1.5.1 Fractional Order Linear Systems

In the fields of dynamical systems and control theory, a fractional-order system is a dynamical system that can be modeled by a fractional differential equation containing non-integer operators. Such systems are said to have fractional dynamics. A general continuous-time dynamical linear system of fractional order can be described by the following form, [91]:

$$a_n\, D^{\alpha_n}\, y(t) + a_{n-1}\, D^{\alpha_{n-1}}\, y(t) + \ldots + a_0\, D^{\alpha_0}\, y(t) = b_m\, D^{\beta_m}\, u(t) + b_{m-1}\, D^{\beta_{m-1}}\, u(t) + \ldots + b_0\, D^{\beta_0}\, u(t) \quad (1.49)$$

where $y(t)$ and $u(t)$ are functions of the fractional derivative operator D of orders α_i, β_j $(i, j = 1, 2, 3...)$, that can be arbitrary real numbers, *i.e.* $(\alpha_i, \beta_j) \in \mathbb{R}^2_+$ and $(a_i, b_j) \in \mathbb{R}^2$. If the ($\alpha_i$ and β_j) are integer multiples of a common factor q, the system is called having commensurate-order, if $(\alpha_i, \beta_j) = kq$, $q \in \mathbb{R}^+$. The system can then be expressed as:

$$\sum_{k=0}^{n} a_k\, D^{kq}\, y(t) = \sum_{k=0}^{m} b_k\, D^{kq}\, u(t) \quad (1.50)$$

If in (Eq. 1.50) the order is $q = (1/r)$, $r \in \mathbb{Z}_+$, the system will be of rational order; and is of $non - commensurate - order$ if no common factor exists [147].

This way, linear time-invariant systems can be classified as given in (Fig. 1.5):

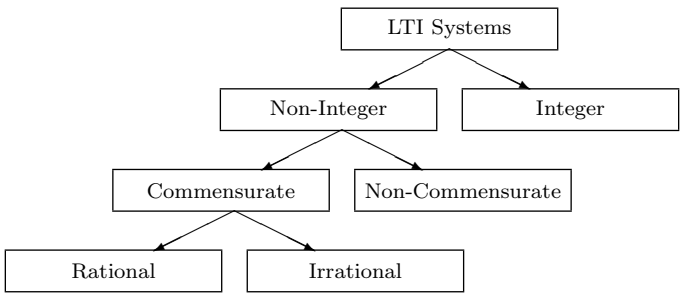

Figure 1.5 Classification of LTI systems

1.5.2 Fractional Order Transfer Functions

Applying the Laplace transform (Eq. 1.17) to (Eq. 1.49) with zero initial conditions, the input-output representation of the fractional-order system can be obtained in the form of a transfer function:

$$G(s) = \frac{Y(s)}{U(s)} = \frac{b_m\, s^{\beta_m} + b_{m-1}\, s^{\beta_{m-1}} + \ldots + b_0\, s^{\beta_0}}{a_n\, s^{\alpha_n} + a_{n-1}\, s^{\alpha_{n-1}} + \ldots + a_0\, s^{\alpha_0}} \tag{1.51}$$

We shall call the number of fractional poles in (Eq. 1.51) the pseudo-order of the system. In the case of a system with commensurate order q, we may take $\sigma = s^q$ and consider the continuous-time pseudo-rational transfer function:

$$G(\sigma) = \frac{\sum_{k=0}^{m} b_k\, \sigma^k}{\sum_{k=0}^{n} a_k\, \sigma^k} \tag{1.52}$$

1.5.3 Time and Frequency Domain Analysis of Fractional Systems

To analyse the dynamical properties of a system, the time and frequency domain can be used. First we begin with the frequency domain analysis.

1.5.3.1 Frequency domain analysis

Frequency domain response may be obtained by substituting $s = j\omega$ in (Eq. 1.51). The complex response for a frequency $\omega \in (0; \infty)$ can then be computed as follows:

$$G(j\omega) = \frac{Y(j\omega)}{U(j\omega)} = \frac{b_m\, (j\omega)^{\beta_m} + b_{m-1}\, (j\omega)^{\beta_{m-1}} + \ldots + b_0\, (j\omega)^{\beta_0}}{a_n\, (j\omega)^{\alpha_n} + a_{n-1}\, (j\omega)^{\alpha_{n-1}} + \ldots + a_0\, (j\omega)^{\alpha_0}} \tag{1.53}$$

where j is the imaginary unit.

In addition, consider the useful relation in (Eq. 1.20) for a non-integer power of the imaginary unit j,

1.5.3.2 Time domain analysis

Another solution involves numerical computation of fractional-order derivatives which is carried out by means of a revised Grünwald-Letnikov definition (Eq. 1.9) rewritten as

$$ {}_{t_0}D_t^{\alpha}\, f(t) = \lim_{h\to 0}\left(\frac{1}{h^{\alpha}}\right) \sum_{j=0}^{\left[\frac{(t-t_0)}{h}\right]} \omega_j^{(\alpha)}\, f(t-jh) \tag{1.54} $$

where h is the computation step-size and $\omega_j^{(\alpha)} = (-1)^j \binom{\alpha}{j}$ can be evaluated recursively from:

$$ \omega_0^{(\alpha)} = 1\,, \qquad \omega_j^{(\alpha)} = \left(1 - \frac{\alpha+1}{j}\right)\omega_{j-1}^{(\alpha)}\,, \quad j = 1,\, 2,\, \ldots \tag{1.55} $$

To obtain a numerical solution for the equation in (Eq. 1.49) the signal $\hat{u}(t)$ should be obtained first, using the algorithm in (Eq. 1.55), where

$$ \hat{u}(t) = b_m\, D^{\beta_m}\, u(t) + b_{m-1}\, D^{\beta_{m-1}}\, u(t) + \ldots + b_0\, D^{\beta_0}\, u(t) \tag{1.56} $$

The time response of the system can then be obtained using the following equation:

$$ y(t) = \frac{1}{\sum_{i=0}^{n} \frac{a_i}{h^{\alpha_i}}} \left[\hat{u}(t) - \sum_{i=0}^{n} \frac{a_i}{h^{\alpha_i}} \sum_{j=1}^{\left[\frac{(t-t_0)}{h}\right]} \omega_j^{(\alpha)}\, y(t-jh)\right] \tag{1.57} $$

The presented method is a fixed step method. The accuracy of simulation therefore may depend on the step size [46, 82, 109].

If the equation (1.49) has time delay L, the resulting delayed response $y_d(t)$ with $y_d(0) = 0$ is obtained such that,

$$ y_d(t) = \begin{cases} y(t-L), & \text{t>L} \\ 0, & \text{otherwise.} \end{cases} \tag{1.58} $$

1.5.4 Discrete Models of Fractional Order Systems

Discrete models of fractional order systems can be obtained using discrete approximations of the fractional integrals and derivatives operators. Thus, a general expression for the discrete transfer function $G(z)$ of the fractional system $G(s)$, can be obtained as [147]:

$$ G(z) = \frac{b_m\, (\omega(z^{-1}))^{\beta_m} + b_{m-1}\, (\omega(z^{-1}))^{\beta_{m-1}} + \ldots + b_0\, (\omega(z^{-1}))^{\beta_0}}{a_n\, (\omega(z^{-1}))^{\alpha_n} + a_{n-1}\, (\omega(z^{-1}))^{\alpha_{n-1}} + \ldots + a_0\, (\omega(z^{-1}))^{\alpha_0}} \tag{1.59} $$

where, $(\omega(z^{-1}))$ denotes the discrete equivalent of the Laplace operator s, expressed as a function of the complex variable z or the shift operator z^{-1}.

As can be seen in the former equations, a fractional-order system has an irrational-order continuous transfer function in Laplace's domain or a discrete transfer function in the z domaine of infinite order. In other words, a fractional-order system has an unlimited memory, and obviously the systems of integer-order are just particular cases of this general case in which the memory is limited. It is clear that only in the case of integer order it is possible to realize a transfer function exactly by using conventional lumped elements (resistances, inductances, and capacitors, in the case of analog realizations), or procedures (finite order difference equations or digital filters in the case of discrete realizations).

Because of this, and taking into account that the final step for applying a fractional controller demands a realizable form of it, in this work some continuous and discrete integer-order approximations of fractional-order operators are presented.

1.5.5 State-Space Representation

Many modern control concepts and methodologies are still applicable to the dynamic systems possessing "FO" behaviors. The State-Space (S-S) representation is such a powerful tool. It can be generally expressed as the following by defining appropriate state variables,

$$\begin{cases} {}_0D_t^{\alpha}x(t) = f(x,u,t) \\ \quad y(t) = g(x) \end{cases} \tag{1.60}$$

where $x \in \mathbb{R}^n$ is the state vector of dimension n, and $0 < \alpha < 2$ is the common factor of the differentiation orders. For linear fractional differential equations in (Eq. 1.49), the (Eq. 1.60) can be simplified as,

$$\begin{cases} {}_0D_t^{\alpha}x(t) = Ax(t) + Bu(t) \\ \quad y(t) = Cx(t) + Du(t) \end{cases} \tag{1.61}$$

where A, B, C and D are system, input and output matrices, respectively.

For integer order state space models, the exponential matrix, $\Phi(t) = e^{At}$ is known as the state transition matrix. It can be analogized accordingly that the generalized exponential

matrix using Mittag-Leffler function, $E_\alpha\left(At^\alpha\right)$, plays the same role for fractional order state-space models. It is called the fractional order state transition matrix and can be obtained by [91],

$$\Phi(t) = \mathcal{L}^{-1}\left\{(s^\alpha I - A)^{-1}\right\}. \tag{1.62}$$

1.5.5.1 Pseudo state-space representation

If the fractional differential equation (1.49) has commensurate order then, for null initial conditions, it admits a pseudo state space representation of the form:

$$\begin{cases} \dfrac{d^\gamma}{dt^\gamma}x(t) = Ax(t) + Bu(t) \\ \qquad y(t) = Cx(t) + Du(t) \end{cases} \tag{1.63}$$

where $x \in \mathbb{R}^n$ is the pseudo state vector, $\gamma = 1/q$ is the fractional order of the system and $A \in \mathbb{R}^{n\times n}, B \in \mathbb{R}^{n\times m}, C \in \mathbb{R}^{p\times n}$ and $D \in \mathbb{R}^{p\times m}$ are constant matrices.

Remark 1.5.1

As for integer order systems, pseudo state variables can be chosen to obtain a controllability or observability canonical form.

Remark 1.5.2

Another way to obtain a fractional order transfer function is to convert from fractional order pseudo state-space expressions, [91]. Consider the pseudo S-S representation in (Eq. 1.61), assuming zero initial conditions, and taking Laplace transformation gives,

$$s^\alpha X(s) = AX(s) + BU(s), \tag{1.64}$$

$$Y(s) = CX(s) + Du(s), \tag{1.65}$$

Then, the transfer function $G(s) = Y(s)/U(s)$ can be derived through:

$$G(s) = C(s^\alpha\, I - A)^{-1}\, B + D, \tag{1.66}$$

If B is a multi-column matrix and/or C is a multi-row matrix, then the resulting $G(s)$ is an FO transfer function matrix rather than a single FO transfer function.

1.5.6 Observability and Controllability

Controllability and Observability represent two major concepts of modern control system theory. For the fractional order systems, the following two results can be demonstrated as their similar in the integer order case [141, 143].

Theorem 1.5.1 (Observability) *: A commensurable fractional order system of the form (Eq. 1.63) is observable if and only if the Observability Matrix given by (Eq. 1.67) is a full rank matrix,*

$$\begin{bmatrix} C \\ CA \\ \vdots \\ CA^{L-1} \end{bmatrix} \tag{1.67}$$

where L is the number of state variables.

Theorem 1.5.2 (Controllability) *: A commensurable fractional order system represented by the state equation system (Eq. 1.63) is controllable if and only if the Controllability Matrix given by (Eq. 1.68) has a full rank,*

$$\begin{bmatrix} B & AB & \dots & A^{L-1}B \end{bmatrix} \tag{1.68}$$

where L is the number of state variables.

1.5.7 Stability Analysis

System stability is always a big concern in control theory due to its importance. There are numerous notions and criteria for different kinds of stabilities, such as bounded-input bounded-output (BIBO) stability, exponential stability, asymptotic stability, Lyapunov stability, robust stability, etc. For FO systems, these criteria need to be extended, and new stability types are proposed.

In order to study stability of a fractional system given by (Eq. 1.49) we consider the following theorem [24, 86].

Theorem 1.5.3 (Matignon's stability theorem) *: A fractional order transfer function* $G(s) = Z(s)/P(s)$ *is stable if and only if the following condition is satisfied in* σ*-plane:*

$$|Arg(\sigma)| > q\frac{\pi}{2}\,, \qquad \forall \sigma \in C\,, \quad P(\sigma) = 0\,, \tag{1.69}$$

where $0 < q \leq 1$ *and* $\sigma := s^q$*. When* $\sigma = 0$ *is a single root of* $P(s)$*, the system cannot be stable. For* $q = 1$ *, this is the classical theorem of pole location in the complex plane: no pole is in the closed right plane of the first Riemann sheet.*

The algorithm for checking the stability of the system in (Eq. 1.51) can be summarized as follows:

1) Find the commensurate order q of $P(s)$, find $a_1, a_2, \ldots, a_n$ in (Eq. 1.52);
2) Solve for σ the equation $\sum_{k=0}^{n} a_k \sigma^k = 0$;
3) If all obtained roots satisfy the condition in (Th.1.5.3), the system is stable.

Stability regions of a fractional-order system are shown in (Fig. 1.6).

Note that there are currently no polynomial techniques, either *Routh* or *Jury* type, to analyze the stability of fractional-order systems [91].

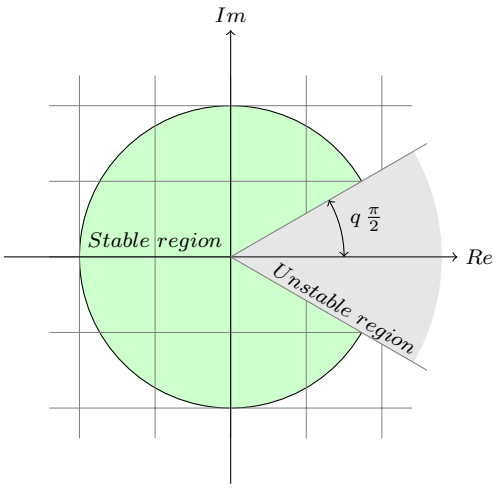

Figure 1.6 LTI fractional-order system stability region for $0 < q \leq 1$

1.5.8 Fractional System Performances

Many previous works have shown that fractional systems present good qualities, in-time response and in-transition dynamic stability (see for instance [103, 134, 18]). For a second order SISO system, represented by the following transfer function:

$$G(s) = \frac{1}{(\frac{s^2}{\omega_n^2} + 2\xi\frac{s}{\omega_n} + 1)^m} \tag{1.70}$$

where: $\omega_n = 10$ rd/s, $\xi = 0.95$.

The step responses for the integer case ($m = 1$) and the fractional order one ($m = 0.55$) are given in (Fig. 1.7), and show the gain in time response.

Let us note that the transfer function given in (Eq. 1.70) is preferred to the model structure given by:

$$G(s) = \frac{1}{\frac{s^2}{\omega_n^2} + 2\xi\left(\frac{s}{\omega_n}\right)^m + 1}, \tag{1.71}$$

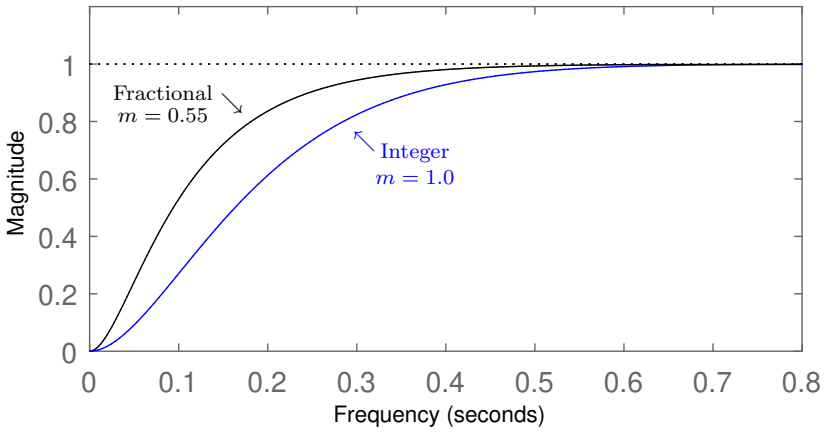

Figure 1.7 Comparative step response (fractional/integer)

Although this latter form could be more familiar for physical and mechanical engineers, it always represents a second order mathematical process model, and the well-known properties of the system presented in (Eq. 1.70) in terms of the fractional order m and the effects of the damping factor ξ on time response [18] make it more realistic, for instance, as a reference model in an adaptive control loop. Moreover, Hartley and Lorenzo have shown [48] a model

of the form:

$$G(s) = \frac{1}{s^{m_1} + as^{m_2} + 1}, \qquad m_1 > m_2 > 0 \tag{1.72}$$

which is more general than (Eq. 1.71), can go into resonance with some conditions on the value of the real constant a, even if $m_1 = 1$.

1.5.9 Time Domain Simulation of Fractional Order Systems

One of the main difficulties with fractional order models is related to time-domain simulation. Often, the analytical expression of a model's output is not simple for implementation. Over the past two decades, many numerical algorithms have been developed using either continuous or discrete rational systems approximating fractional models. The problem of obtaining a continuous or discrete suitable realizable form in control applications can be regarded as a problem of obtaining rational approximation of irrational transfer function. In a given frequency band of practical interest, the fractional order model and its rational approximation have the same dynamics. A good overview of existing continuous and discrete time approximations of fractional operators is given in [147]. They can be classified in two types "direct and indirect methods".

1.5.9.1 Direct method

These methods are based on a numerical approximation of the non-integer operator; the fractional derivation is replaced by its discrete-time equivalent. As a result, a discrete-time transfer function similar to (Eq. 1.59) is obtained. The $(\omega(z^{-1}))$ term can be computed using various approximation methods. The most common are *Euler's*, *Tustin's*, *Simpson's*, or *Al-Alaoui's* approximations [147, 2]. These analogue-to-digital open-loop design methods lead to irrational z-transforms which are then approximated either by a truncated Taylor's series expansion or a continuous fraction expansion in order to obtain a recurrent equation directly used for simulation [4]. Different types of approximations can be used in this context; the most commonly used method is that directly related to the Grünwald-Letnikov (GL) definition [113]. This method is very simple to use. However, the simulation requires, for each step, the computation of sums of increasing dimension with time. This makes real-

time simulation hard to achieve and amplify greatly any noise present in the data. This is a real constraint when this approximation is used for model identification and parameter estimation.

In [37], a new technique for numerical simulation of fractional systems using Digital Adjustable Fractional Integrator (DAFI), obtained by discretization of an optimal analog variable fractional integrator, was proposed. This technique leads to one-step forward recurrent equation directly used for numerical simulation and parameters identification of different fractional order systems with a very high speed compared to the classical methods. Moreover, the memory is considerably reduced and the accuracy is increased. Practical use of embedded processors for fractional digital filtration of signals in real time is then possible.

1.5.9.2 Indirect method

These methods are based on the simulation of the continuous fractional model with the help of a specific operator or representation [105, 2, 147, 23, 19]. Fractional behavior of a given system is usually limited in a frequency range of interest, the fractional order model and its rational approximation have the same dynamics.

In [19] a design of an analog variable fractional order differentiator and integrator, in a given frequency band, was presented. The main feature of this analog variable fractional order integrator or differentiator is that its frequency characteristics can be changed without redesigning a new one. This gives a useful tool to approximate and simulate different fractional systems using fixed fractional order filter structure.

1.6 Realization of Fractional Order Systems

Realization of fractional systems includes the realization of analogue fractional systems and the realization of digital fractional systems.

1.6.1 Analogue Realization of Fractional Operators

Analogue fractional systems, such as the fractional controllers and fractional filters, can be used widely in engineering. All fractional systems rely on the fractional order integrator and the fractional-order differentiator as basic elements. Many efforts have been made to design analogue fractional-order integrators and differentiators. Most of these analogue realization methods are based on networks of resistors, capacitors or inductors.

1.6.1.1 Implementation of fractional order integrator

The approximation of fractional order integrator operator by a rational function in a given frequency band has the form (Eq. 1.40):

$$H_I(s) = \frac{K_I}{s^\lambda} = \frac{K_I}{\left(1+\frac{s}{\omega_c}\right)^\lambda} \approx K_I \frac{\prod_{i=0}^{n-1}\left(1+\frac{s}{z_i}\right)}{\prod_{i=0}^{n}\left(1+\frac{s}{p_i}\right)}\,, \tag{1.73}$$

The decomposition into simple elements of the rational function approximating the fractional order integrator $H_I(s)$ gives:

$$H_I(s) = \sum_{i=0}^{N}\left(\frac{h_i}{1+\frac{s}{p_i}}\right)\,, \tag{1.74}$$

where, h_i are the residues of the poles given by (Eq. 1.73).

It can be seen that (Eq. 1.74) corresponds to the impedance of an RC network of the Forster type of 1^{st} form as shown in (Fig. 1.8): The impedance of this network is given by:

$$Z(s) = \sum_{i=0}^{N}\left(\frac{R_i}{1+R_iC_is}\right)\,, \tag{1.75}$$

From (Eq. 1.74) and (Eq. 1.75), and for $i = 1, 2, 3, ...N-1$, we can write,

$$R_i = h_i\,, \quad C_i = \frac{1}{p_ih_i} \tag{1.76}$$

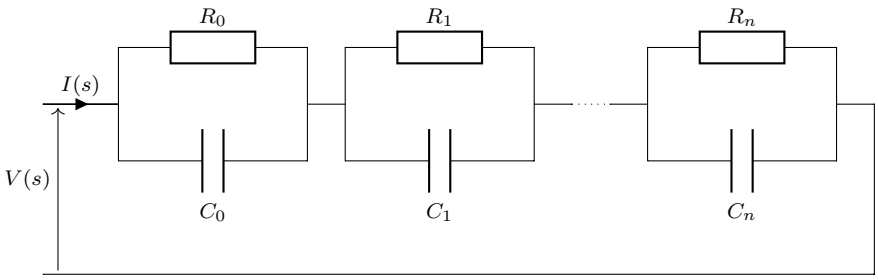

Figure 1.8 Equivalent network of a fractional order integrator operator

1.6.1.2 Implementation of fractional order derivative

In the same way, the rational approximation of the fractional order derivative can be given by the following form:

$$G_D(s) = K_D s^{\mu} = K_D \left(1 + \frac{s}{\omega_c}\right)^{\mu} \approx K_D \frac{\prod_{i=0}^{N} \left(1 + \frac{s}{z_i}\right)}{\prod_{i=0}^{N} \left(1 + \frac{s}{p_i}\right)}, \tag{1.77}$$

The decomposition into simple elements of the obtained rational function gives:

$$G_D(s) = G_0 + \sum_{i=0}^{N} \left(\frac{g_i s}{1 + \frac{s}{p_i}}\right), \tag{1.78}$$

where, g_i are the residues given by (Eq. 1.66).

It can be seen that (Eq. 1.78) corresponds to the admittance of the Forster-type of 2^{nd} form as shown in (Fig. 1.9): The admittance of this network is given by:

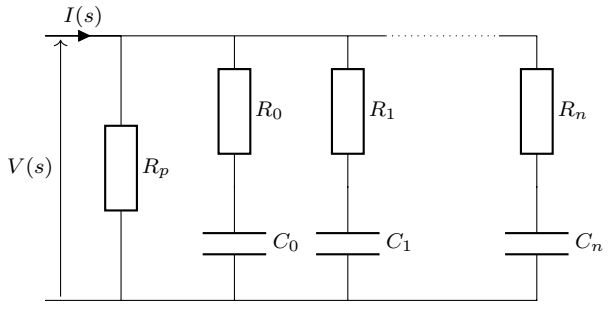

Figure 1.9 Equivalent network of a fractional derivative operator

$$Y(s) = \frac{1}{R_p} + \sum_{i=0}^{N} \left(\frac{C_i s}{1 + R_i C_i s} \right) , \tag{1.79}$$

From (Eq. 1.78) and (Eq. 1.79), and for $i = 1, 2, 3, ...N$, we can write

$$C_i = g_i , \quad R_i = \frac{1}{C_i g_i} \tag{1.80}$$

1.6.2 Digital Realization of Fractional Systems

Based on the definition of fractional calculus, the calculation of the output of a fractional system depends on the long-range history of the input. Because of the limitation of calculation speed and storage space, the digital realization of fractional systems is difficult. The commonly used methods of approximate digital realization of fractional systems are frequency domain methods and time domain methods. Currently both methods offer limited success in fitting the fractional system.

Frequency domain methods include Oustaloup method [102, 107], Carlson method [17], Matsuda method [87], and so on. Frequency-domain fitting techniques can fit the magnitude of the frequency response very well, but cannot guarantee the stable minimum-phase fitting. Time domain methods are mainly based on fitting the impulse response or the step response of the system. An effective time domain impulse response invariant discretization method was discussed in [23, 26, 27, 75]. There, a technique for designing discrete-time Infinite Impulse Response (IIR) filters to approximate the continuous-time fractional-order filters is proposed, keeping the impulse response of the continuous-time fractional-order filter and the impulse response of the approximate discrete-time filter almost the same.

1.7 Applications of Fractional Calculus

The concept of fractional calculus has great potential to change the way we see, model and analyze complex systems. We can say that ignoring fractional calculus is just like ignoring fractional, irrational or complex numbers. It provides good opportunity to researchers and engineers for revisiting the origins. The theoretical and practical interests of using fractional order operators are increasing. The application domain of fractional calculus is ranging from accurate modeling of the microbiological processes to the analysis of astronomical images. In the next section, we will present a brief review of applications of fractional calculus in various scientific and engineering disciplines.

1.7.1 Control Theory and Engineering

The accuracy and robustness of control systems are becoming imperative these days. The dynamic nature of control systems requires them to be modeled using the fractional calculus. In control engineering the concept of the fractional operations is mostly used in fractional system identification [47], biomimetic (bionics) control [28], feedback control systems [110], trajectory control of redundant manipulators [40], temperature control [112], Model Reference based adaptive control [149], passive vibrational control [93], fractional PI^{λ} controller [81] and fractional PD^{α} controllers [157].

1.7.2 Signal Processing

In the last decade, the use of fractional calculus in signal processing has tremendously increased. In signal processing, the fractional operators are used in the design of differentiator and integrator of fractional order [59], fractional order FIR differentiator [138], IIR type digital fractional order differentiator [85] and for modeling the speech signal [5]. A brief survey of application of fractional calculus in signal processing is presented in [25].

1.7.3 Image Processing

In image processing, fractional calculus (fractional differentiation) is used for enhancing image quality, image restoration and edge detection [85]. In particularly fractional calculus is used in satellite image classification [119] and astronomical image processing [132].

1.7.4 Electromagnetic Theory

The use of fractional calculus in electromagnetic theory has emerged in the last two decades. In 1998, Engheta [42] introduced the concept of fractional curl operators and this concept is extended by Naqvi [95]. Engheta's [41] work gave birth to the new field of research in Electromagnetics, namely, 'Fractional Paradigms in Electromagnetic Theory'. Nowadays fractional calculus is widely used in Electromagnetics to explore new results; for example, Faryad [43] used fractional calculus for the analysis of a Rectangular Waveguide.

1.7.5 Communication

Chaotic Communication and Chaos synchronization are becoming very popular nowadays. The concept of fractional calculus is recently introduced for secure chaotic communication and very satisfactory results have been achieved [58]. In [154], authors have used fractional calculus for informational network traffic modeling.

1.7.6 Probability Theory

G. Cottone used fractional operators for the probabilistic characterization of random variable and some remarkable results are discussed in [31].

1.7.7 Biology

In Biology, fractional calculus is used in neuron modeling [3], biophysical processes [39], modeling of complex dynamics of tissues [80], modeling of infectious diseases [33] etc.

1.8 Conclusion

The aim of this chapter is to present relevant literature to this research and to provide a theoretical framework. We essentially intended to make the researcher familiar with the main concepts of the fractional calculus (in both time and frequency domain) which is fundamental for the formal analysis of fractional-order linear time invariant systems, as well as the dynamical properties (stability, observability and controllability, time transient and steady-state responses, and frequency response) usually considered in classical control theory. With this aim, we have introduced two preliminary sections, the first devoted to the fundamental definitions of fractional-order operators in both time and Laplace domain, and the second to the analytical and numerical solutions of the fractional-order operators. Then, we have introduced two preliminary subsections, application of fractional calculus in control and applications of fractional calculus.

A more detailed treatment of fractional calculus can be, however, found in many books [89, 100, 113, 123].

Chapter 2

FRACTIONAL ORDER ROBUST CONTROL

This Chapter presents the fractional order robust control with an overview of the most popular fractional order robust controllers such as, CRONE controller and the fractional order $PI^{\lambda}D^{\mu}$ Controller. The well known Bode's ideal loop is also presented which is used next for the main contribution of this thesis.

2.1 Introduction

In the control theory, the ultimate objective is to develop a robust controller that shows satisfactory performance in the real operating environment where the plant shows different dynamic behavior than that of its model [84]. The interest for this type of characteristics has its origins in the seminal works of Bode [13] in 1945s. The main idea of these works was the robustness problem while designing a feedback amplifier insensitive to variations in the amplifier gain. To solve this problem, Bode has suggested an open loop transfer function $(\omega_{gc}/s)^{\gamma}$ where $1 < \gamma < 2$ and ω_{gc} is the gain crossover frequency, also called Bode's Ideal Transfer Function (BITF). Thus, the use of fractional calculus concepts in automatic control was begun with Bode. Manabe [83] attempted to use non-integer integral

and its application to control systems in the 1960s. Quantitative feedback theory [50] can be interpreted as fractional control, though its formulation does not refer explicitly to fractional derivation. However, the works of Oustaloup have really popularized fractional control. The author developed three generations of fractional order controller, known as CRONE control. Podlubny [115] proposed a fractional $PI^{\lambda}D^{\mu}$ controller and also proved that this controller structure is more suitable to regulate a fractional system in comparison to classical PID controller. Fractional $PI^{\lambda}D^{\mu}$ controllers was defined as a generalization of the classical PID, where the fractional orders λ and μ are supplementary tuning knobs used to improve the performances of the PID controller [140]. However, the ability of satisfying conflicting performance requirements is ensured at the cost of complexity in the selection of controller parameters. A good review of tuning and implementation methods for $PI^{\lambda}D^{\mu}$ as well as for other schemes of fractional order controller such as CRONE, TID, and fractional order lead-lag compensator can be found in [111]. Great number of publications have been proposed, mainly focused on techniques of fractional controllers tuning (see for example [91, 116, 11, 90, 142, 156, 145]). Though, in their comparative results the different authors insist on the interest of the parameters λ and μ, they do not present simple and general principles giving guidelines for the tuning of these parameters in order to satisfy conventional control design objectives, particularly robustness objectives.

Recently, Djouambi *et. al.*, [36] have proposed a simple technique to design fractional order controllers using the Bode's ideal transfer function as a reference model of the open-loop transfer function. However, the author assumes that the process must be minimum phase, stable and not oscillatory. Therefore, in this chapter, a generalization of the above method is proposed to the case where no assumptions on the stability and oscillatory conditions are needed for any minimum phase systems.

The remainder of this chapter consists of three main parts as follows.

Part 1 is dedicated to the study of properties of non-integer integration action and non-integer derivation action as well as the characteristics of BITF loop. The second part presents the principle results of CRONE control. In the third part, the BITF loop is used as a reference model to design a fractional order robust controller.

2.2 Characteristic of a Fractional Order Control System

In control theory, fractional order control was not until the resurgence of the study of the non-integer derivative operator, and the application of the fractional calculus in engineering [100]. In the early of nineties, the CRONE controller (see previous Section) was proposed to offer new solutions to control problems [108], such as robust performances; a constant maximum value of the unit-step closed-loop response. Often known as Iso-damping property, this property is independent of system steady state gain or pole/zero frequencies variations.

2.2.1 Concept of Iso-damping Using Fractional Order Controllers

The concept of having iso-damping property i.e., overshoot independent of the system gain has remarkable usage in the field of control science. This concept is only possible by the use of fractional order operators. For a linear system this relates to the fact that the open loop phase curve of the Bode plot is almost flat. Mathematically this implies that the derivative of the phase with respect to the frequency is zero at some specified frequency known as the tangent frequency ω_c. Thus, the iso-damping property can be mathematically written as,

$$\left.\frac{d\angle G\left(s\right)}{ds}\right|_{s=j\omega_c} = 0 \tag{2.1}$$

or alternatively as

$$\left.\angle\frac{dG(s)}{ds}\right|_{s=j\omega_c} = \left.\angle G(s)\right|_{s=j\omega_c} \tag{2.2}$$

When this condition is ensured, the Bode phase plot is locally flat implying that the system would be robust to variation in system gain [22].

2.2.2 Basic Fractional Order Control Actions

The effects of the basic control actions of type Ks^{μ} for $\mu \in [-1,\ 1]$ will be examined in this section. The basic control actions traditionally considered will be particular cases of this general case, in which:

1) Proportional action: μ=0,
2) Integral action: μ=-1,

3) Derivative action: μ=1.

The generalization to non-integer-orders of traditional controllers or control schemes translates into more tuning parameters and more adjustable time and frequency responses of the control system, allowing the fulfilment of robust performance.

2.2.2.1 Fractional integral action

The main effects of the integral actions can be summarized as follows,

- it makes the system response slower,
- decreases the system relative stability,
- eliminates the steady-state error for inputs for which the system had a finite error.

It is worth noting that effects of PID controller actions, as well as effects of fractional PID controller actions ($1/s^{\mu}$) with $\mu < 1$, are analyzed using complex plane, time domain and frequency domain methods. Let's consider the example with the closed loop system shown in (Fig. 2.1).

A. Complex plane analysis

In the complex plane, root locus of the system is displaced towards the right half plane after applying the integral action. Mathematically, the root locus of the system with control action is governed by,

$$1 + Ks^{\mu}G(s) = 0 \tag{2.3}$$

Its magnitude and phase can be given as,

$$|K| = \frac{1}{|s^{\mu}||G(s)|}$$

$$Arg[s^{\mu}G(s)] = (2n+1)\pi, \qquad n = 0, \mp 1, \mp 2, \ldots \tag{2.4}$$

$s = |s|e^{j\theta}$ can be written as,

$$s^{\mu} = |s|^{\mu}\, e^{j\mu\theta} \tag{2.5}$$

The conditions of phase can be further expressed as,

$$Arg[s^{\mu}G(s)] = Arg[G(s)] + \mu\theta = (2n+1)\pi, \qquad n = 0, \mp 1, \mp 2, \ldots \tag{2.6}$$

Therefore, it is obvious that, by choosing $\mu \in (-1, 0)$, the root locus is displaced towards the right half plane.

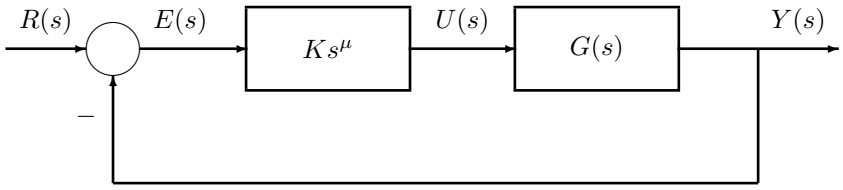

Figure 2.1 Fractional integral action $\mu \in (-1,\, 0)$

B. Frequency domain analysis

In frequency domain, a pole at zero adds $-20\,dB/dec$ in the magnitude curve and decreases the phase plot by $\pi/2\,rad$. The effect of fractional order integral is explained as follows.

The magnitude curve in the frequency domain is given as:

$$20\,log[s^{\mu}G(s)]_{s=j\omega} = 20\,log|G(j\omega)| + 20\mu\,log\omega, \tag{2.7}$$

and the phase plot is given by,

$$Arg[s^{\mu}G(s)]_{s=j\omega} = Arg|G(j\omega)| + \mu\,\frac{\pi}{2}, \tag{2.8}$$

Therefore, by varying the value of μ between -1 and 0, it is possible to introduce a constant increment in the slope of the magnitude curve by introducing a fractional order integrator, which varies between -20 and $0\,dB/dec$. Similarly, a constant delay in phase plot, which varies between $-\frac{\pi}{2}$ and $0\,rad$.

C. Time domain analysis

By introducing a fractional order integrator, there are clear cut effects over the transient response, which consists of the decrease in the rise time, increase of the settling time and the overshoot. Mathematically, these effects can be studied considering the error signal of the following form,

$$e(t) = \sum_{j=0}^{n} (-1)^j\, u_0(t - jT), \qquad n = 0,\, \mp 1,\, \mp 2, \ldots, n \tag{2.9}$$

where u_0 represents the unit step input. Its Laplace equivalent is given as,

$$E(s) = \sum_{j=0}^{n} (-1)^j \left(\frac{e^{-jTs}}{s} \right) \tag{2.10}$$

Therefore, the control action can be expressed as,

$$\begin{aligned} u(t) &= \mathcal{L}^{-1} \{U(s)\}, \\ &= K \sum_{j=0}^{n} (-1)^j \left(\frac{e^{-jTs}}{s^{1-\mu}} \right), \\ &= K \sum_{j=0}^{n} \frac{(-1)^j}{\Gamma(1-\mu)} (t - jT)^{-\mu} u_0(t - jT) \end{aligned} \tag{2.11}$$

It is clear that the control action over the error signal, vary between the effects of a proportional action $\mu = 0$ (square signal) and an integral action $\mu = -1$ (straight line curve). For the intermediate value of μ, the control action increases for a constant error, which results in the elimination of the steady state error and decrease when error is zero, resulting a more stable system.

2.2.2.2 Fractional derivative action

Same as fractional integral action, the derivative action of fractional order controller can be analyzed in complex domain, frequency domain and time domain. For example, consider the close loop system as shown in (Fig. 2.2).

A. Complex plane analysis

In the complex plane, root locus of the system is displaced towards the left half plane after applying the derivative action.

B. Frequency domain analysis

In frequency domain, a derivative action of a controller adds a slope of $+20\,dB/dec$ in the magnitude plot and adds $\pi/2\,rad$ in phase plot. Similarly, in its fractional counterpart, fractional derivative can add a slope of $0 - 20\,dB/dec$, when $\beta \in (0, 1)$ is varied. Similarly, a constant delay in phase plot, which varies between 0 and $\pi/2\,rad$.

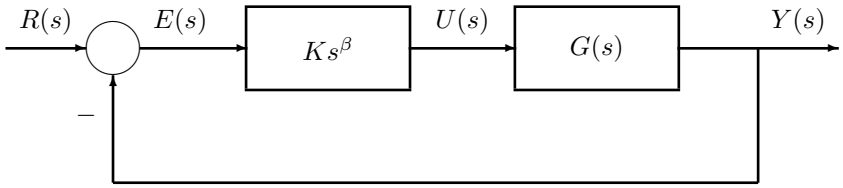

Figure 2.2 Fractional derivative action $\beta \in (1,\, 0)$

C. Time domain analysis

In the time domain, a decrease in the overshoot and the settling time is observed. This can be studied using the trapezoidal error signal given as,

$$e(t) = tu_0(t) - (t-T)\,u_0(t-T) - (t-2T)\,u_0(t-2T) + (t-3T)\,u_0(t-3T) \tag{2.12}$$

where u_0 is the unit step input. The Laplace transform of (Eq. 2.12) can be written as,

$$E(s) = \frac{1}{s^2} - \frac{e^{-Ts}}{s^2} - \frac{e^{-2Ts}}{s^2} + \frac{e^{-3Ts}}{s^2} \tag{2.13}$$

Therefore, the control action can be expressed as,

$$\begin{aligned} u(t) &= \mathcal{L}^{-1}\left\{U(s)\right\}, \\ &= \mathcal{L}^{-1}\left\{\frac{1}{s^{2-\beta}} - \frac{e^{-Ts}}{s^{2-\beta}} - \frac{e^{-2Ts}}{s^{2-\beta}} + \frac{e^{-3Ts}}{s^{2-\beta}}\right\}, \\ &= \frac{K}{\Gamma(2-\beta)}\left\{t^{1-\beta}\,u_0(t) - (t-T)^{1-\beta}\,u_0(t-T) - (t-2T)^{1-\beta}\,u_0(t-2T)\right\} \\ &+ \frac{K}{\Gamma(2-\beta)}\left\{(t-3T)^{1-\beta}\,u_0(t-3T)\right\} \end{aligned} \tag{2.14}$$

The effects of the fractional order control over the error signal vary between the effects of a proportional action $\beta = 0$ (trapezoidal signal) and a derivative action $\beta = 1$ (square signal).

2.2.3 Bode's Ideal Transfer Function

Bode, in his study on design of feedback amplifiers [13], has suggested an ideal shape of the open-loop transfer function $L(s)$ of the form,

$$L(s) = \left(\frac{\omega_c}{s}\right)^{\gamma} \tag{2.15}$$

for some $\gamma \in \mathbb{R}$, where ω_c is the gain cross-over frequency, that is, $|L(j\omega_c)| = 1$. The parameter γ determines both the slope of the magnitude curve on a *log-log* scale and the phase margin of the system, and may assume integer as well non-integer values. In fact, the transfer function $L(s)$ is a fractional-order transfer function for non-integer γ. The magnitude and phase of (Eq. 2.15) are,

$$\begin{cases} M_G(\omega) = \left(\frac{\omega_c}{s}\right)^{\gamma} \\ \Phi_G(\omega) = \angle G(j\omega) = -\gamma\frac{\pi}{2} \end{cases} \tag{2.16}$$

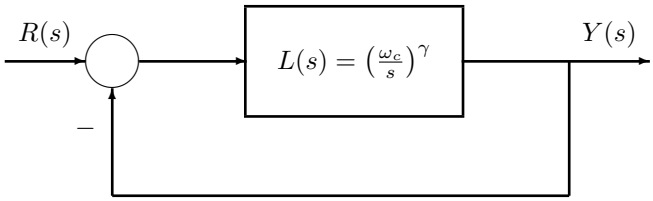

Figure 2.3 Bode's ideal loop diagram $L(s)$

Obviously, the amplitude curve is a straight line of constant slope $-20\gamma\, dB/dec$, and the phase curve is a horizontal line at $-\gamma\pi/2$ rad. The Nyquist curve consists, simply, of a straight line through the origin.

This choice of $L(s)$ gives a closed-loop system with the desirable property of being insensitive to gain changes ($Gain\, Margin = \infty$) and the phase margin of the system remains $\pi(1-\gamma/2)$ rad, independent of the gain. This is why closed loop system has a strongly robustness to gain variation.

Next, we study the step-response of the closed-loop system consist of the fractional order transfer function $L(s)$ given in (Eq. 2.15) with unity feedback,

$$T(s) = \frac{L(s)}{L(s)+1} = \frac{1}{1+\left(\frac{s}{\omega_c}\right)^{\gamma}} \tag{2.17}$$

We start by obtaining the unit step response of fractional-order transfer function $T(s)$. The output $y(t) = \mathcal{L}^{-1}[T(s)R(s)]$, when the input is a unit step $R(s) = 1/s$. Thus, the step-response would be,

$$y(t) = \mathcal{L}^{-1}\left\{\frac{\omega_c^{\gamma}}{s(\omega_c^{\gamma}+s^{\gamma})}\right\} = 1 - \sum_{n=0}^{\infty}\frac{[-(\omega_c t)^{\gamma}]^n}{\Gamma(1+\gamma\, n)} \tag{2.18}$$

which results in,

$$y(\infty) = \lim_{t\to\infty} y(t) = 1, \quad y(0^+) = \lim_{t\to 0^+} y(t) = 0.$$

Figure (2.4), shows the overshoot M_p, peak-time T_p, rise-time T_r, settling-time T_s, and the step-response of the fractional system $T(s)$ for $\omega_c = 1$ and different γ. Using these results and (Fig. 2.3), it is relatively easy to find suitable values ω_c and γ based on design specifications.

Now, let's consider a variation in the gain of the transfer function $T(s)$. For this reason, we consider $(\omega_c)^\gamma = A$ and (Eq. 2.17) can be rewritten as,

$$T(s) = \frac{L(s)}{L(s)+1} = \frac{A}{A+s^\gamma},$$

Therefore, in order to check the robustness of the closed-loop system $T(s)$, a variation in the nominal gain A is introduced as $\{0.1A,\ A,\ 10A\}$. Figure (2.5), illustrates the step responses of the system $T(s)$ for $\gamma = 1.5$ and different values of A.

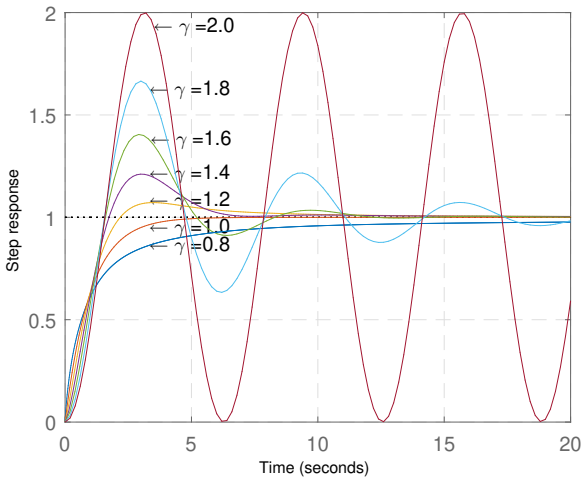

Figure 2.4 Time response characteristics of $T(s)$ for $\omega_c = 1$ and different γ

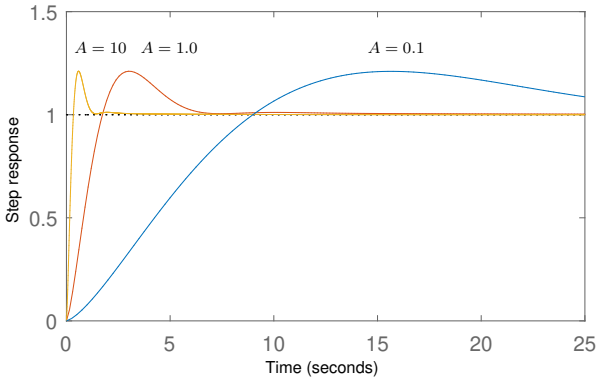

Figure 2.5 Time response characteristics of $T(s)$ for $\gamma = 1.5$ and different A

Motivated by the results of (Fig. 2.5) and the characteristics discussed in this subsection, the closed-loop of (Fig. 2.3), will be used as a reference model (in Section 2.5) to develop a new strategy for tuning of fractional controllers based on this fractional reference model.

2.3 CRONE Controller

CRONE being the French acronym of "Commande Robuste d'Ordre Non Entier" means robust control of non-integer order, represent the first framework for non-integer order operator application in the automatic control area. The CRONE through three generations, operates properties of this operator, with orders strictly real for first and second generations and complex orders for the third generation [102].

2.4 Fractional Order PI$^{\lambda}$D$^{\mu}$ Controller

The fractional order PID controller denoted by PI$^{\lambda}$D$^{\mu}$ [115], or FO-PID controller, where λ and μ are two additional parameters to the integral and the derivative components of the classical PID controller. The FO-PID controller provides a control effort $u(t)$ given by,

$$u(t) = k_p\, e(t) + k_i\, D^{-\lambda}\, e(t) + k_d\, D^{\mu}\, e(t), \qquad \lambda,\, \mu\, > 0, \tag{2.19}$$

The corresponding controller transfer function is defined as the ratio of the controller output $U(s)$ and error $E(s)$ as,

$$C(s) = \frac{U(s)}{E(s)} = \left(k_p + \frac{k_i}{s^{\lambda}} + k_d\, s^{\mu}\right), \tag{2.20}$$

where λ and μ are positive real numbers, k_p, k_i, k_d are the controller gains. For $\lambda = 1$ and $\mu = 1$, we obtain the classical PID controller. If $\lambda = 0$ ($k_i = 0$) we obtain a fractional PD$^{\mu}$. If $\mu = 0$ ($k_d = 0$) we obtain a fractional PI$^{\lambda}$. All these types of controllers are particular cases of the PI$^{\lambda}$ D$^{\mu}$. Figure (2.6), shows the parallel structure of a fractional order PID controller.

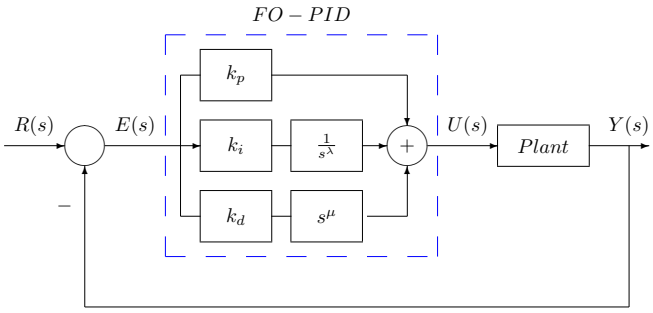

Figure 2.6 Parallel structure of FO-PID controller

It is quite natural to conclude that by introducing more general control actions of the form PI$^{\lambda}$ D$^{\mu}$, one could achieve more satisfactory performances between positive and negative effects of classical PID, and combining the fractional order actions one could develop more powerful and flexible design methods to satisfy the controlled system specifications. In other words, the generalization to non-integer-orders of traditional controllers or control schemes translates into more tuning parameters and more adjustable time and frequency responses of the control system, allowing the fulfilment of robust performance.

Another variant of fractional order PID controller is the FO[PID] controller may be used which uses only one integro-differential order parameter. The transfer function of the FO[PID] controller is given by [32]:

$$C(s) = \left(k_p + \frac{k_i}{s} + k_d\, s \right)^{\lambda}, \tag{2.21}$$

The FO-PID can be seen as a generalization of the PID controller from "points to a plane". Figure (2.7), shows the schematic representation of the PID and the FO-PID controller on the λ, μ plane. It is evident that the P, PI, PD and PID controllers are just four points on the plane and the FO-PID controller can have any value in the plane. Thus, the designer

essentially has a higher degree of freedom and can use these additional tuning knobs to fine tune his controller design for specific applications. Figure (2.8) shows the frequency response of this controller for the following values of (Tab. 2.1):

Table 2.1 Fractional PID vs PID controller parameters

Controller	Parameters				
	k_p	k_i	k_d	λ	μ
PID	1.0	1.0	1.0	1.0	1.0
FO-PID	1.0	1.0	1.0	0.8	0.8

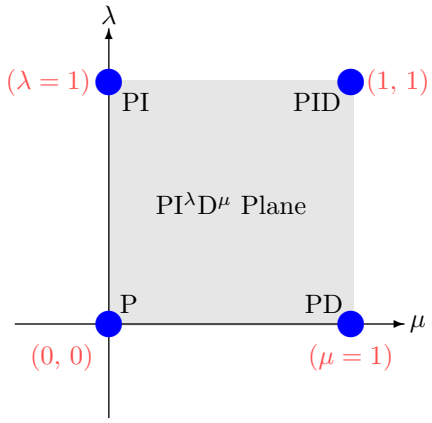

Figure 2.7 Generalization of the PID controller from point to plane

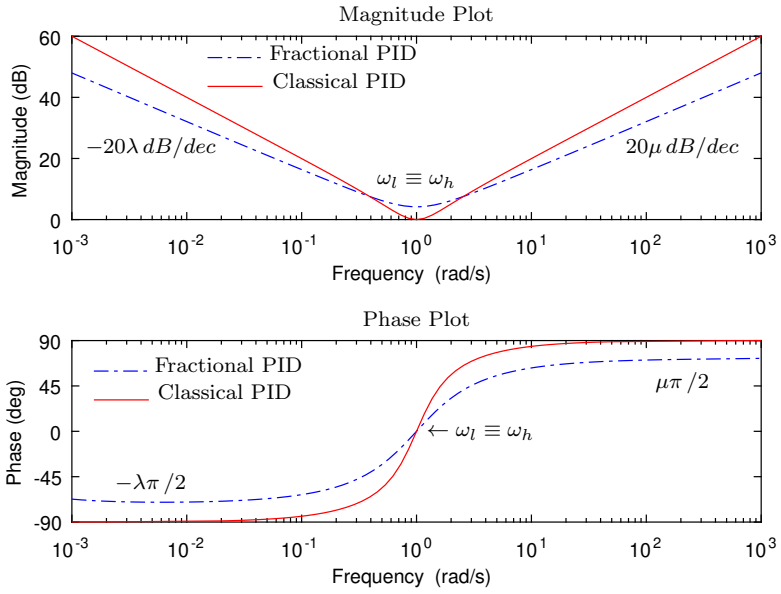

Figure 2.8 Frequency response of PID vs FO-PID controller

Tuning Methods for Fractional Order PID Controllers

The tuning methods for FO-PID controllers may be roughly divided into three categories [141]: empirical tuning rules, analytical methods, and optimization-based methods. Tuning rules are relations obtained empirically between the controller parameters and the plant model. A comprehensive review of tuning rules for Fractional Order PID Controllers may be found in [120].

Analytical methods consist of deriving analytically the controller parameters from the plant model. Most of the analytical methods applied in FO-PID controllers tuning are based on the Internal Model Control (IMC) method [121]. This is straightforward for fractional order plants [141], and adaptations of the IMC method may be employed for integer order plants, as in [77]. There are also methods based on the frequency domain (e.g., *Lanusse et al.,* in [72]).

Optimization-based methods consist of formulating the controller design as an optimization problem, in which the controller parameters are used as decision variables. One of the most popular optimization-based tuning methods available in the literature is the one proposed by [92]. There are also methods based on minimizing performance indices, like error integrals [155, 73]. Other authors combine both ideas [135, 124].

Since a FO-PID controller should only be used if it can outperform a conventional PID controller, it is necessary to use an optimization-based method [137], otherwise there would be no guarantee that the designed FO-PID provides better performance and robustness than some (possibly optimal) PID controller adjusted to meet the same criteria. Thus, the method proposed here is optimization-based.

2.5 Fractional Robust Controller Design Using Bode's Ideal Transfer Function

Frequency domain design of process controllers are popular since the robustness measures like gain and phase margins can easily be assigned with such a technique. Recently iso-damping in control system design has emerged due to the fact that the performance degradation needs to be considered with variation in system's gain and mere stability measures like gain margin is not sufficient. In this chapter, a new tuning technique for Fractional Order Controllers (FOC) based Bode's ideal transfer function as a reference model has been proposed with simulation examples so that the resulting closed-loop system has the desirable feature of being robust to gain variations with step responses exhibiting an iso-damping property for a range of system's gain while also meeting the user specified (desired) performances.

2.5.1 Control Design Structure

Let's consider the unity feedback system represented in (Fig. 2.9), where, $C(s)$ is the fractional order controller and $G_p(s)$ is a minimum phase plant.

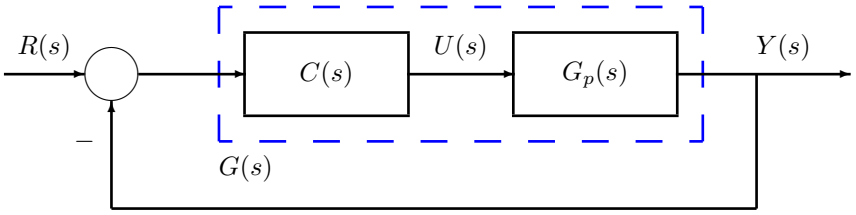

Figure 2.9 Closed loop control system

The open loop transfer function of the feedback control system of (Fig. 2.9) is given by,

$$G(s) = C(s) \times G_p(s)\,, \tag{2.22}$$

To ensure the iso-damping property for the control system, $G(s)$ must be close to the Bode's ideal transfer function (Eq. 2.15), as [144, 29].

$$G(s) \approx L(s) = \frac{1}{\left(\frac{s}{\omega_u}\right)^{\alpha}} \quad with\, 1 < \alpha < 2\,,\,, \tag{2.23}$$

The proposed tuning method consists of two steps [56]. In the first step, the open loop reference fractional integrator $L(s)$, after its design according to the desired control performances, must be approximated by a rational stable transfer function $L_a(s)$ using the Charef's approximation method presented in Section (1.4.1.2). The approximation $L_a(s)$ can be then given in the frequency band of interest $[\omega_c, \omega_{max}]$ by,

$$L_a(s) = L_0 \frac{\prod_{i=0}^{N-1} \left(1 + \frac{s}{z_i}\right)}{\prod_{i=0}^{N} \left(1 + \frac{s}{p_i}\right)}, \tag{2.24}$$

where,

$$N = Integer \left[\frac{\log(\frac{\omega_{max}}{p_0})}{\log(ab)}\right] + 1, \tag{2.25}$$

p_i and z_i $(i = 0, 1, \ldots N)$ are given by,

$$\begin{cases} p_i = p_0(ab)^i\,, & i = 0, 1, \ldots N \qquad \text{with } p_0 = \omega_c\sqrt{b} \\ z_i = z_0(ab)^i\,, & i = 0, 1, \ldots N-1 \qquad \text{with } z_0 = ap_0 \end{cases} \tag{2.26}$$

where

$$(p_i, z_i) \in (\mathbb{R}^+)^2,\ a = 10^{\left[\frac{y}{10(1-\alpha)}\right]} \text{ and, } b = 10^{\left[\frac{y}{10\alpha}\right]},$$

Let's write $L_a(s)$ as:

$$L_a(s) = \frac{L_Z(s)}{L_D(s)L_R(s)} \tag{2.27}$$

where,

$$L_Z(s) = L_0 \prod_{i=0}^{N-1} \left(1 + \frac{s}{z_i}\right),$$

$L_D(s)$ a polynomial representing some poles of $L_a(s)$ which will be used as the desired poles for plant pre-correction and $L_R(s)$ the polynomial of the remaining poles of $L_a(s)$.

In the second step, a standard pole placement technique (Fig. 2.10), is used to align the poles of the plant transfer function $G_p(s)$ with the desired stable poles $L_D(s)$ of the rational transfer function approximation $L_a(s)$. As a default choice, the closest poles to those of the plant can be considered.

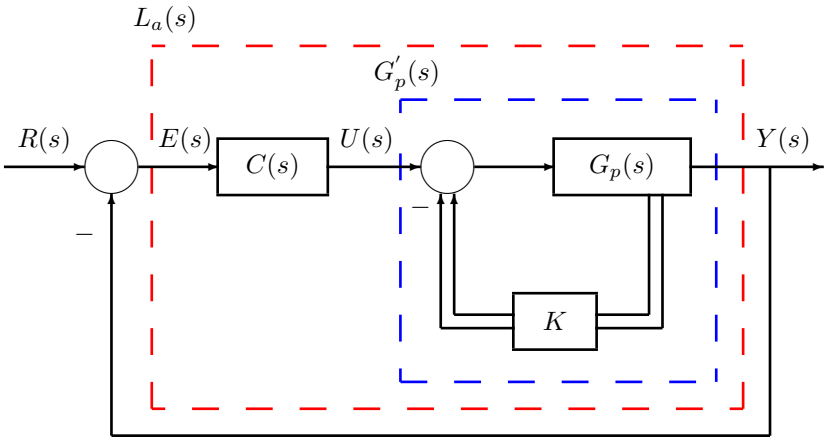

Figure 2.10 Closed loop control system with Pole Placement Algorithm

A pre-corrected stable plant $G'_p(s)$ will be then obtained where all its poles are part of those of the reference approximation $L_a(s)$. Thus, $G'_p(s)$ can be written as:

$$G'_p(s) = \frac{G'_{pz}(s)}{L_D(s)}, \tag{2.28}$$

Hence, the open loop of the control system can be then considered to be equal to the reference transfer function as,

$$C(s) \times G'_p(s) = L_a(s), \tag{2.29}$$

The transfer function of the FOC is then obtained as:

$$C(s) = \frac{L_a(s)}{G'_p(s)} = \frac{L_Z(s)}{L_R(s) \times G'_{pz}(s)}, \tag{2.30}$$

In this new conception method, $C(s)$ must be causal, this means that the relative degree N_r between the degree of the denominator and the degree of the numerator of $C(s)$ must be negative or equal to zero. If $C(s)$ is not causal, which corresponds to N_r positive then, at least N_r poles located outside the band $[\omega_c, \omega_{max}]$ can be added to $C(s)$ to guarantee its causality. The controller $C(s)$ will be then given by,

$$C(s) = \frac{L_Z(s)}{L_R(s) \times G'_{pz}(s)} \times \frac{1}{\prod_{i=0}^{N_r} \left(1 + \frac{s}{p_{ci}}\right)}, \tag{2.31}$$

where $p_{ci} = p_0(ab)^i,\ i = N+1, \ldots N_r$ with $p_0 = \omega_c\sqrt{b}$,

2.5.2 Illustrative Examples

Example 2.5.2.1

As a first example, let's consider the transfer function of the plant $G_p(s)$ given by [36],

$$G_p(s) = \frac{k_n(1+s/50)}{s(1+s)(1+s/10)(1+s/100)} \tag{2.32}$$

where $k_n = 1$ is the nominal value. The specifications of the control design are,

- Phase margin = 62°;
- Unity gain crossover frequency $\omega_u = 5\,rad/s$.

To achieve these specifications in a frequency range $[\omega_l, \omega_h] = [0.1\omega_u, 10\omega_u] = [0.5\,rad/s, 50\,rad/s]$ around ω_u, the open loop reference Bode's ideal function should be designed as (see Section 2.2.3),

$$L(s) = \frac{1}{(s/5)^{1.3}} \tag{2.33}$$

Using the Charef's method discussed above, $L(s)$ is approximated by,

$$\begin{aligned} L(s) \approx\ L_a = & \frac{1769.9(s+0.1456)(s+0.7543)(s+3.907)(s+20.24)}{(s+0.08891)(s+0.05)(s+0.4605)(s+2.385)(s+12.35)(s+63.99)} \\ & \times \frac{(s+104.8)(s+542.9)}{(s+331.4)(s+1717)} \end{aligned} \tag{2.34}$$

Using equation (Eq. 2.27), the poles of $L_a(s)$ that are close to the poles of the original process $G_p(s)$ are,

$$L_D(s) = (s+0.05)(s+0.4605)(s+12.35)(s+63.99) \tag{2.35}$$

and the remaining poles and zeros of the approximation $L_a(s)$ are,

$$\begin{aligned} \frac{L_Z(s)}{L_R(s)} = & \frac{1769.9(s+0.1456)(s+0.7543)(s+3.907)(s+20.24)(s+104.8)}{(s+0.08891)(s+2.385)(s+331.4)(s+1717)} \\ & \underline{(s+542.9)} \end{aligned} \tag{2.36}$$

Now, using the pole placement algorithm (state feedback $u = -Kx$), the process poles ($s = 0$, $s = -1$, $s = -10$ and $s = -100$) are adjusted to be aligned respectively with the

desired poles of the $L_D(s)(s = -0.05,\ s = -0.4605,\ s = -12.35,$ and $s = -63.99)$. Using the *MATLAB Control Toolbox* then, the state feedback gain matrix K can be obtained as,

$$K = [-34.1495\ \ -280.7289\ \ -594.8061\ 18.1961].$$

Hence, the new obtained transfer function of the adjusted process $G_p^{'}(s)$ is given as,

$$\begin{aligned} G_p^{'}(s) &= \frac{20(s+50)}{(s+0.05)(s+0.4605)(s+12.35)(s+63.99)} \\ &= \frac{20(s+50)}{L_D(s)} \end{aligned} \tag{2.37}$$

As we can see, the poles of the adjusted process $G_p^{'}(s)$ in the (Eq. 2.37) are now aligned and covered in the transfer function of $L_a(s)$ of the equation (Eq. 2.34). Thus, the controller's transfer function $C(s)$ can be obtained from equation (Eq. 2.30) as,

$$C(s) = \frac{L_a(s)}{G_p^{'}(s)} = \frac{L_Z(s)}{20(s+50)\ \times\ L_R(s)}, \tag{2.38}$$

$$C(s) = \frac{1769.9(s+0.1456)(s+0.754)(s+3.907)(s+20.24)(s+104.8)(s+542.9)}{20(s+50)(s+0.08891)(s+2.385)(s+331.4)(s+1717)}, \tag{2.39}$$

From (Eq. 2.39) we can see that $C(s)$ is not causal with $N_r = 1$. Thus, at least one pole should be added to the transfer function $C(s)$. Using (Eq. 2.31) the additional pole is, $s_r = p_0(ab)^9 = -8891$.

Finally, the proper controller transfer function is then given by

$$C(s) = \frac{1.5737e7(s+0.1456)(s+0.754)(s+3.907)(s+20.24)(s+104.8)(s+542.9)}{20(s+50)(s+0.08891)(s+2.385)(s+331.4)(s+1717)(s+8891)} \tag{2.40}$$

Figure (2.11) and (2.12) show the Bode plots of the original plant's transfer function $G_p(s)$, the adjusted plant's transfer function $G_p^{'}(s)$, the open loop transfer function $C(s) \times G_p^{'}(s)$, and the reference model $L_a(s)$. It can be seen that, in the given frequency band of interest $[0.5,\ 50]\, rad/s$, the phase curve of the open loop $C(s) \times G_p^{'}(s)$ overlaps the flat phase of the reference model $L_a(s)$ around the gain crossover frequency with a phase margin about 62°.

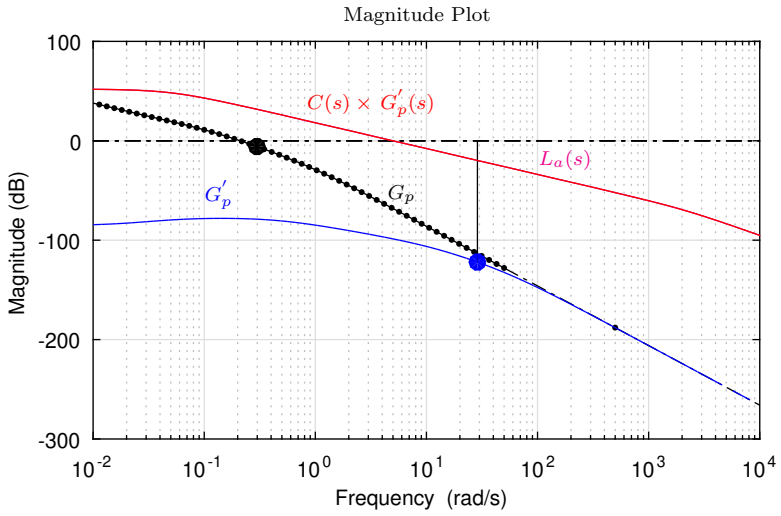

Figure 2.11 Magnitude plot of $G_p(s)$, $G_p'(s)$, $C(s) \times G_p'(s)$ and $L_a(s)$

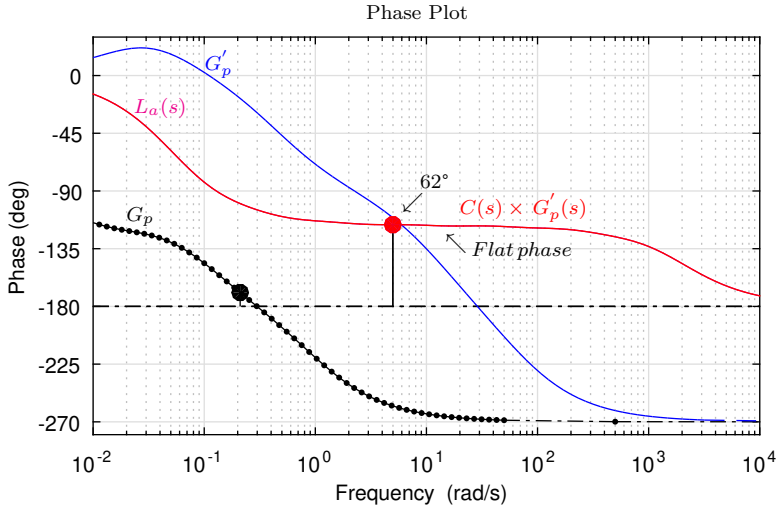

Figure 2.12 Phase plot of $G_p(s)$, $G_p'(s)$, $C(s) \times G_p'(s)$ and $L_a(s)$

In order to check the robustness of the control system, a variation in the nominal plant gain k_n is introduced as $\{0.5k_n, k_n, 1.5k_n\}$. The step responses are illustrated in (Fig. 2.13). The figure shows that the step responses are maintained in a constant overshoot (iso-damping property) in spite of the plant gain variations. From these observations, one can conclude that the designed controller, tuned by the proposed method, is robust against gain variations with an iso-damping property around the gain crossover frequency.

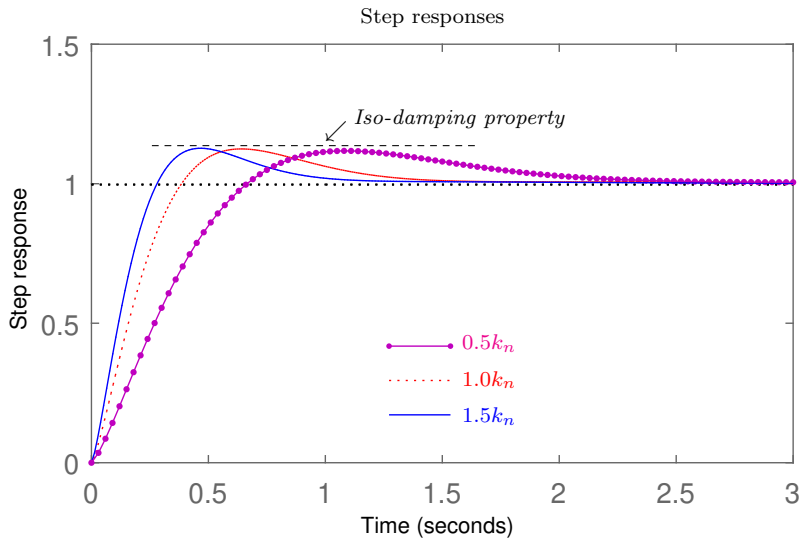

Figure 2.13 Step responses of the plant with a gain variation $\{0.5k_n, k_n, 1.5k_n\}$

Example 2.5.2.2

To more illustrate the effectiveness of the proposed tuning method, let's consider a pair of complex-conjugate poles system given by,

$$G_p(s) = \frac{k_n(s+2)}{s^2+2s+3}, \tag{2.41}$$

where $k_n = 1$ is the nominal value. The specifications of the design are,

- Phase margin = 55°;
- Unity gain crossover frequency $\omega_u = 3\,rad/s$.

To achieve these specifications in a frequency range $[\omega_l,\, \omega_h] = [0.3\,rad/s,\, 30\,rad/s]$ around ω_u, the open loop reference Bode's ideal function should be designed as,

$$L(s) = \frac{1}{(s/3)^{1.4}} \tag{2.42}$$

Using the Charef's method, $L(s)$ is approximated to,

$$\begin{aligned} L_a \approx & \frac{874.47(s+1948)(s+462)(s+109.6)(s+25.98)(s+6.161)(s+1.461)}{(s+4620)(s+1096)(s+259.8)(s+61.61)(s+14.61)(s+3.464)(s+0.0462)} \\ & \times \frac{(s+0.3464)(s+0.08215)}{(s+0.03)(s+0.1948)(s+0.8215)} \end{aligned} \tag{2.43}$$

Using (Eq. 2.27), the poles of $L_a(s)$ that are close to the poles of the original process $G_p(s)$ are,

$$L_D(s) = (s + 0.1948)(s + 0.8215) \tag{2.44}$$

and the remaining poles and zeros of the approximation $L_a(s)$ are,

$$\begin{aligned}\frac{L_Z(s)}{L_R(s)} = &\frac{874.47(s + 1948)(s + 462)(s + 109.6)(s + 25.98)(s + 6.161)(s + 1.461)}{(s + 4620)(s + 1096)(s + 259.8)(s + 61.61)(s + 14.61)(s + 3.464)} \\ &\times \frac{(s + 0.3464)(s + 0.08215)}{(s + 0.0462)(s + 0.03)}\end{aligned} \tag{2.45}$$

The transfer function $G_p^{'}(s)$ is,

$$G_p^{'}(s) = \frac{k_n(s + 2)}{(s + 0.1948)(s + 0.8215)} = \frac{k_n(s + 2)}{L_D(s)} \tag{2.46}$$

with the state feedback gain matrix $K = [-0.9837 \ -2.8400]$. Thus, the controller's transfer function $C(s)$ can be obtained from (Eq. 2.30) for $k_n = 1$ as

$$C(s) = \frac{L_a(s)}{G_p^{'}(s)} = \frac{L_Z(s)}{(s + 2)L_R(s)}, \tag{2.47}$$

Finally,

$$\begin{aligned}C(s) \approx &\frac{874.47(s + 1948)(s + 462)(s + 109.6)(s + 25.98)(s + 6.161)(s + 1.461)}{(s + 4620)(s + 1096)(s + 259.8)(s + 61.61)(s + 14.61)(s + 3.464)(s + 2)} \\ &\times \frac{(s + 0.3464)(s + 0.08215)}{(s + 0.0462)(s + 0.03)}\end{aligned} \tag{2.48}$$

Figure (2.14) and (2.15) shows the Bode plots of the adjusted plant's transfer function $G_p^{'}(s)$, the open loop transfer function $C(s) \times G_p^{'}(s)$, and the reference model $L_a(s)$.

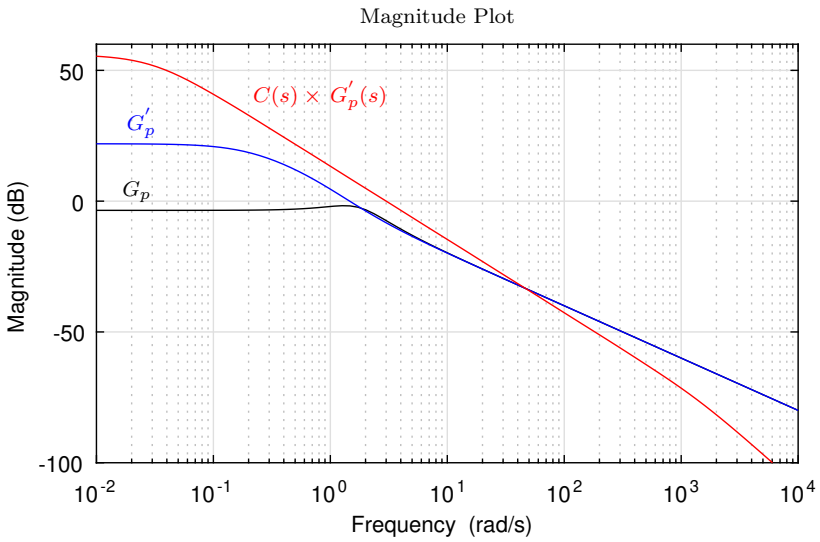

Figure 2.14 Magnitude plot of G_p, $G_p'(s)$, and $C(s) \times G_p'(s)$

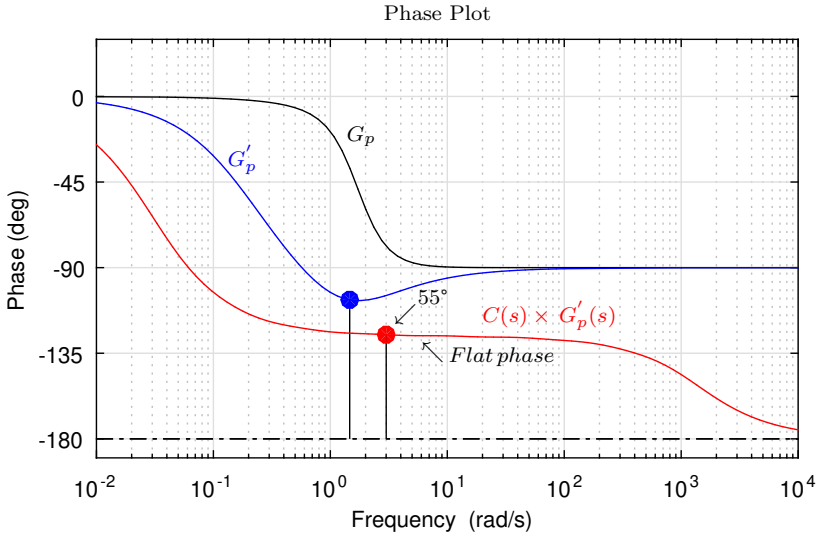

Figure 2.15 Phase plot of G_p, $G_p'(s)$, and $C(s) \times G_p'(s)$

In (Fig. 2.15), one can see that, in the given frequency band of interest $[0.3, 30]\, rad/s$, the phase curve of the open loop $C(s) \times G_p'(s)$ is flat around the gain crossover frequency and almost is about 55°.

In order to check the robustness of the control system, a variation of $\mp 50\,\%$ in the nominal gain k_n is introduced as $\{0.5k_n,\ k_n,\ 1.5k_n\}$. The step responses are shown in (Fig. 2.16).

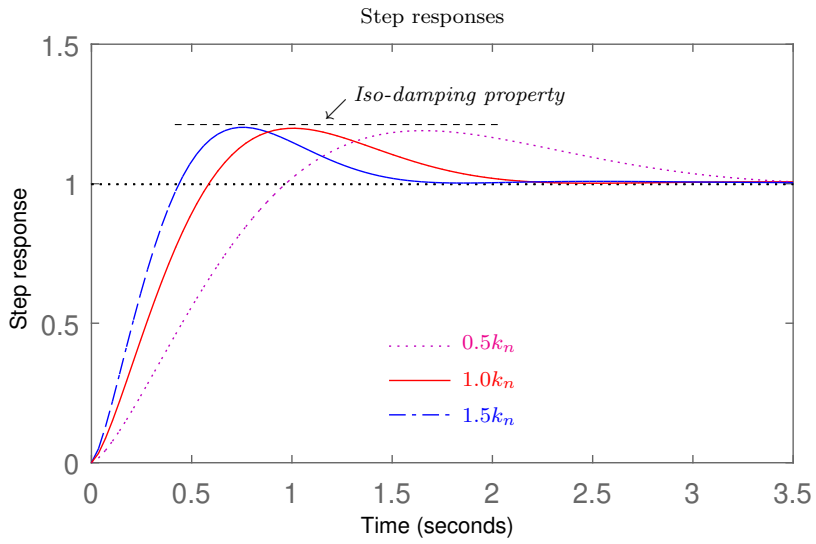

Figure 2.16 Step responses of the plant with a gain variation $\{0.5k_n, k_n, 1.5k_n\}$

The figure (2.16) shows that the step responses are maintained in a constant overshoot (iso-damping property) in spite of the plant gain variations. From these observations, one can conclude that the designed controller, tuned by the proposed method, makes the unity feedback control system robust to gain variations with an iso-damping property around the gain crossover frequency.

Example 2.5.2.3

Let's consider the transfer function of unstable plant $G_p(s)$ given by,

$$G_p(s) = \frac{k_n(s^2+1)}{s^2(s^2-1)-1} \tag{2.49}$$

where $k_n = 1$ is the nominal value. The specifications of the design are,

- Phase margin = 69°;

- Unity gain crossover frequency $\omega_u = 10\,rad/s$.

The plant poles are at $s = \pm 1.272$ and $\pm j0.7862$. The system is clearly unstable.

To achieve these specifications in a frequency range $[\omega_l, \omega_h] = [1\,rad/s, 100\,rad/s]$ around ω_u, the open loop reference Bode's ideal function should be designed as,

$$L(s) = \frac{1}{(s/10)^{1.23}} \tag{2.50}$$

Using the Charef's method, $L(s)$ is approximated to,

$$L_a(s) \approx \frac{11142(s+0.3318)(s+2.333)(s+16.4)(s+115.3)(s+810.6)}{(s+0.2119)(s+0.1)(s+1.49)(s+10.47)(s+73.62)(s+517.6)(s+3639)} \quad (2.51)$$

Using (Eq. 2.27), the poles of $L_a(s)$ that are close to the poles of the original process $G_p(s)$ are,

$$L_D(s) = (s+0.2119)(s+0.1)(s+1.49)(s+10.47) \quad (2.52)$$

and the remaining poles and zeros of the approximation $L_a(s)$ are,

$$\frac{L_Z(s)}{L_R(s)} = \frac{11142(s+0.3318)(s+2.333)(s+16.4)(s+115.3)(s+810.6)}{(s+73.62)(s+517.6)(s+3639)} \quad (2.53)$$

The transfer function $G_p^{'}(s)$ is,

$$G_p^{'}(s) = \frac{k_n(s^2+1)}{(s+0.2119)(s+0.1)(s+1.49)(s+10.47)} = \frac{k_n(s^2+1)}{L_D(s)} \quad (2.54)$$

with the state feedback gain matrix $K = [12.2719\ 20.3518\ 5.1192\ 1.3306]$. Thus, the controller's transfer function $C(s)$ can be obtained from (Eq. 2.30) for $k_n = 1$ as

$$C(s) = \frac{L_a(s)}{G_p^{'}(s)} = \frac{L_Z(s)}{(s^2+1)L_R(s)}, \quad (2.55)$$

Finally,

$$C(s) = \frac{11142(s+0.3318)(s+2.333)(s+16.4)(s+115.3)(s+810.6)}{(s^2+1)(s+73.62)(s+517.6)(s+3639)}, \quad (2.56)$$

Figure (2.17) and Figure (2.18) show the Bode plots of the adjusted plant's transfer function $G_p^{'}(s)$, the open loop transfer function $C(s) \times G_p^{'}(s)$, and the reference model $L_a(s)$.

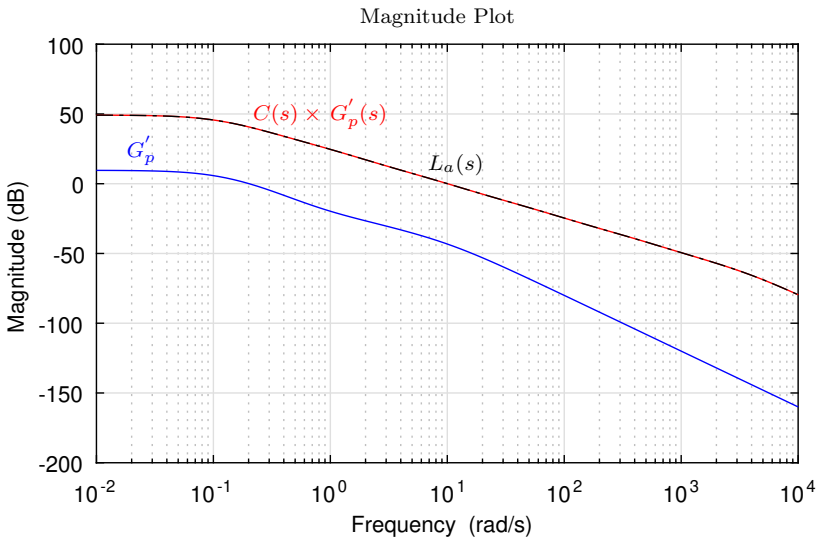

Figure 2.17 Magnitude plot of G_p, $G_p'(s)$, $C(s) \times G_p'(s)$ and $L_a(s)$

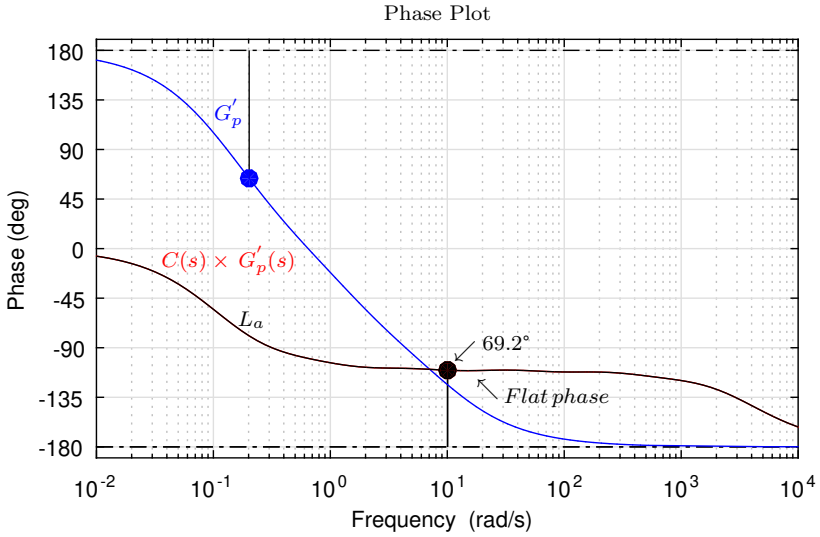

Figure 2.18 Phase plot of G_p, $G_p'(s)$, $C(s) \times G_p'(s)$ and $L_a(s)$

From the phase Bode plot shown in (Fig. 2.18), one can see that, in the given frequency band of interest $[1,\ 100]\, rad/s$, the phase curve of the open loop $C(s) \times G_p'(s)$ overlaps the flat phase of the reference model $L_a(s)$ around the gain crossover frequency and is about 69°.

In order to check the robustness of the control system, a variation of $\mp 50\,\%$ in the nominal gain k_n is introduced as $\{0.5k_n,\ k_n,\ 1.5k_n\}$. The step responses are illustrated in (Fig. 2.19).

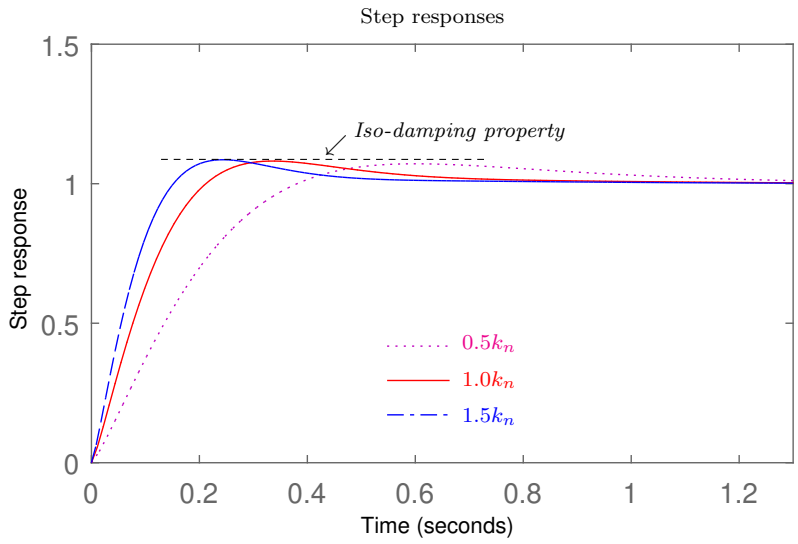

Figure 2.19 Step responses of the plant with a gain variation of $\{0.5k_n, k_n, 1.5k_n\}$

Figure (2.19) shows that the step responses are maintained in a constant overshoot (iso-damping property) in spite of the plant gain variations.

From these observations, one can conclude that the proposed controller, tuned by the proposed method, stabilizes the unity feedback control system and makes it robust against gain variations with an iso-damping property around the gain crossover frequency.

Example 2.5.2.4

In order to compare the effectiveness of the proposed method with the classical PID and the CRONE controller, let's consider the unity feedback control system of a DC motor whose transfer function $G_p(s)$ is given as [102],

$$G_p(s) = \frac{1}{\frac{s}{\omega_n}\left(1 + \frac{s}{\omega_0}\right)} \tag{2.57}$$

where $\omega_n = 16.98$ is the nominal natural frequency and $\omega_0 = 50$.
The specifications of the design are,

- Phase margin = 45°;

- Unity gain crossover frequency $\omega_u = 500\, rad/s$.

To achieve these specifications in a frequency range $[\omega_l,\, \omega_h] = [50\,rad/s,\, 5000\,rad/s]$ around ω_u, the open loop reference Bode's ideal function should be designed as (see Section 2.2.3),

$$L(s) \approx \frac{1}{(s/500)^{1.5}} \tag{2.58}$$

Thus, with the state feedback gain matrix $K = [-16.8800\ 140.6000]$, the controller's transfer function $C_{FOC}(s)$ can be obtained as,

$$\begin{aligned} C_{FOC}(s) \approx & \frac{3.4946 \times 10^6 (s+14.75)(s+59.53)(s+240.3)(s+970.2)(s+3917)}{849(s+6.844)(s+111.5)(s+450.3)(s+1818)(s+7339)} \\ & \times \frac{(s+1.581\times 10^4)(s+6.383\times 10^4)}{(s+2.963\times 10^4)(s+1.196\times 10^5)} \end{aligned} \tag{2.59}$$

The transfer functions of the CRONE and classical PID controllers, tuned to achieve the same specifications, are given respectively by [102]:

$$C_{CRONE}(s) = C_0 \frac{(1+s/z_1)(1+s/z_2)(1+s/z_3)(1+s/z_4)(1+s/z_5)}{(1+s/p_1)(1+s/p_2)(1+s/p_3)(1+s/p_4)(1+s/p_5)} \tag{2.60}$$

where,

$$\begin{aligned} & C_0 = 4.84; \\ & z_1 = 0.5495\,rd/s;\ z_2 = 2.747\,rd/s;\ z_3 = 13.783\,rd/s;\ z_4 = 68.692\,rd/s;\ z_5 = 343.46\,rd/s; \\ & p_1 = 1.9234\,rd/s;\ p_2 = 6.144\,rd/s;\ p_3 = 30.72\,rd/s;\ p_4 = 153.6\,rd/s;\ p_5 = 1202.1\,rd/s. \end{aligned}$$

$$C_{PID}(s) = C_0 \frac{(1+s/(z_1))(1+s/(z_2))}{(1+s/(p_1))(1+s/(p_2))} \tag{2.61}$$

where,

$$\begin{aligned} & C_0 = 728.7; \\ & z_1 = 4.0824\,rd/s;\ z_2 = 204.12\,rd/s; \\ & p_1 = 0.6804\,rd/s;\ p_2 = 1224.72\,rd/s; \end{aligned}$$

Figure (2.20) shows the Bode plots of the adjusted plant's transfer function $G_p^{'}(s)$ with the proposed controller $C_{FOC}(s) \times G_p^{'}(s)$ and the plant $G_p(s)$ with the $CRONE$ and the classical PID controller.

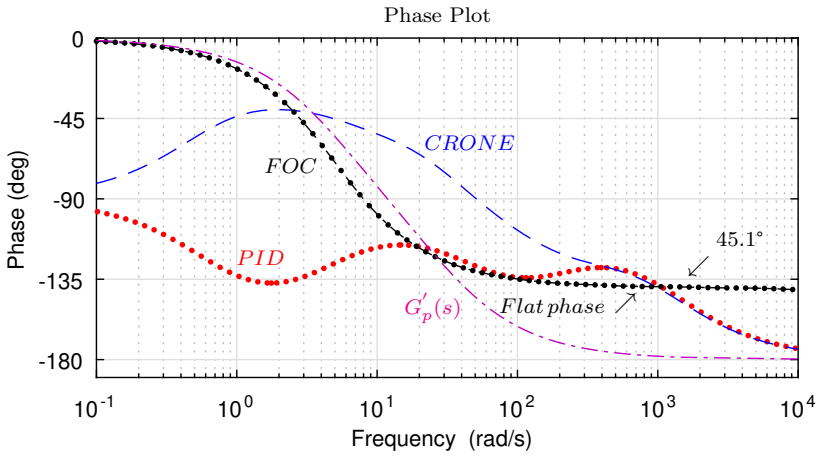

Figure 2.20 Phases Bode plot of the open loop transfer functions for each controller

From the phase Bode plot shown in (Fig. 2.20), one can see that in the given frequency band of interest, the proposed controller gives best phase flatness around the gain crossover frequency and is about 45°.

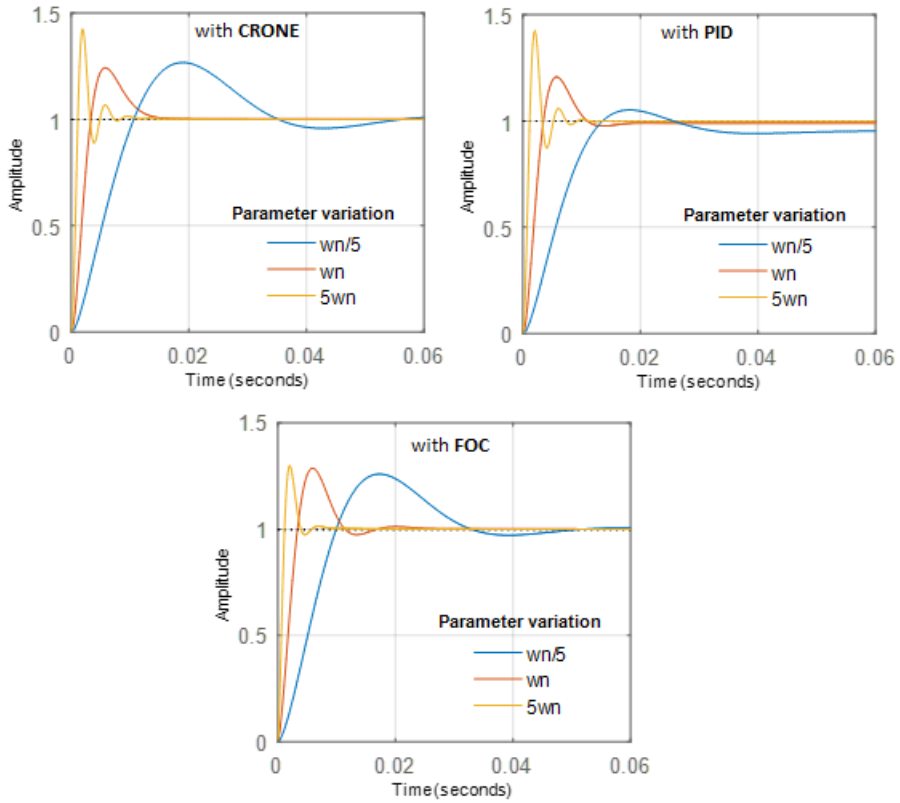

Figure 2.21 Step responses of the considered system for each controller

In order to check the robustness of the controlled system with the three controllers, a variation in the nominal parameter ω_n is introduced as $\{\omega_n/5,\ \omega_n,\ 5\omega_n\}$. The step responses are illustrated in (Fig. 2.21) for each controller.

From the closed loop responses plot shown in (Fig. 2.21), for different values of plant parameter ω_n one can remark that the proposed controller $C_{FOC}(s)$ gives the best robustness results versus plant parameter variations.

Example 2.5.2.5

Another comparative example is a first order plus time delay (FOPTD) plant whose transfer function $G_p(s)$ is given as [126],

$$G_p(s) = \frac{k_n\, e^{-0.01s}}{(0.4s+1)} \tag{2.62}$$

where $k_n = 1$ is the nominal value.

Three controllers are designed for the plant (Eq. 2.62), namely:

- a classical PI controller $C_1(s)$ designed in [126] based on analytical tuning method:

$$C_1(s) = 2.46369 + \left(\frac{33.06090}{s}\right), \tag{2.63}$$

- a fractional controller $C_2(s)$ tuned as in [15] using analytical design method based fractional reference model:

$$C_2(s) = 69.6041\,\frac{1}{s}\left(\frac{1}{s^{0.5}} + 0.4\,s^{0.5}\right), \tag{2.64}$$

- the proposed fractional controller $C_3(s)$ tuned as discussed in Section 2.5.1:

$$\begin{aligned} C_3(s) = {} & \frac{1778.3(s+1122)(s+281.8)(s+70.79)(s+17.78)(s+4.467)}{(s+2239)(s+562.3)(s+141.3)(s+35.48)(s+8.913)(s+0.5623)} \\ & \times \frac{(s+1.122)(s+0.2818)}{(s+0.1413)(s+0.1)} \end{aligned} \tag{2.65}$$

with state feedback gain matrix $K = [-0.2610]$.

The controllers $C_1(s)$, $C_2(s)$, and $C_3(s)$ are designed to satisfy the followings specifications,

- Unity gain frequency $\omega_c = 10\,rad/s$;
- Phase margin $\Phi_m = 45°$.

In order to check the robustness of the control system with the three controllers, a variation in the nominal plant gain k_n is introduced as $\{k_n/5,\ k_n,\ 5k_n\}$. The step responses are illustrated in (Fig. 2.22) for each controller.

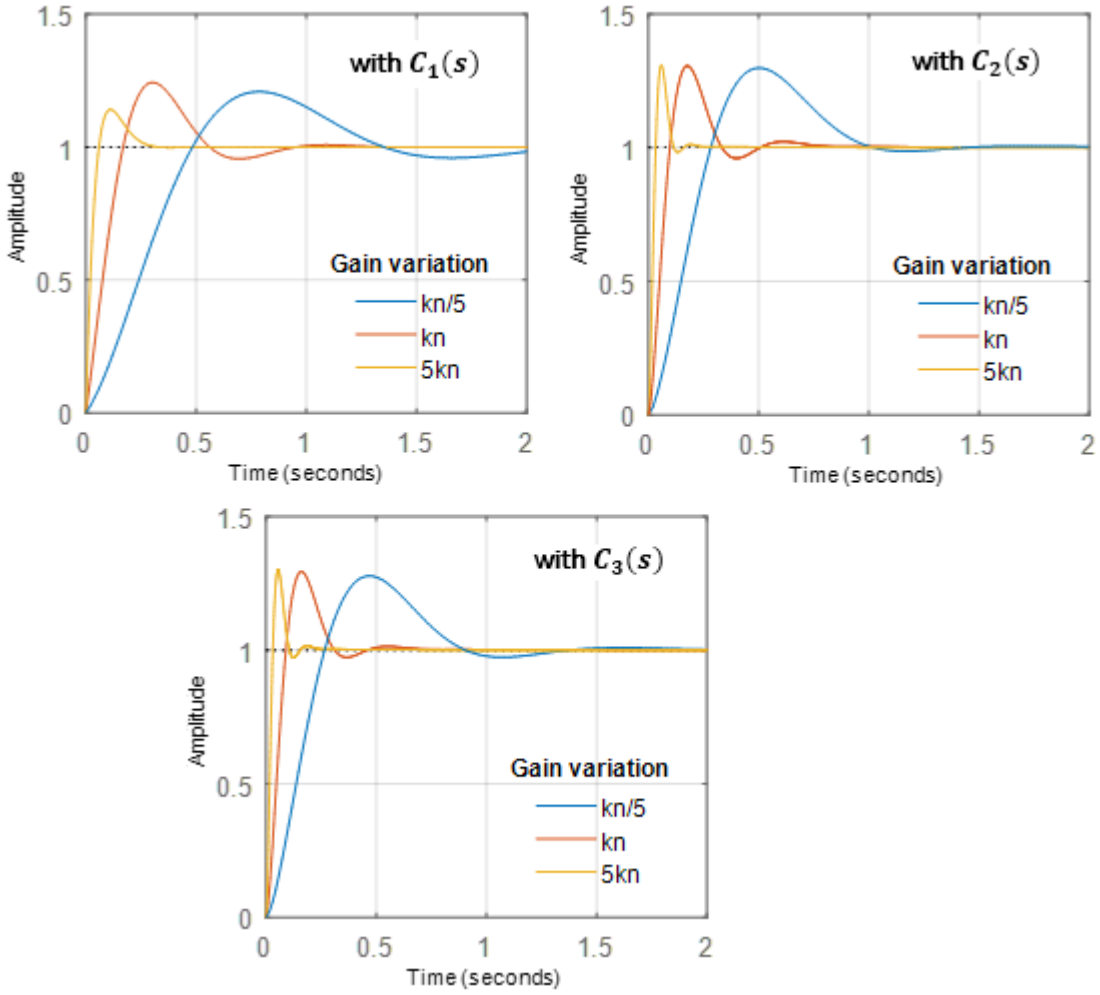

Figure 2.22 Step response of the considered system for each controller

From (Fig. 2.22), we see that the controller $C_1(s)$ gives poor performance, while in (Fig. 2.22) the controllers $C_2(s)$, and $C_3(s)$ ensure best results of iso-overshoot (iso-damping) property and relatively enhanced with $C_3(s)$ controller.

Table (2.5.2) shows performance comparison results of the controlled system using the Matlab command *"StepInfo"* with the three controllers, in which appears that the proposed controller is clearly the best one.

Table 2.2 Performance comparison of the control system with the three controllers with ($k_n = 1$)

Property	Controller		
	$C_1(s)$	$C_2(s)$	$C_3(s)$
Rise Time	0.1297	0.0702	0.0650
Settling Time	0.8462	0.6550	0.4015
Settling Min	0.9167	0.9051	0.9052
Settling Max	1.2430	1.3060	1.2934
Overshoot	24.296	30.604	29.393
Undershoot	0.000	0.000	0.000
Peak	1.2430	1.3060	1.2934
Peak Time	0.2978	0.1776	0.1601

In this section, a new simple and useful tuning technique of fractional order controllers (FOC) has been proposed to achieve user-specified gain and phase margins using the so-called Bode's ideal transfer function as a reference model. The basis of this method is to use a standard pole placement technique to align each pole of the plant transfer function with the nearest one given by the Rational Transfer Function Approximation (RTFA) of the fractional order integrator. The set of the aligned poles are then removed from the RTFA. The transfer function of the FOC is then obtained by multiplying the remaining poles of the RTFA with the inverse of the zeros of the plant transfer function. This inverse imposes that the system must be a minimum phase. Simulations results show that the proposed method is simple, effective, can ensures the iso-damping property for the control system and can be investigated to cover processes that have complex-conjugate poles or unstable conditions.

2.6 Design of PI$^{\lambda}$ Using Bode's Integrals Based Online Estimation Algorithm

The fractional-order proportional-integral-derivative controller denoted by PI$^{\lambda}$D$^{\mu}$, is a generalization of the classical PID controller, where λ and μ are two additional parameters related to its integral and derivative components. In general form, the transfer function of PI$^{\lambda}$D$^{\mu}$ is given by [32]:

$$C(s) = k_p + \frac{k_i}{s^{\lambda}} + k_d s^{\mu} \tag{2.66}$$

As it was mentioned in the Section 2.4, for $\mu = 0\,(k_d = 0)$, the fractional controller (Eq. 2.66) is reduced to PI$^{\lambda}$, with a transfer function of the form,

$$C(s) = k_p + \frac{k_i}{s^{\lambda}} \tag{2.67}$$

The transfer function (Eq. 2.67) is known as fractional order PI controller, a particular case of (Eq. 2.66).

Motivated by the remarkable characteristic performance in terms of robustness and the numerous methods proposed for synthesis and control design of the PI$^{\lambda}$D$^{\mu}$ controllers, sometimes called Non-Integer Order PID, in this section, we propose a recursive tuning technique of the reduced controller (Eq. 2.67) in the time domain using the Bode's ideal loop as a reference model for a first order process.

2.6.1 Synthesis Algorithm of Non-Integer Order PI

Consider the unity negative feedback control scheme shown in (Fig. 2.23),

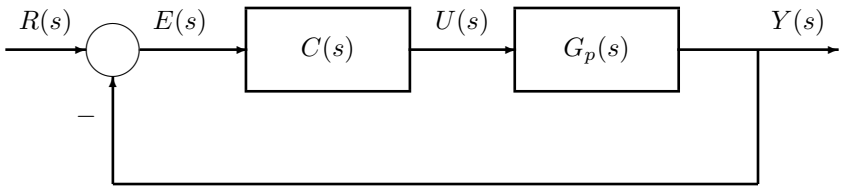

Figure 2.23 Closed-loop control system

where, $G_p(s)$ is the process transfer function and $C(s)$ is an FO-PI controller which is used to achieve the desired closed-loop transfer function. Consider $G_p(s)$ as a first order process without time delay with the transfer function,

$$G_p(s) = \frac{k_c}{(\tau\, s + 1)} \tag{2.68}$$

2.6.1.1 Tuning of the Non-Integer Order λ

According to the structure shown in (Fig. 2.23), the nominal open-loop transfer function is obtained as,

$$\frac{Y(s)}{E(s)} = C(s) \times G_p(s) \tag{2.69}$$

If the considered controller is given by (Eq. 2.67) for the process (Eq. 2.68). Then, (Eq. 2.69) can be written as:

$$\frac{Y(s)}{E(s)} = \frac{k_c \left(k_p\, s^{\lambda} + k_i\right)}{s^{\lambda}(\tau\, s + 1)} \tag{2.70}$$

The design of the PI$^{\lambda}$ controller adapted to the problem discussed here is based on solving an optimization problem using the recursive least squares algorithm extended to non-integer orders [34, 38]. A time domain method using Bode's ideal transfer function (Eq. 2.15) is used to estimate the controller coefficients k_p, and k_i (see next Section). The fractional order λ of the integral action is tuned based on ISE minimization between the desired step response, produced by a fractional-order transfer (BITF), and the step response of the system with the PI$^{\lambda}$ controller.

The setting of the two parameters μ and ω_u of the Bode's ideal loop (Eq. 2.15) is carried out according to the desired performances. Data of the identification are obtained by a simulation in time domain of the Bode's ideal loop excited by a Pseudo-Random Binary Sequence (PRBS).

2.6.1.2 Online Estimation of the Parameters k_p, and k_i

According to the structure shown in (Fig. 2.23), the nominal closed-loop transfer function is obtained as,

$$\frac{Y(s)}{R(s)} = \frac{C(s)G_p(s)}{1 + C(s)G_p(s)} \tag{2.71}$$

Then, resulting in:

$$\frac{Y(s)}{R(s)} = \frac{k_c \left(k_p\, s^{\lambda} + k_i\right)}{s^{\lambda}(\tau\, s + 1) + k_c \left(k_p\, s^{\lambda} + k_i\right)} \tag{2.72}$$

The non-integer order differential equation corresponding to (Eq. 2.72) can be expressed as,

$$\tau\, \frac{d^{\lambda+1} y(t)}{dt^{\lambda+1}} + \frac{d^{\lambda} y(t)}{dt^{\lambda}} = k_c\, k_i \left(r(t) - y(t)\right) + k_c\, k_p \frac{d^{\lambda}\left(r(t) - y(t)\right)}{dt^{\lambda}} \tag{2.73}$$

A matrix form of (Eq. 2.73) can be given by:

$$Y(t,\theta) = \tau\, \frac{d^{\lambda+1} y(t)}{dt^{\lambda+1}} + \frac{d^{\lambda} y(t)}{dt^{\lambda}} = \theta(t)\, \phi^{T}(t) \tag{2.74}$$

where,

$$\theta^{T}(t) = [k_i,\ k_p] \tag{2.75}$$

and,

$$\phi(t) = k_c \begin{bmatrix} (r(t) - y(t)) \\ \frac{d^{\lambda}(r(t) - y(t))}{dt^{\lambda}} \end{bmatrix} \tag{2.76}$$

The numerical evaluation of $\phi(t)$ is achieved using the Grünwald-Letnikov approximation of a non-integer derivative defined by [89],

$$\begin{aligned} {}_{a}D_{t}^{\alpha} y(t) &\approx \frac{1}{h^{\alpha}} \sum_{k=0}^{N} (-1)^{k} \binom{\alpha}{k} y(t - kh) \\ N &= Integer \left[\frac{(t-a)}{h}\right], \\ \binom{\alpha}{k} &= \frac{\alpha(\alpha-1)\ldots(\alpha-k+1)}{k!} \end{aligned} \tag{2.77}$$

Knowing that h is the sampling step, and the variable α is a real number. Thus, the sampled vector $\phi(K)$ can be given, at a moment K, by:

$$\phi(K) = k_c \begin{bmatrix} (r(t) - y(t)) \\ \frac{1}{h^{1}} \sum_{k=0}^{N} (-1)^{k} \binom{1}{k} \left(r(K-k) - y(K-k)\right) \end{bmatrix} \tag{2.78}$$

The estimation of parameters vector θ can be obtained by minimizing the quadratic criterion of least squares based on the equation error, defined by:

$$J_t(\hat{\theta}) = \frac{1}{K} \sum_{k=0}^{N} \left[Y(k) - \hat{Y}(k,\hat{\theta})\right]^{2} \tag{2.79}$$

where,

$$Y(k) = \frac{\tau}{h^\alpha}\sum_{k=0}^{K}(-1)^k\binom{\alpha+\lambda}{k}y(K-k) + \frac{1}{h^\alpha}\sum_{k=0}^{K}(-1)^k\binom{\alpha}{k}y(K-k) \tag{2.80}$$

$y(k)$ is the time domain output of the Bode's ideal loop (BIL) excited by an input of PRBS type and $\hat{Y}(k,\hat{\theta}) = \hat{\theta}(k)\hat{\phi}^T(k)$. The principle of this technique can be summarized by the block diagram of (Fig. 2.24), whose the block B.I.L represents the Bode's Ideal Loop and the block P.A.A represents the Parametric Adaptation Algorithm.

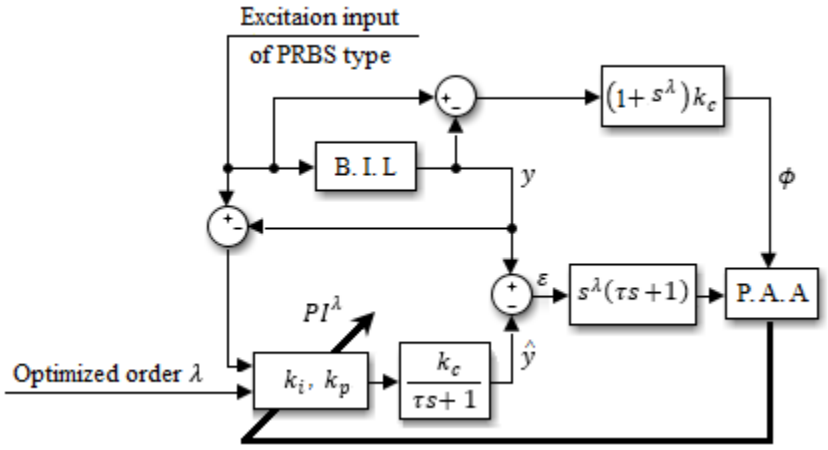

Figure 2.24 Unity-feedback control system with PI$^\lambda$ controller

Thus, using the recursive least squares algorithm [107], the parameters vector $\hat{\theta}(k)$ estimated at time $t = Kh$ can be given by,

$$\begin{cases} \hat{\theta}(K) &= \hat{\theta}(K-1) + \dfrac{F(K-1)\phi(K)}{1+\phi^T(K)F(K-1)\phi(K)}er(k) \\ F(K) &= F(K-1) - \dfrac{F(K-1)\phi(K)\phi^T(K)F(K-1)}{1+\phi^T(K)F(K-1)\phi(K)} \\ er(k) &= Y(K) - \hat{\theta}^T(K-1)\phi(K) \end{cases} \tag{2.81}$$

with $F(0) = \frac{1}{0.001}I$ and $\hat{\theta}^T(0) = \left[\hat{k}_p(0),\ \hat{k}_i(0),\ \right] = [0,\ 0]$

2.6.2 Illustrative Example

This section presents a descriptive example of parameters determination of a unity feedback PI$^\lambda$ controller using the discussed method in the previous section, as well as a comparative analysis of robustness with integer order PI to ensure the same specifications.

Consider a continuous time transfer function relating the speed of a motor armature to the input voltage [30],

$$G(s) = \frac{k}{(1.45\,s + 1)} \quad k_n = 0.25 \text{ (nominal value)} \tag{2.82}$$

The imposed frequency domain specifications of the control are, $\omega_c = 1.5$ and $\varphi_m = 60°$. These specifications mean that a transitional frequency at unity gain of $\omega_u = 1.5\ rad/s$ in a frequency band:

$$[\omega_l,\ \omega_h] = [0.1\omega_u,\ 10\omega_u] = [0.15\ rad/s,\ 15\ rad/s]$$

To ensure these specifications around ω_u, the Bode's ideal transfer function (open-loop of the model) must be[11],

$$L(s) = \left(\frac{1}{s/\omega_\mu}\right)^\mu = \left(\frac{1}{s/1.5}\right)^\mu \tag{2.83}$$

where,

$$\mu = 2\left(1 - \frac{\varphi_m}{\pi}\right) = 1.33$$

For different values of $\lambda = [0.8 - 1.4]$, the corresponding parameters k_p, and k_i can be calculated using the recursive least squares algorithm proposed in the previous section.

Figure (2.25) shows the plant step responses using different values of $\lambda = [0.8 - 1.4]$ with the corresponding k_p, and k_i values. The case $\lambda = 1.0$ corresponds to the integer order PI controller.

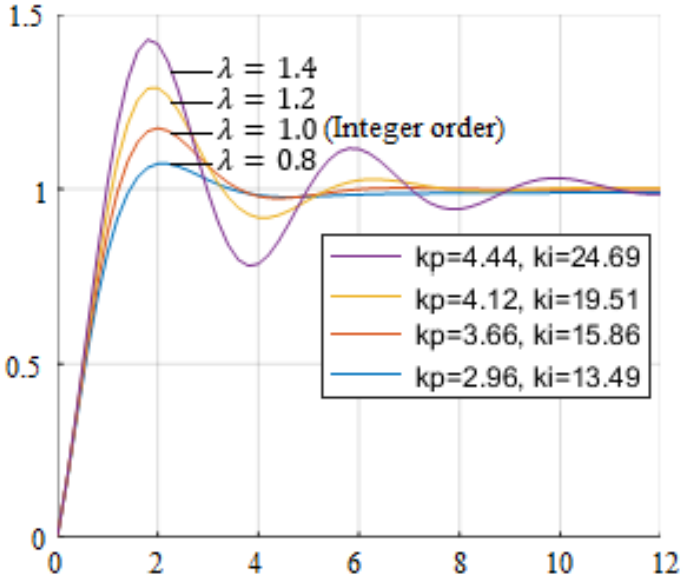

Figure 2.25 Step response for different values of λ=[0.8 1.0 1.2 1.4]

To design a fractional controller PI$^{\lambda}$ for the physical plant (Eq. 2.82), the parameter λ is set to 1.168, with the initialization:

$$F(0) = \frac{1}{10^{-4}} I$$

and, $\hat{\theta}^T(0) = \left[\hat{k}_p(0),\ \hat{k}_i(0)\right] = [0,\ 0]$.
The established values of the parameters k_p, and k_i are then,

$$k_p = 3.9548, \text{ and } k_i = 16.6233.$$

Thus, the obtained transfer function of the fractional order controller PI$^{\lambda}$ is,

$$C_{FOPI}(s) = \left(3.9548 + \frac{16.6233}{s^{1.168}}\right), \tag{2.84}$$

Figure (2.26) shows the estimation evolution of the parameters k_p, and k_i.

The choice of λ equal to $1,168$ is justified by minimization of a performance indice criterion. The ISE (Integral Square Error) is chosen as performance measure since it is one of the most commonly used for tuning of PID controller.

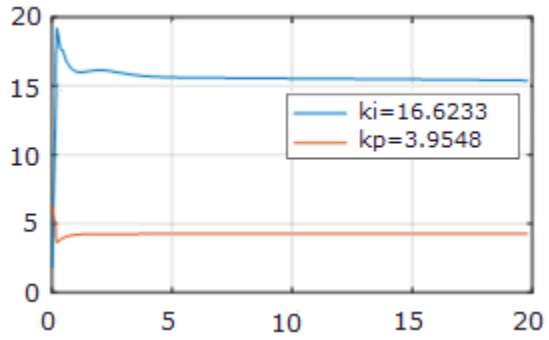

Figure 2.26 Evolution of parametric estimation as a function of time.

For the robust performance test, the plant gain is considered changing with a variation range of $k = [0.25/2,\ 0.25,\ 0.25 \times 2]$, the nominal gain value is $k = 0.25$.

The step responses for different values of k are illustrated in (Fig. 2.27). The parameter λ is set to 1.1 which gives satisfactory robustness against gain variation.

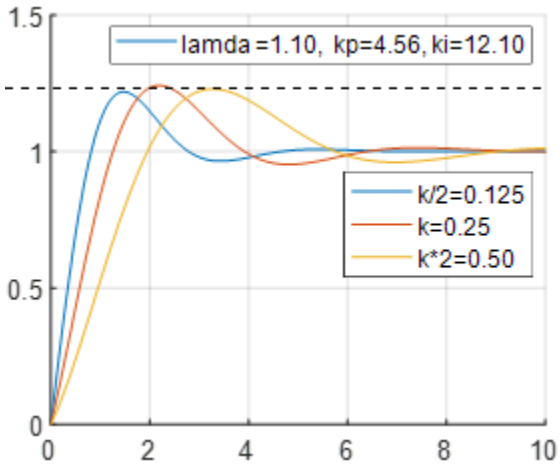

Figure 2.27 Step responses of the controlled system for different values of k

Figure (2.27) exhibits an iso-damping property. This means that the control system with the designed fractional order (PI$^{\lambda}$) controller is robust to gain variations.

The transfer function of the classical PI controller obtained by setting $\lambda = 1.0$ integer case (proposed control) to ensures the same specifications is given by,

$$C_{PI}(s) = \left(3.8215 + \frac{11.4411}{s}\right), \tag{2.85}$$

Figure (2.28) illustrates the step responses with $\lambda = 1.0$ and $k = [0.25/2,\ 0.25,\ 0.25 \times 2]$.

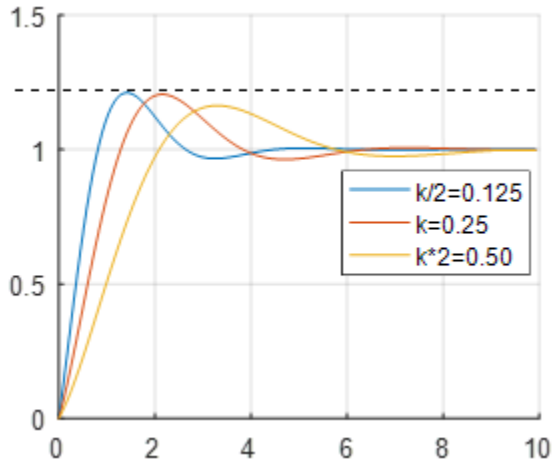

Figure 2.28 Plant step responses for different values of k and $\lambda = 1.0$ (integer case)

From this figure we see that the designed integer PI controller provides poor performances.

In order to have a realistic form of the fractional controller given in (Eq. 2.84), an approximation of non-integer integration operator is obtained by a stable and achievable filters presented in [107].

In this section, a simple technique is presented to determine fractional order PI controller parameters using Bode's Ideal Transfer Function (BITF). The BITF is used as the reference model. After having fixed the parameters (μ and ω_{μ}) of the BITF according to the desired performances, the order of the integration in PI$^{\lambda}$ controller is tuned freely until satisfactory performances. The controller coefficients are then estimated online using the Bode's ideal loop as a reference model. The unit step response of the controlled system was obtained as having the same characteristic as the BITF. The success of the presented method is demonstrated by a simulation example.

2.7 Conclusion

The fractional order robust control has become more and more interesting, the motivation for a such control comes from the consideration of using the idea of "constant phase" of the open loop transfer function around the transitional frequency at unity gain. For this idea, the so-called Bode's ideal function can be used as reference model for the open loop of the control system. Once the Bode's ideal function parameters are set according to the desired performances, the feedback control system is robust against the variation in gain, the step response of the controlled system exhibits an iso-damping property and the control strategy is said fractional order robust control. In this chapter, two new techniques have been developed to obtain step responses as having the same characteristic as the Bode's ideal transfer function.

- The first technique is based on a pre-compensation of the plant using a standard pole placement algorithm, thus, each pole of the plant transfer function is aligned with some poles in the Rational Approximation (RA) of the reference model and the transfer function of the fractional order controller is then obtained by gathering the remained poles and zeros of the RA. The most innovative character of the proposed method is its simplicity and its remarkable performances in terms of robustness towards the variation of the static gain. Simulation of some illustrative examples confirms and validates the proposed method,

- The second technique is based on a fractional PI controller where its coefficients are estimated recursively in the time domain using the Bode's ideal loop as a reference model. The order of the integration in PI^{λ} controller is tuned freely until satisfactory response. We showed, by an example of simulation, that the robustness against the gain variations accomplished by the fractional order PI^{λ} controller is clearly better than that of integer order PI controller.

Chapter 3

FRACTIONAL ORDER ADAPTIVE ROBUST CONTROL

This Chapter considers robustness criteria in plant parameter changes case by exploring the adaptive control design using fractional order operators.

3.1 Introduction

Adaptive control is an active field in the design of control systems to deal with systems with unknown constant or slowly time-varying parameters. The basic idea of adaptive control is to employ a parameter adaptation scheme to estimate those unknown parameters and replace the unknown parameters in the feedback controller with their estimates. Adaptive control is essentially nonlinear control due to the involvement of dynamic parameter adaptive law, no matter it is applied to linear systems or nonlinear systems. The key difference between adaptive controllers and linear controllers is the adaptive controller's ability to adjust itself to handle unknown model uncertainties. More detailed overviews of adaptive control are given by M'Saad [76], and Najim [94].

Adaptive control is roughly divided into two categories: direct and indirect.

- In the indirect approach, the parameters of the plant model are estimated online and

use the estimated model information to adjust the controller. These controllers are referred to as self-tuning controllers,

- In the second approach (direct), the plant model is reparametrized in terms of the controller parameters. This allows the controller parameters to be estimated directly. This parametrization is possible using the minimum variance or model reference control method.

In this work, direct MRAC method is considered, where the only updated parameters are those of the controller.

However, in a number of cases, related to the desired control objectives and structure of the plant model, the important question is to know in which case it is necessary to opt for an adaptive control? In control theory dealing with adaptive control, there are several cases in which fixed-gain controllers can give the same performance as adaptive controllers. Figure (Fig. 3.1) illustrates a way of proceeding to choose between adaptive controllers and fixed-gain controllers.

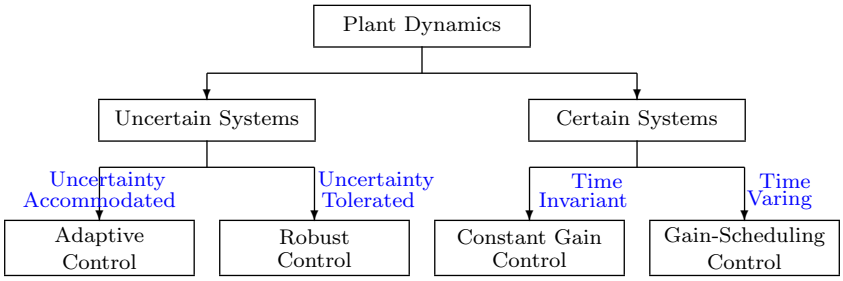

Figure 3.1 Classes of automatic control for dynamical systems

As mentioned in the previous chapters, fractional calculus came into being one of the most powerful mathematical tool for modelling real world and complex systems. In spite of its complicated mathematical background, fractional calculus can successfully be used in various strategies and schemes of control systems. Over the few last years, the idea of introducing fractional calculus and systems in adaptive control strategy has become a rapidly growing research topic [64]. Since the pioneering works of Vinagre *et. al.*, [149], and Ladaci and Charef [65] a decade ago, a great number of fractional adaptive control approaches

have been developed. Some researchers have been interested in the Fractional Order Model Reference Adaptive Control (FO-MRAC) [66], [12, 150, 1]; others have investigated the fractional adaptive PID control domain [96]. Fractional order adaptive High-Gain control [69, 21], fractional IMC-based adaptive control [68] and robust fractional order adaptive control [67] have also been introduced. Very recently fractional adaptive extremum seeking control has been investigated in Neçaibia *et. al.*, [97].

The fractional adaptive control laws provides new maneuver margins to the design engineers for control parameters tuning thanks to the fractional operators, making it possible to improve significantly the controlled system's behavior and robustness [61].

In the remainder of this chapter, we show how we can enhance the adaptive control performances by introducing fractional dynamics in the adaptation algorithm. We will emphasize, especially on Model Reference Adaptive Control (MRAC). Two main reasons have encouraged this orientation of the fractional order control:

- The MRAC control is based on the choice of a reference model which specifies the closed loop desired performances by the designer. Moreover, many research works have shown that the dynamic characteristics of a fractional order system are better than those of an integer order system [103, 134, 18] (see Section 1.5.8.).

- The simplicity of the MRAC control law, which allows the introduction of a high order model (rational approximation of fractional order models) without destabilizing the control loop.

The reference model of the MRAC system is extended to its fractional-order version, and to go furthermore, the MRAC control law has been also modified as fractional-order MIT rule which provides an extra degree of freedom.

We have carefully interested in the robust adaptive control concept, in particular, via classic technique of MRAC algorithm robustification, known as parallel feedforward filter [9], by choosing an appropriate fractional order filter.

3.2 Model Reference Adaptive Control

MRAC is an important part of adaptive control systems. The expected output is generated by a reference model (the desired performance of the closed loop control system). The parameter of the controller (adaptation gain) is adjusted according to the error signal which is defined as the difference between the system output and the model output, see (Fig. 3.2). This control system can be regarded as a subset of direct adaptive system (solved via MIT and/or the *Lyapunov* rules). In this case, the desired performance is given by the reference model connected to the system input reference signal u. The control loop will be adjusted by the output signal of the model through the adaptation mechanism. In addition to normal feedback structure, adaptive controls employ extra loop, namely, "adaptation loop" (represented by gray rectangle) to compensate any variations in the dynamics of the process and to compensate the disturbances.

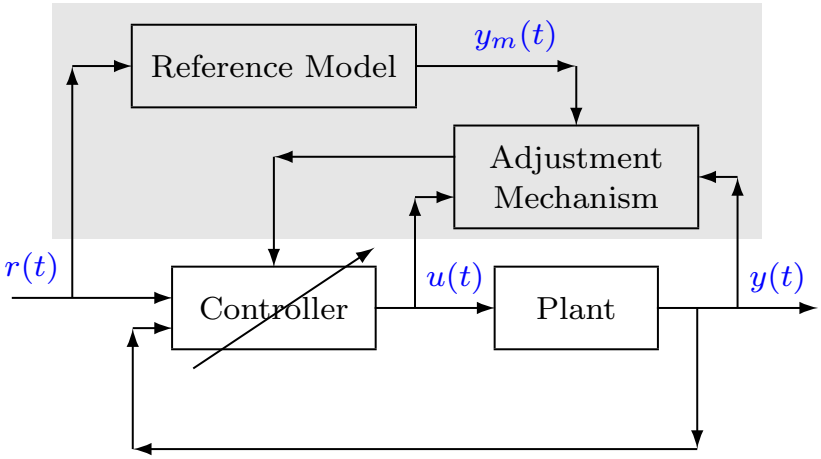

Figure 3.2 Model Reference Adaptive Controls (parameter adaptation)

Given a controllable plant $G_p(s)$ with input output signals $u(t)$ and $y(t)$ respectively, presented by the following transfer function,

$$G_p(s) = k_p \frac{N_p(s)}{D_p(s)} \tag{3.1}$$

The reference model, which is directly connected to the reference signal $r(t)$ is depicted by,

$$G_m(s) = k_m \frac{N_m(s)}{D_m(s)} \tag{3.2}$$

where, $N_m(s)$ and $D_m(s)$ are Hurwitz polynomials of degree m and n respectively, and k_m is the gain of the system. It is assumed that the structure of the controlled system is known, and only its parameters are unknown. The control objective is to make $y(t)$ track the reference model output $y_m(t)$ as closely as possible through the parameters adaptation. The control law must have the ability to follow perfectly or asymptotically the reference response. The two most popular methods of designing the controller's adaptation law are:

- The steepest descent (MIT rule) method,

- The Lyapunov stability method,

3.2.1 MRAC with MIT-Based Adaptation Law

This scheme can be achieved by means of the sensitivity concept via the gradient descent method. Let θ be the parameter vector specifically designed to minimize a certain loss function J, such as,

$$J(\theta) = \frac{1}{2}e(t)^2 \tag{3.3}$$

where, $e(t) = y_m(t) - y(t)$. Then, to minimize $J(\theta)$, it is logical to vary the parameters in the opposite direction shown by $dJ/d\theta$, that is:

$$\frac{d\theta}{dt} = -\gamma\frac{dJ}{d\theta} = -\gamma\, e\frac{\delta\, e}{\delta\theta} \tag{3.4}$$

where γ is a positive constant representing descent rate, and $\delta\, e/\delta\, \theta$ is the *sensitivity derivative* of the system.

3.2.2 MRAC with Lyapunov-Based Adaptation Law

Despite the intuitive nature of the MIT rule, however, it should be pointed out the stability of the system is not guaranteed, as it really depends on the value of γ. To overcome its limitation, one may consider the Lyapunov method, with this method, the stability is guaranteed [7]. More details about Lyapunov-Based Adaptation Law can be found in [7].

3.2.3 MRAC with Feed-Forward Configuration

In several application problems the system may have noises and disturbances. In this case, the MRAC algorithm shows its limits which can damage the quality of the product or gives an unsatisfactory result. For this reasons, many modifications and compensations of the reference model control algorithm have emerged in order to improve the "robustness" of the controlled system [71, 74]. The so-called Feed-Forward Compensation (FFC) is considered in many works [9, 70] as a robust control. The basic idea of using FFC configuration is shown in (Fig. 3.3), where the FFC is inserted in parallel with the controlled process.

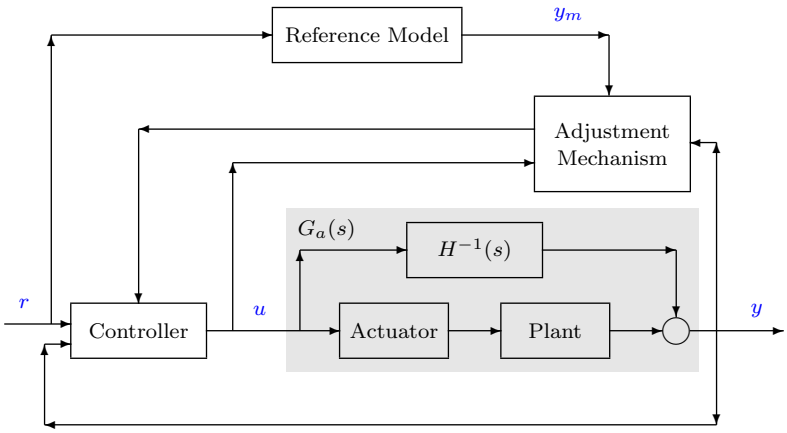

Figure 3.3 Diagram of MRAC using FFC configuration

The FFC configuration can only be used if some prior knowledge about the controlled plant is given. The FFC approach is related to the concept of "almost positivity" condition [10], which can guarantee the stable implementation of the adaptive control strategy. If there is reason to know that the controlled plant satisfies the "almost positivity" condition then, the adaptive control strategy can be immediately safely implemented.

3.2.3.1 Main concepts of robust control

The term "robust", seems to have been introduced (into statistics) by Box in 1953, refers to tests which are not greatly affected by violations of their assumptions: robust meant strong, healthy, sufficiently tough to withstand life's adversities.

In control theory, robust system is a system capable of meeting requirements (stability or

performance measures) even in the presence of model and/or disturbance uncertainty. While a robust control is an approach to controller design that explicitly deals with uncertainty.

Now let's consider a typical feedback system shown in (Fig. 3.4), where $G_p(s)$ is the plant transfer function; $C(s)$ is the controller transfer function. Very often the plant $G_p(s)$ is not exactly known, or more precisely is only known to belong to certain set of plants. In this case, we say the plant is uncertain and call the set which the plant belongs to the uncertainty set. The purpose of robust control is to design the controller $C(s)$ so that the feedback system behaves in a desired manner: for each possible plant $G_p(s)$ in the uncertainty set. Although the controller design is the ultimate goal, a typical robust control theory progresses in three stages [118]:

- Uncertainty description: Construct a mathematical description of the uncertainty set.
- Robustness analysis: Determine if the feedback system behaves in a desired manner for each G_p in the uncertainty set when a controller is given.
- Robust controller design: Design a controller C to satisfy the robustness requirement.

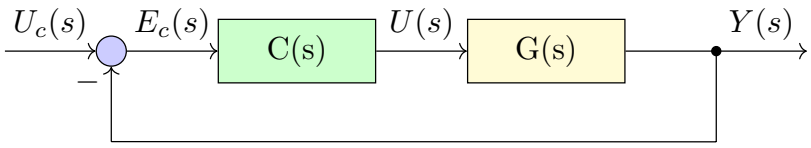

Figure 3.4 The Standard Feedback System

Over the past several decades, there has been an increasing interest in robust control. On one hand, uncertain parameters or disturbances exist inherently in the aeronautics and astronautics, advanced manufacturing, and other complex engineering systems. On the other hand, uncertain parameters or disturbances seriously affect the stability, accuracy, and reliability of underlying control systems. Therefore, robust control has become a challenging problem in international control field, for example, H_∞ control, H_2 control, Variable Structure Control (VSC), LQG Control, Adaptive Control (AC), and so forth. In adaptive robust control several successful methods were published such as [152] and [153].

3.2.3.2 Design problem

Process control objectives are generally determined by the process operating conditions and by the pre-imposed specifications. They are originally formulated in terms of physical, technological or economic parameters. The requirements on the control can typically can be grouped into four categories:

1) **Stability**: The operating point of the closed-loop system must be asymptotically stable.

2) **Asymptotic regulation**: For a given class of control inputs and external disturbances, asymptotic regulation ($\lim_{t\to\infty} y(t) - u_r(t) = 0$) must be realized.

3) **Dynamic requirements**: The performances of the closed-loop system must satisfy a set of given specifications such as the bounds on the step responses, requirement of a certain degree of non-interaction between the different signals, etc.

4) **Robustness**: The properties of the closed-loop system (1-3) must be preserved under a given class of variations in the dynamics of the open loop.

The major difficulty of the design problems (1-4) is that the aspects of performance and uncertainty must be evaluated simultaneously to obtain a good compromise. As the optimal control theory is interested in the performance aspect (1-3), we are mainly concerned with the uncertainties and robustness aspect (4).

In several practical applications the design specifications should not be considered as definitively fixed. They are often contradictory.

The control problem considered here will have to be solved by means of a regulator with FeedBack and FeedForward.

3.2.3.3 Main Definitions

Definition 3.2.1 (Strictly Positive Real Systems) *A strictly proper $m \times m$ transfer matrix is a Strictly Positive Real (SPR) system if it has n poles and $n - m$ zeros, and if all its poles and zeros are placed in the left half-plane.*

Definition 3.2.2 (Almost Positive Real Systems) *A system is Almost Positive Real Systems (ASPR) if there exists an unknown constant feedback gain matrix K_y, such that the resulting closed-loop transfer function is strictly positive real.*

3.2.3.4 Principle of Robust MRAC with Feed-Forward

In general, if a system described by $m \times m$ transfer matrix $G_p(s)$ of n order can be stabilized by a suitable feedback matrix $H(s)$ of $p \leq n$ order, then, the augmented controlled system,

$$G_a(s) = G_p(s) + H^{-1}(s) \tag{3.5}$$

becomes ASPR.

Many previous works have proposed improper PD controllers of the form:

$$H^{-1}(s) = K\left(1 + \frac{s}{s_0}\right) \tag{3.6}$$

which can stabilize many real processes for sufficiently high K values.

A feed-forward action can be then, chosen as follows:

$$H(s) = \frac{H_p}{\left(1 + \frac{s}{s_0}\right)} \tag{3.7}$$

Steps of how to design a suitable augmentation $H^{-1}(s)$ will be detailed in the next part of this chapter.

The aim of this introductory part is to emphasize the basic concepts and schemes pertinent to adaptive control techniques involved in our research work, where we present the Model Reference Adaptive Control with its control laws for direct and indirect methods. A modification of this control using a parallel Feedforward also interests this work. Another approach to adaptive control based on Feedback Adaptive Control and applicable to a certain class of linear systems is discussed.

These different approaches can be subject to more or less significant modifications to introduce fractional order operators in order to obtain an improvement in the performance of the adaptive control loop.

3.3 Fractional Order Model Reference Adaptive Control

The main objective of this section is to show how we can improve the performance of the Adaptive Control, by introducing a fractional dynamic in the adaptation algorithm.

There are several research works in the literature where, authors have already tried to introduce fractional calculus into conventional Model Reference Adaptive Control systems [45, 62], and we have slightly tried to extend in the sequel the control strategy of (Fig. 3.2) as depicted in (Fig. 3.10) and (Fig. 3.23).

In the sequel, let the abbreviation FO-MRAC stands for Fractional-Order Model Reference Adaptive Control system and FO-PID for Fractional Order PID controller.

3.3.1 FO-MRAC-Based Fractional Order $PI^{\lambda}D^{\mu}$ Regulator

In this technique, a fractional order model reference adaptive control based FO-PID regulator is introduced by making use of MIT rule with the concept of Bode's ideal loop transfer function, the aim of this work is to benefit from the fractional calculus approach to improve the closed-loop performance to obtain more robustness for the control system. The structure used in this method is the scheme depicted in (Fig. 3.2).

3.3.1.1 Fractional order reference model

The adaptive control scheme is constructed on the principle of forcing the closed loop system to follow a chosen reference model. Many research works have shown that the use of fractional order system as reference model in the MRAC algorithm can improve the dynamic characteristics with respect to response time and disturbance rejection [66]. The fractional reference model is designed based on BITF. The BITF is given by (see Section 2.2.3.),

$$L(s) = \left(\frac{\omega_c}{s}\right)^{\gamma}, \qquad \gamma \in \mathbb{R} \tag{3.8}$$

where ω_c is the gain cross-over frequency, that is, $|L(\omega_c)| = 1$. The transfer function of the closed-loop system is given by:

$$F(s) = \frac{L(s)}{L(s)+1} = \frac{1}{1+\left(\frac{s}{\omega_c}\right)^{\gamma}} \tag{3.9}$$

As in classical control designs, some system properties and constraints are fixed at the beginning such as the overshoot M_p, peak time T_p, rise time T_r, time constant T_c, and settling time T_s. References [11, 83] give us the following expressions to construct the fractional-order transfer function F(s).

- The overshoot M_p:

$$M_p = \frac{y_{max} - y(\infty)}{y(\infty)}, \qquad M_p \approx 0.8(\gamma - 1)(\gamma - 0.75) \tag{3.10}$$

- The rise time T_r:

$$T_r \approx \frac{0.131(\gamma + 1.157)^2}{(\gamma - 0.724)\omega_c}, \qquad 1 < \gamma < 2 \tag{3.11}$$

- The settling time T_s (for 2% and 5% criterion):

$$T_s(2\%) \approx \frac{4}{cos\left(\pi - \frac{\pi}{\gamma}\right)\omega_c} = \frac{4}{\xi\omega_c}, \qquad 1.39 < \gamma < 2 \tag{3.12}$$

$$T_s(5\%) \approx \frac{3}{cos\left(\pi - \frac{\pi}{\gamma}\right)\omega_c} = \frac{3}{\xi\omega_c}, \qquad 1.44 < \gamma < 2 \tag{3.13}$$

where $\xi = cos\left(\pi - \frac{\pi}{\gamma}\right)$ is the damping ratio of the fractional closed-loop control system.

3.3.1.2 Control strategy

In this section, we have interested in the reference model based direct adaptive control, and in particular, to the method using MIT law presented in (3.2.1), MIT rule is given by:

$$\frac{d\theta}{dt} = -\gamma\frac{dJ}{d\theta} = -\gamma\, e\frac{\delta\, e}{\delta\theta} \tag{3.14}$$

3.3.1.3 Application to a speed control of a DC motor

The application proposed to this method is the speed control of a DC motor [57]. The control design and results are simulated in Matlab Simulink environment.

A. Description and modeling of the DC motor

The plant considered in this work is a DC motor (Fig. 3.5) simulated by Matlab/Simulink, the aim of this work is to control the DC motor speed to get the desired speed [57]. The parameters' values are listed in (Tab. 3.1).

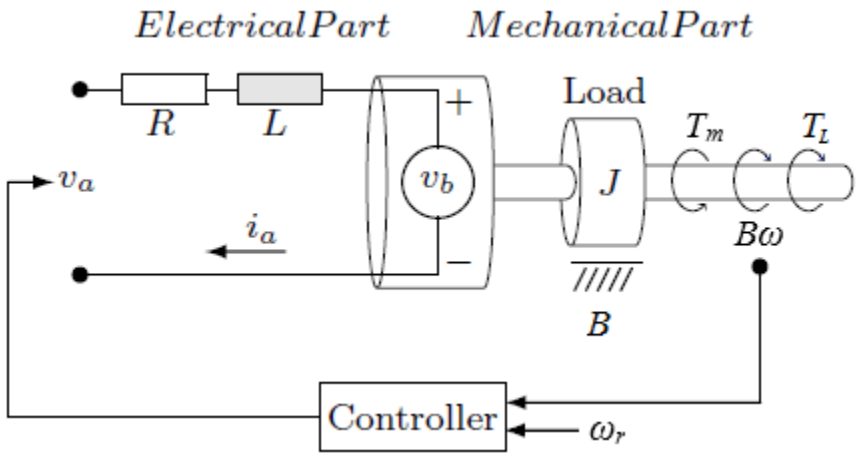

Figure 3.5 Simplified scheme of a DC motor

Mechanical equation:

Applying the Newton's law we have,

$$J\,\frac{d\omega(t)}{dt} = T_m - T_L - B\,\omega(t) \tag{3.15}$$

where ω is the shaft angular speed of the motor, B is a constant represents the friction in the bearings of the motor and the load.

Electrical equation:

From kirchhoff's voltage law we have,

$$L\,\frac{di_a(t)}{dt} = v_a(t) - R\,i_a(t) - v_b(t) \tag{3.16}$$

Electro-mechanical coupling:

The back EMF is proportional to speed as,

$$v_b(t) = k_b\omega(t)$$

The motor torque is proportional to current as,

$$T_m(t) = k_m\,i_a(t)$$

After Laplace transformation we can obtain transfer function of DC motor as,

$$\frac{\Omega(s)}{V_a(s)} = \frac{k_m}{(Ls+R)(Js+B)+k_m\,K_b} \tag{3.17}$$

As shown in (Eq. 3.17) the system output is the rotational speed Ω and the system input is the armature voltage V_a.

Thus, the block diagram can be schematized as in (Fig. 3.6).

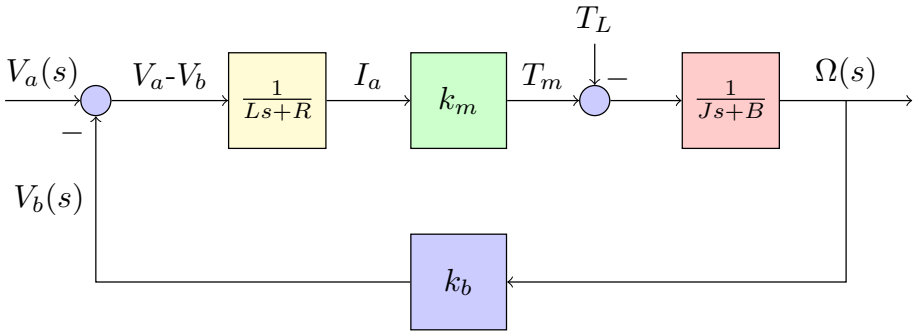

Figure 3.6 Block diagram of a DC motor

Table 3.1 DC motor parameters

Parameter	Value
Inertia Moment	$J = 0,02Kg.m^2$
Coefficient of friction	$B = 0,2N.ms$
Back EMF constant	$K_b = 0,15V/rads^{-1}$
Torque constant	$K_m = 0,15Nm/A$
Resistance	$R = 2.0Ohm$
Inductance	$L = 0.5H$

Substituting the parameters of (Tab. 3.1) in (Eq. 3.17) then, the transfer function of the DC motor is:

$$\frac{\Omega(s)}{V_a(s)} = \frac{15}{s^2+14s+42.25} \tag{3.18}$$

The open loop response of the DC motor for step input is shown in (Fig. 3.7).

By considering the poles of the system (Eq. 3.18) and the open loop step response of the transfer function, the system is stable.

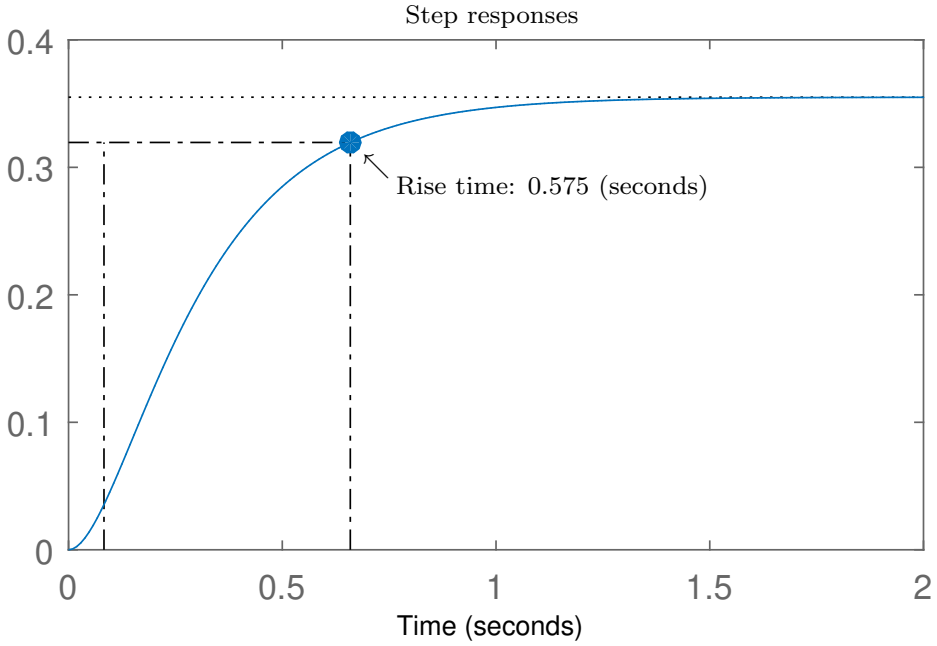

Figure 3.7 System open loop response for step input

Using MATLAB *pidTuner* of Control System Toolbox, PID controller parameters are tuned to satisfy the desired performances presented in Table 3.2. The closed loop response of the DC motor for step input is shown in (Fig. 3.8).

Table 3.2 Parameters of the tuned PID with the desired performance

Parameter		Value
Performance	Rise time	0.3 s
	Settling time	0.5 s
	Overshoot	$\leq$2%
Controller	k_p	6.5
	k_i	20.75
	k_d	0.475

Now to maintain the performance of (Tab. 3.2) in the presence of disturbances and load perturbation, the motor requires suitable (in terms of robustness) speed controller. For this aim, in the next step, we will use the fractional order approach to design a fractional order model reference adaptive control that can offers an improvement in the quality of the speed response of the DC motor (Eq. 3.17).

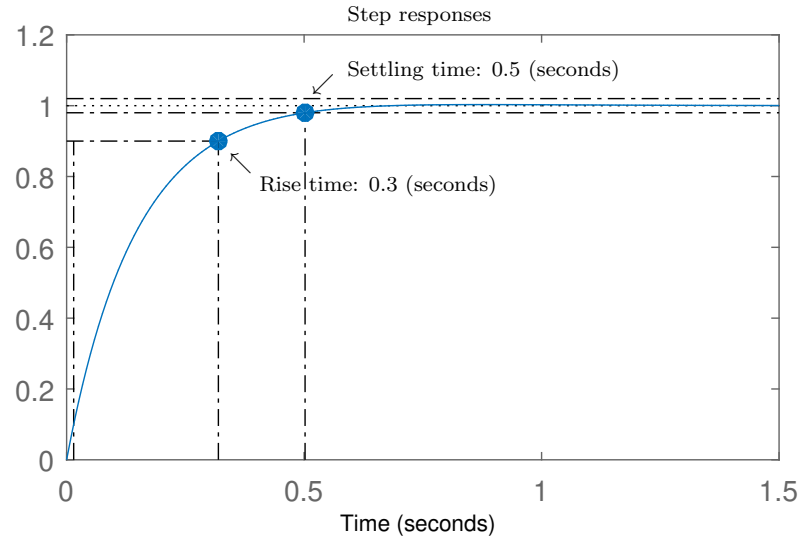

Figure 3.8 Closed loop system response for a step input

B. Design of FO-MRAC for the DC motor

Basically, the model reference adaptive controller is constructed on a simple concept. Using the general representation of adaptive control scheme given in (Fig. 3.2), the adaptive control scheme adopted for our application can be given as,

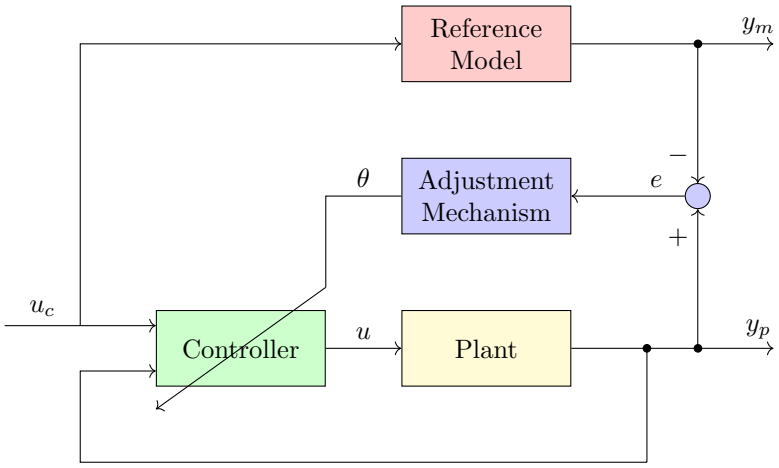

Figure 3.9 Schematic diagram of MRAC

The model approximation error can be defined as:

$$e = y_p - y_m \tag{3.19}$$

where y_p is the controlled process output, and y_m is the reference model output, e is called the tracking error.

Whenever responses of reference model and control system differ, it causes increasing amplitude of e and MRAC updates the adaptation parameter θ by minimizing a convex cost function $J(\theta)$ via MIT rule:

$$J(\theta) = \frac{1}{2}\, e^2(t) \tag{3.20}$$

The change of adaptation parameter towards the negative gradient of $J(\theta)$ was achieved using (Eq. 3.14). The control law u, is the combination of a control action u_c, and vector θ, as represented in (Eq. 3.21) and (Eq. 3.22).

$$u = \theta\, u_c \tag{3.21}$$

$$\theta = k_0/k \tag{3.22}$$

For the plant,

$$\frac{Y_p(s)}{U(s)} = k\, G(s) \tag{3.23}$$

where k is unknown parameter, the aim is to force (Eq. 3.23) look like (Eq. 3.24).

$$\frac{Y_m(s)}{U_c(s)} = k_0\, G(s) \tag{3.24}$$

Using,

$$G_m(s) = k_0\, G(s) \tag{3.25}$$

this means that reference model is scalar multiplied by plant model.

$$G_p(s) = k\, G(s) \tag{3.26}$$

Figure (Fig. 3.10), illustrates basic blocks of adjustment mechanism for the parameter θ.

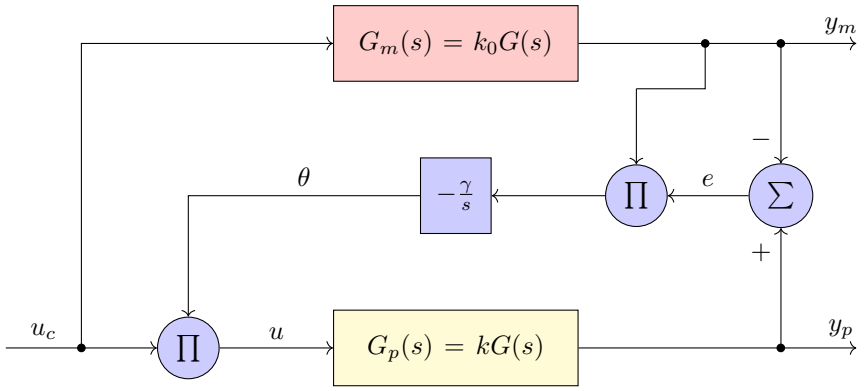

Figure 3.10 Adaptation of feed-forward gain

Substituting (Eq. 3.21−3.26) in (Eq. 3.19), gives us.

$$e = kG(s)U(s) - G_m(s)U_c(s) \tag{3.27}$$

$$e = kG(s)\theta\, U_c(s) - k_0 G(s)U_c(s) \tag{3.28}$$

Applying the MIT rule (Eq. 3.14), we get:

$$\frac{d\theta}{dt} = -\left(\gamma^{'}\,\frac{k}{k_0}\right)\, y_m\, e = -\gamma\, y_m\, e \tag{3.29}$$

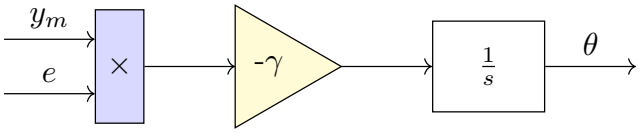

Figure 3.11 Adaptive mechanism block diagram

Reference model :

Substituting the desired performance of (Tab. 3.2) in (Eq. 3.10−3.13).

$$T_s = 0.5, T_r = 0.3, \xi = 0.9217, \alpha = 1.027, \omega_c = 6.51 rd/s.$$

Then, the required parameters for the Bode's model can be derived as follow,

$$L(s) = \left(\frac{6.51}{s^{1.027}}\right) \tag{3.30}$$

Leading to the closed loop,

$$F(s) = \frac{1}{1 + 0.153s^{1.027}} \tag{3.31}$$

The well-established Oustaloup's approximation method is, is an approximation method allowing to express the fractional order transfer function into an approximate integer order one (see Section 1.4.1.1.). For $\omega_b = 10^{-3}$ and $\omega_h = 10^{-3}$, Oustaloup's approximation gives the rational transfer function (Eq. 3.32), which will serve as a reference model for the proposed adaptive controller.

$$F(s) \approx \frac{s^7 + 1224s^6 + 2.094 \times 10^5 s^5 + 5.695 \times 10^6 s^4 + 2.507 \times 10^7 s^3 + 1.787 \times 10^7 s^2}{\begin{array}{c} 185.4s^7 + 3.615 \times 10^4 s^6 + 1.134 \times 10^6 s^5 + 9.588 \times 10^6 s^4 + 2.773 \times 10^7 s^3 \\ +2.024 \times 10^6 s + 3.206 \times 10^4 \\ \hline +1.816 \times 10^7 s^2 + 2.029 \times 10^6 s + 3.206 \times 10^4 \end{array}} \tag{3.32}$$

Figure (3.12), shows how the fractional model reference based on Bode's transfer function overlaps the desired performance.

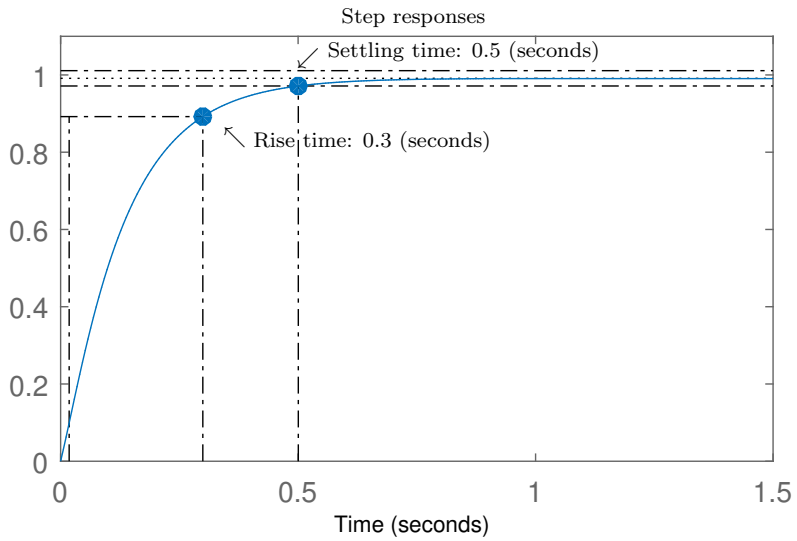

Figure 3.12 Step response of the fractional model reference

The reason of designing the reference model in this way is to avoid the bad dynamics in

higher order frequency, by taking benefit from Bode's closed loop transfer function which presents the interesting property of being robust to gain changes.

The control signal $U_c(s)$ is provided by a FO-PID controller in closed loop unity feedback system. Here, FO-MRAC provides adaptation by scaling control effort of closed-loop PID controller [114]. Figure (3.13) shows the FO-PID used in closed loop unity feedback.

This approach comes out the advantage of easily transformation of fractional $PI^{\lambda}D^{\mu}$ control system into adaptive $PI^{\lambda}D^{\mu}$ control systems. In our simulation studies, we are using the following parameters for the fractional PID, (to satisfy the performance of (Tab. 3.2)).

$$k_p = 31.8, \qquad k_i = 116, \qquad k_d = 3.3,$$

$$\lambda = 1.0185, \qquad \mu = (\lambda/2) = 0.509$$

The obtained transfer using the Oustaloup's approximation method is called from Simulink through the LTI System block as depicted below,

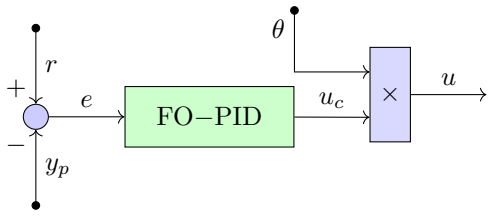

Figure 3.13 Fractional PID controller

C. Simulation results

A numerical simulation example is presented in this section by applying the designed FO-MRAC for the DC motor Speed Control (Eq. 3.18).

Figure (3.14) shows plant and reference model output, in which we can see that the plant output tracks the desired performance with perfect behavior. Figure (3.15) shows the tracking error that is very minimized.

Figure (3.16), illustrates the tracking when the plant is subjected to random output disturbances of amplitude of 0.02. Figure (3.17) shows the corresponding tracking error.

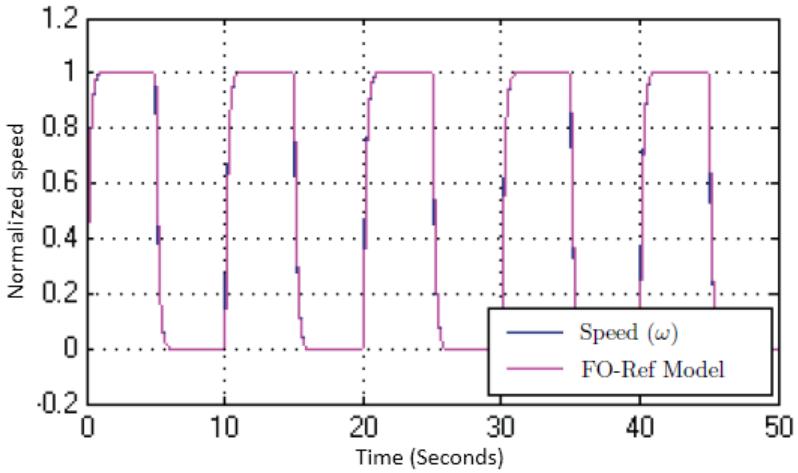

Figure 3.14 Plant output with particular value of $\lambda = 0.01$

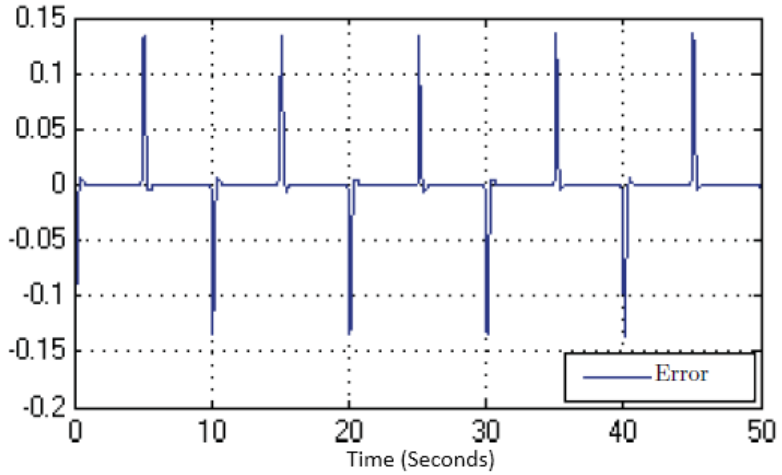

Figure 3.15 Tracking error

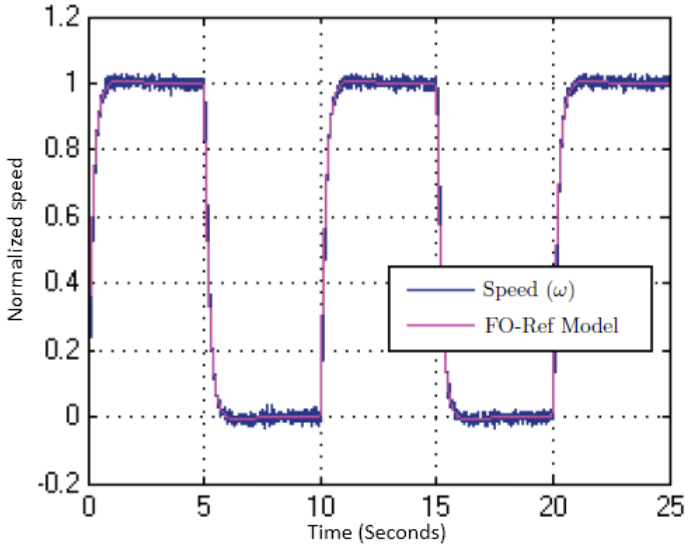

Figure 3.16 Process output with random output disturbances

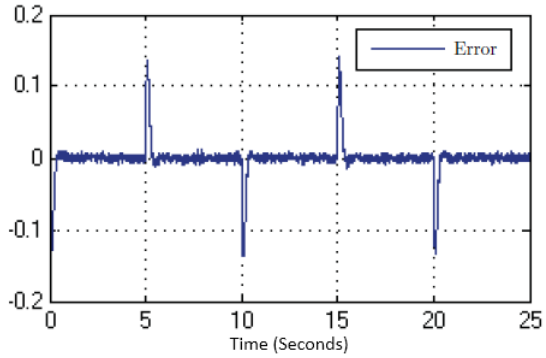

Figure 3.17 Tracking error with random output disturbances

Figure (3.18), illustrates DC motor output with a load applied at t=3 (sec). Figure (3.19), is the tracking error with the applied load which is minimized to zero.

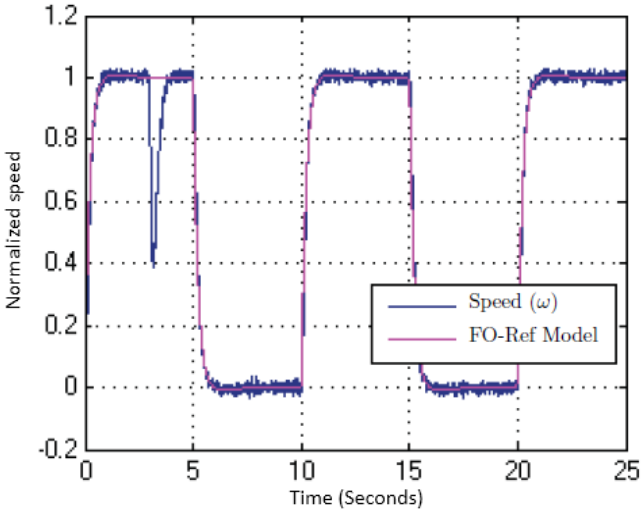

Figure 3.18 Disturbance rejection test at t=3 (sec)

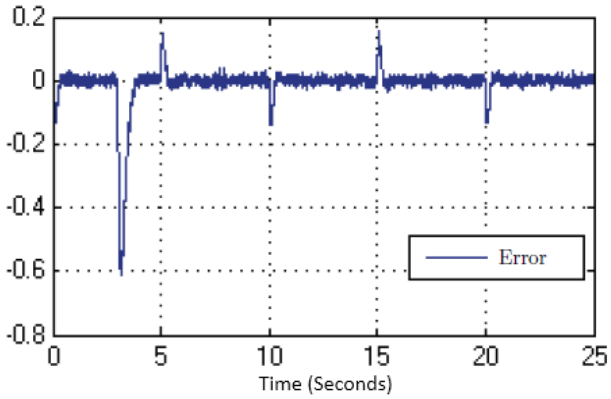

Figure 3.19 Tracking Error with the applied load

Figure (3.20), shows the plant output with impulse disturbance. Figure (3.21). demonstrates the corresponding tracking error.

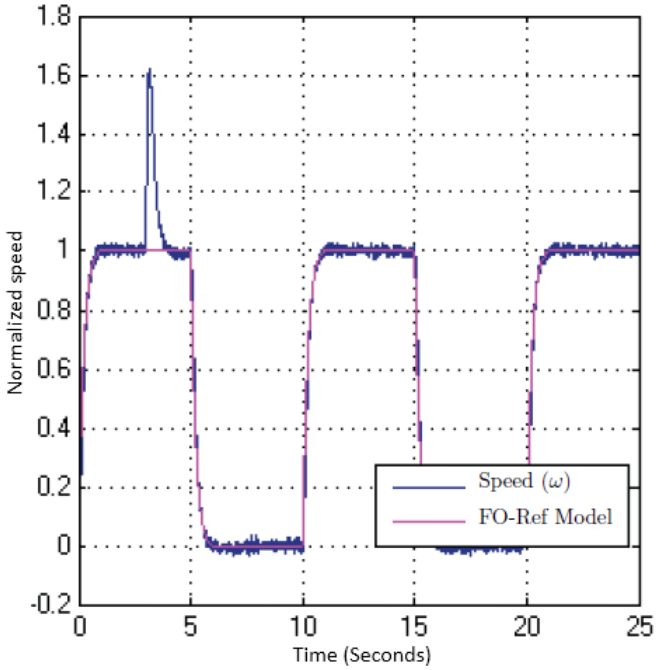

Figure 3.20 Output of the DC motor with impulse disturbance

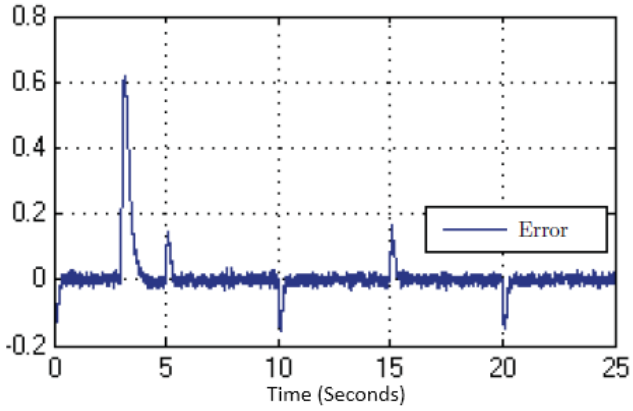

Figure 3.21 Tracking error of the output with disturbance

This work presents a simulation study for designing a FO-MRAC based PID control for the DC motor speed using MIT rule. From the simulation, we see that the designed controller drives the process response to mimic the desired performance of the fractional reference model. The work is achieved with the following remarks:

- The adaptation gain is achieved, but beyond a certain limit ($\gamma < 5$) the system performance becomes poor. Need much tuning to get acceptable response.

- More advanced controllers could be formed from other methods such as, Modified (normalized) MIT, and Lyapunov direct and indirect methods.

3.3.2 Adaptive Fractional PI$^{\lambda}$ Controller Tuning Scheme

Many methods for tuning of fractional order PID controllers have been presented in the literature. Gain phase margin, crossover frequency, high frequency noise rejection, maximum sensitivity and the iso-damping property are the main specifications that have been considered to design FO-PID controllers [92]. Among these methods are "Fractal Robustness and Parameter Tuning PI$^{\lambda}$D$^{\mu}$ Controllers" proposed in [35] and the "Analytical Design Method for Fractional Order Controller Using Fractional Reference Model" presented in [15].

Many schemes have been proposed to introduce fractional order controllers into the adaptive control strategies, in order to maintain robustness properties and to allow more design freedom and resulting in a robust adaptive control. In most of these schemes the tuning of the fractional orders is not showed explicitly.

The objective of this section is to develop a new design scheme in order to tune the adaptive fractional-order PID controller with the aim of satisfying gain and phase margin specifications over the given range of the plant parameters variation. The controller tuning is based on bode's ideal function which is applicable to FOPTD processes.

3.3.2.1 Design method

The transfer function form used to model a large number of industrial processes to a first order plus time delay (FOPTD) can be written as,

$$G(s) = \frac{Y(s)}{U(s)} = \frac{k\, e^{-Ls}}{\tau\, s + 1} \tag{3.33}$$

where L is the time delay, $k \in [k_{min}, k_{max}]$ is the static gain and τ is the time constant.

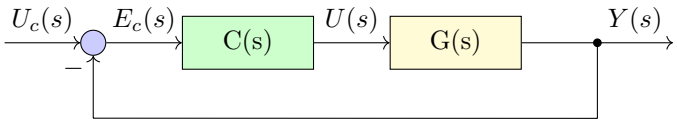

Figure 3.22 Closed loop control system

where, $C(s)$ is a fractional order controller defined as [15],

$$C(s) = k_p \left(\frac{1 + T_d\, s}{s^{\alpha}} \right) \tag{3.34}$$

where, k_p is the proportional gain, T_d is the derivative time of the controller, and $1 < \alpha < 2$. Equation (Eq. 3.34) can also be rewritten as,

$$C(s) = k_p \left(\frac{1}{s^\alpha} + T_d \, s^{1-\alpha} \right) \tag{3.35}$$

which is a particular case of a fractional $\mathrm{PI}^\alpha\mathrm{D}^\lambda$ controller, where, $\lambda = 1 - \alpha$. The fractional order α is calculated using analytical design method (detailed in the next section) to satisfy the desired gain and phase margins A_m and ϕ_m respectively.

A. Analytical design tuning method (Offline tuning)

As mentioned previously, the fractional order α is determined using analytical design method to satisfy the desired gain and phase margins A_m and ϕ_m respectively. The analytical design method chosen is described in [15] as follows, with $T_d = \tau$. The open loop of the (Fig. 3.22) is,

$$C(s)G(s) = \frac{k_p k \, e^{-Ls}}{s^\alpha} \tag{3.36}$$

Then, the gain and the phase expressions are given respectively,

$$|C(j\omega)G(j\omega)| = \frac{k_p k}{\omega^\alpha} \tag{3.37}$$

$$\phi = -L\omega - \alpha \frac{\pi}{2} \tag{3.38}$$

with the desired specifications A_m and ϕ_m. The controlled system should satisfy,

$$A_m = \frac{1}{|C(j\omega_p)G(j\omega_p)|} \tag{3.39}$$

and,

$$\phi_m = \pi + \arg[C(j\omega_g)G(j\omega_g)] \tag{3.40}$$

where ω_g and ω_p are the gain and phase crossover frequencies of the open-loop system, with,

$$|C(j\omega_g)G(j\omega_g)| = 1 \tag{3.41}$$

and,

$$\arg[C(j\omega_p)G(j\omega_p)] = -\pi \tag{3.42}$$

By substitution, we can write the gain relations as,

$$\frac{kk_p}{{\omega_g}^{\alpha}} = 1 \tag{3.43}$$

$$\frac{{\omega_p}^{\alpha}}{kk_p} = A_m \tag{3.44}$$

and the phase relations as,

$$\phi_m = \pi - L\omega_g - \alpha\frac{\pi}{2} \tag{3.45}$$

$$\pi = \alpha\frac{\pi}{2} + L\omega_p \tag{3.46}$$

From (Eq. 3.43) and (Eq. 3.44), we obtain the gain and the phase crossover frequencies as,

$$\omega_g = \frac{\pi - \phi_m - \alpha\frac{\pi}{2}}{L} \tag{3.47}$$

$$\omega_p = \frac{\pi - \alpha\frac{\pi}{2}}{L} \tag{3.48}$$

Using (Eq. 3.41) and (Eq. 3.44), we obtain a new nonlinear relation,

$$A_m = \left(\frac{\pi - \alpha\frac{\pi}{2}}{\pi - \phi_m - \alpha\frac{\pi}{2}}\right)^{\alpha} \tag{3.49}$$

Using a numerical method, the fractional order α can be determined for each desired gain and phase margin values A_m and ϕ_m.

Equation (Eq. 3.49) shows that the specified gain and phase margins depend only on the fractional order α. Therefore, any variation of the gain k has no effect on the closed loop control system performance. So that, the system is robust to gain variations.

The proportional gain is given by,

$$k_p = \frac{\omega_p^{\alpha}}{kA_m} = \frac{\omega_g^{\alpha}}{k} \tag{3.50}$$

At this point, the value of α calculated in (Eq. 3.49) and the value k_p calculated in (Eq. 3.50) using nominal values for the gain k, are useful for the next stage of the proposed tuning scheme.

In the sequel, the results of the offline tuning method described above is investigated to design a robust fractional order PI-based model reference adaptive control, using Bode's ideal loop and the fractional order MIT rule. The resulting fractional order controller can be used to serve as a robust adaptive PI control for first order plus time delay plants with unknown variations of gain k.

B. MRAC and the MIT rule approach (Online tuning)

To obtain a FO-MRAC based solution of the PI$^{\lambda}$ controller which will be more appropriate for application in the case of gain and parameters variation of the plant, we slightly modify the control strategy of (Fig. 3.9) as depicted in (Fig. 3.23). As a result the control law parameters k_p and k_d are now updated online.

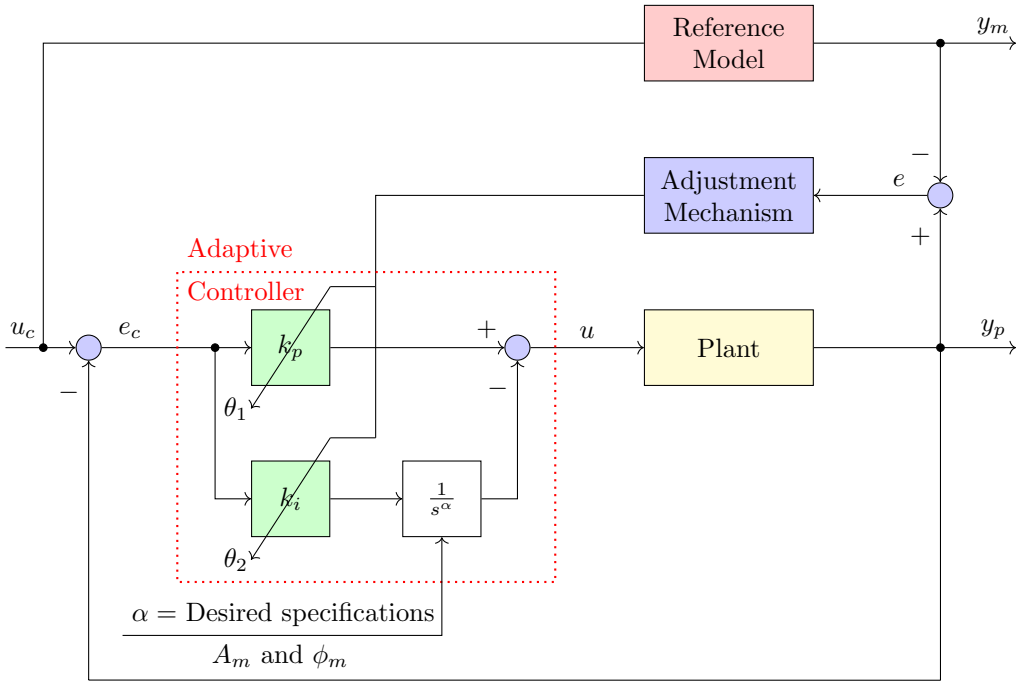

Figure 3.23 Schematic diagram of fractional order PI-MRAC controller

The fractional order LTI controller (Eq. 3.34) with the analytical method described above is investigated to design a robust fractional order PI-based model reference adaptive control using Bode's ideal loop and the fractional order MIT rule. The resulting fractional order controller can be used to serve as a robust adaptive PI control for First Order Plus Time Delay (FOPTD) with unknown variations of gain k.

C. Fractional order model reference adaptive PI controller

In this section, the parameter adaptation laws for a PI control algorithm using the MIT rule are detailed. The controller of (Fig. 3.9), is an adaptive Proportional-Integral (PI)

controller defined as,

$$C(s) = k_p + \frac{k_i}{s^\alpha} \tag{3.51}$$

The control law u, in (Fig. 3.9), is considered as,

$$U(s) = C(s) \times E_c(s) \tag{3.52}$$

where U is the control variable, E_c is the control error (defined as $E_c = U_c - Y$), U_c is the reference and Y is the output. Substituting (Eq. 3.51) in (Eq. 3.52) yields,

$$U(s) = -k_p Y(s) + \frac{k_i(U_c(s) - Y(s))}{s^\alpha} \tag{3.53}$$

Rearranging (Eq. 3.53) gives us,

$$U(s) = \frac{k_i U_c(s) - (k_p s^\alpha + k_i)Y(s)}{s^\alpha} \tag{3.54}$$

where the tuning of the fractional order α is done with the same way as in (Eq. 3.35). In other words, the parameter α is calculated using (Eq. 3.49) to satisfy gain and phase margin specifications.

The parameters k_p and k_i are adjusted using MRAC structure to compensate the controlled plant against any disturbances or parametric variations.

Equation (Eq. 3.54) can be written as,

$$U(s) = \frac{k_i}{s^\alpha} U_c(s) - \frac{k_p s^\alpha + k_i}{s^\alpha} Y(s) \tag{3.55}$$

Now, let's consider the following control law form,

$$U(s) = \theta_1 U_c(s) - \theta_2 Y(s) \tag{3.56}$$

Comparing with (Eq. 3.55) yields,

$$\theta_1 = \left[\frac{k_i}{s^\alpha}\right] \quad \text{and} \quad \theta_2 = \left[\frac{k_p s^\alpha + k_i}{s^\alpha}\right] \tag{3.57}$$

C.1. Initial values of the adaptive algorithm (of k_p and k_i)

As mentioned above, the parameters of the controller k_p and k_i are adjusted using an adaptive PI control algorithm. Furthermore, it is possible to use the value of k_p calculated in

(Eq. 3.50), and $k_i = k_p T$ as initial conditions to initiate the adaptive algorithm. Thus, three parameters can be tuned in this structure (k_p, k_i and α) as follows,

- **In offline tuning:**

  - α is tuned in offline from (Eq. 3.49),

  - the initial value of k_p calculated from (Eq. 3.50) and $k_i = k_p T$.

- **In online tuning**

  - α must be remain fixed,

  - k_p and k_i adjusted using MIT-based MRAC algorithm.

As a result, a robustness to variations in the gain of the plant is fulfilled (fractional operators and the MRAC algorithm) and the controlled plant satisfies gain and phase margins specifications.

With the initial values given to the parameters (k_p and k_i) for the adaptive algorithm based on gain and phase margins specifications, it is possible to say that the adaptive algorithm can start from the right initial conditions, so the stability of the controlled plant is ensured and improved.

C.2. Reference model

Another contribution of this work is the fractional property of the model reference used for the MRAC algorithm, which is based on Bode's ideal loop. Considering the same gain and phase margins specifications (A_m, ϕ_m) adopted for the system (Eq. 3.33), a fractional order model reference is obtained as the closed loop of (Eq. 3.36) as,

$$\frac{Y_m(s)}{U_c(s)} = \frac{C(s)G(s)}{1 + C(s)G(s)} = \frac{k_p k e^{-Ls}}{s^\alpha + k_p k e^{-Ls}} \tag{3.58}$$

Which clearly has unit steady state gain. The initial values of α, k_p and k_i are calculated from (Eq. 3.49) and (Eq. 3.50) respectively, with the nominal values of k.

Equation (Eq. 3.58) is used to serve as a Bode's ideal loop-based Model Reference for the adaptive control algorithm proposed in this work.

Applying the control law (Eq. 3.56) to the system (Eq. 3.33) gives us,

$$Y(s) = \frac{\theta_1 k e^{-Ls}}{(\tau\, s + 1) + \theta_2 k e^{-Ls}} U(s) \tag{3.59}$$

Now, let's derive the adaptation rules for the controller parameters k_p and k_i. Using the adjustment rule (Eq. 3.34), the next relations are given,

$$\frac{d\theta}{dt} = \begin{cases} \frac{d\theta_1}{dt} & = -\gamma \times \frac{\partial J}{\partial \theta_1} = -\frac{\partial J}{\partial e} \times \frac{\partial e}{\partial y} \times \frac{\partial y}{\partial \theta_1} \\ \frac{d\theta_2}{dt} & = -\gamma \times \frac{\partial J}{\partial \theta_2} = -\frac{\partial J}{\partial e} \times \frac{\partial e}{\partial y} \times \frac{\partial y}{\partial \theta_2} \end{cases} \tag{3.60}$$

Solving (Eq. 3.59) for θ_1 and θ_2 and substituting in (Eq. 3.60) gives,

$$\frac{d\theta_1}{dt} = -\gamma\, e \times \left(\frac{k e^{-Ls}}{(\tau\, s + 1) + \theta_2 k e^{-Ls}} \right) U_c(s) \tag{3.61}$$

$$\frac{d\theta_2}{dt} = \gamma\, e \times \left(\frac{k e^{-Ls}}{(\tau\, s + 1) + \theta_2 k e^{-Ls}} \right) Y(s) \tag{3.62}$$

In Laplace domain (Eq. 3.61) and (Eq. 3.62) can be written as,

$$\theta_1 = \frac{-\gamma^{'}\, e}{s} \left(\frac{k e^{-Ls}}{(\tau\, s + 1) + \theta_2 k e^{-Ls}} \right) U_c(s) = \left[\frac{k_i}{s^\alpha} \right] \tag{3.63}$$

$$\theta_2 = \frac{\gamma^{'}\, e}{s} \left(\frac{k e^{-Ls}}{(\tau\, s + 1) + \theta_2 k e^{-Ls}} \right) U_c(s) = \left[\frac{k_i + k_p s^\alpha}{s^\alpha} \right] \tag{3.64}$$

where $\gamma^{'} = k\gamma$.

From (Eq. 3.65) the model output is derived as,

$$Y_m(s) = \frac{k_p k e^{-Ls}}{s^\alpha + k_p k e^{-Ls}} U_c(s) \tag{3.65}$$

when the output Y in (Eq. 3.59) is close to its ideal Y_m in (Eq. 3.65) the following approximation can be done,

$$(\tau\, s + 1) + \theta_2 k e^{-Ls} \cong \frac{k_p k e^{-Ls}}{s^\alpha + k_p k e^{-Ls}} \tag{3.66}$$

where in the second side of (Eq. 3.66) k_p is substituted by initial values. While, k can be replaced by nominal values. Therefore, (Eq. 3.63) and (Eq. 3.64) are approximated to,

$$\frac{k_i}{s^\alpha} = -\frac{\gamma}{s} e \left(\frac{e^{-Ls}}{s^\alpha + k_p k e^{-Ls}} \right) U_c(s) \tag{3.67}$$

$$k_p = \frac{\gamma}{s} e \left(\frac{e^{-Ls}}{s^\alpha + k_p k e^{-Ls}} \right) (Y(s) - U_c(s)) \tag{3.68}$$

3.3.2.2 Illustrative examples

In order to show the effectiveness of the proposed adaptive control scheme, an example is chosen from the literature. The plant is a heating furnace which was modelled in [156] by,

- **Integer order model (IOM)**

$$G_{\text{IOM}} = \frac{1}{73043s^2 + 4893s + 1.93} \tag{3.69}$$

- **Fractional order model (FOM)**

$$G_{\text{FOM}} = \frac{1}{14994s^{1.31} + 6009s^{0.97} + 1.69} \tag{3.70}$$

According to [156], the fractional order model was more exact than the integer order one. To apply the proposed adaptive control, the integer order model (Eq. 3.69) should be approximated by a first order plus time delay system which is given in [156] by,

$$G_{\text{FOPTD}} = \frac{0.51813e^{-14.97s}}{2520.2609s + 1} \tag{3.71}$$

The design specifications required for this plant are,

- Gain margins, $A_m = 3.13$,
- Phase margins $\phi_m = 60$ degrees,

Applying the tuning equation 3.49, the obtained fractional order is $\alpha = 1.0134$,

From (Eq. 3.29) , $k_p = 0.0619$, with $T_d = \tau$, $k_i = 156.0315$. As mentioned above, these values will be used to initiate the adaptive PI algorithm parameters.

- **Design of the fractional order adaptive PI controller**

The proposed fractional model reference of the control system can be given by,

$$G_m = \frac{0.0321e^{-14.97s}}{s^{1.0134} + 0.0321e^{-14.97s}} \tag{3.72}$$

The delay time term is approximated by 2^{nd} order Pade approximation. Fractional order operator approximation is done in the frequency band $[10^{-3} - 10^{3}]$ rad/s with the order 5. The controlled plant response and the fractional model reference are given in (Fig. 3.24).

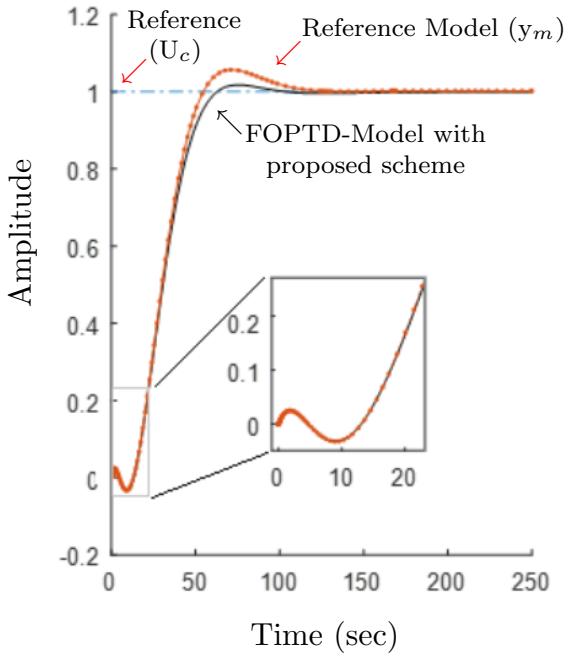

Figure 3.24 Controlled plant and model responses

As can be seen from this figure, there is an excellent model-following for time $t < 50$ seconds, the controlled plant and the model performance are overlapped due to the initial conditions given to the adaptive control algorithm. The control law given to the system is depicted in (Fig. 3.25).

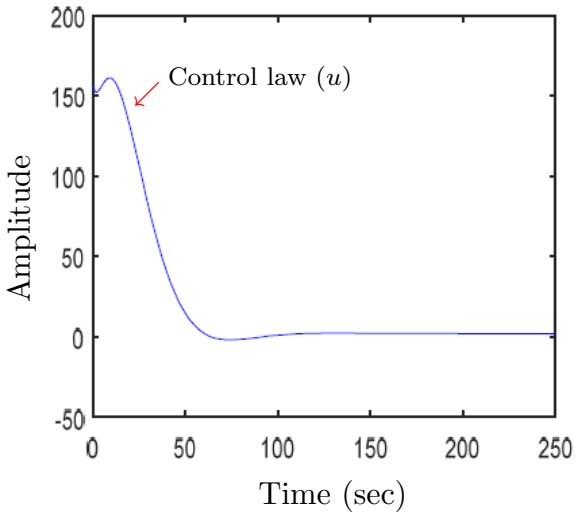

Figure 3.25 The control law

An integer order PID controller is designed according to Åström-Hägglund tuning algorithm [6] for the integer order model (Eq. 3.69) as,

$$C_{IO}(s) = 305.38 + \frac{10.18}{s} + 2290.35s \tag{3.73}$$

A fractional order $PI^{\lambda}D^{\mu}$ controller is designed according to the tuning algorithm in [156] for the fractional model (Eq. 3.70) as,

$$C_{FO}(s) = 736.8054 + \frac{0.5885}{s^{0.6}} - 818.420s^{0.35} \tag{3.74}$$

In order to compare the results of the proposed scheme for the plant model (Eq. 3.72) with the two controllers (Eq. 3.73) and (Eq. 3.74), a comparison of the three strategies of control is shown in (Fig. 3.26).

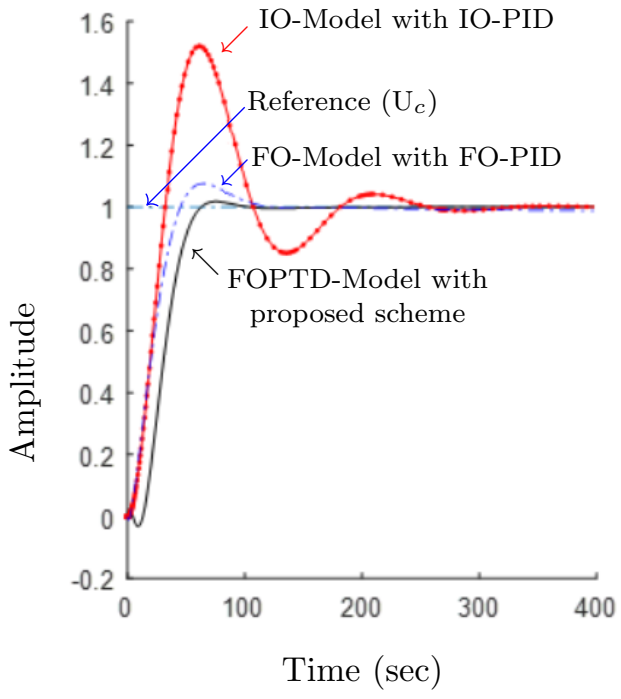

Figure 3.26 Comparison of the three strategies of control

IO: Stands for Integer Order.

FO: Stands for Fractional Order.

FOPTD: stands for First Order Plus Time Delay Model.

MATLAB *StepInfo* command is used to compute the step response characteristics, the results for the three controllers are recorded in (Tab. 3.3).

Table 3.3 Results of the "stepinfo" command for the three strategies of control

Performances	- FOPTD model with FO-MRAC PI (Proposed)	IO model with IO-PID	FO model with FO-PID
Rise Time	31.5208	21.8900	30.5475
Settling Time	53.9381	167.1491	83.2827
Settling Min	0.9294	0.8521	0.9103
Settling Max	1.0172	1.5206	1.0761
Overshoot	1.7187	52.0575	7.6145
Undershoot	3.2214	0	1.0228
Peak	1.0172	1.5206	1.0761
Peak Time	76.3258	61.2695	64.4210

From the (Tab. 3.3), the performances of the controlled plant are improved. The plant response is much faster with smaller overshoot when the fractional adaptive controller PI is applied.

In this part, a novel design scheme is proposed to tune fractional order adaptive PI controller for a class of First Order Plus Time Delay (FOPTD) plants. Two ideas have been presented to improve the Fractional Order Model Reference Adaptive Control (FO-MRAC) namely,

- The Fractional Order MRAC tuning scheme is improved; where initial parameters of the adaptive algorithm are fixed in offline first, then an online tuning is performed to achieve the robustness of the controlled plant against parametric variations,

- The second idea is the new fractional order Model Reference tuning form which is introduced using the plant model.

Through an illustrative example, simulation results show the effectiveness of the proposed scheme.

3.3.3 Robust MRAC with Fractional Order FeedForward

In this section, a fractional order adaptive robust control solution for disturbed systems is presented, based on the work of Bar-kana [10, 9], which uses the basic property of process stabilization and a simple parallel feed-forward in order to guarantee the robust stability of the adaptive non-linear regulator [63].

3.3.3.1 Control strategy

In this section, we have interested in the fractional order Feed-Forward configuration similar to that of integer order one (Eq. 3.5) of the forme:

$$H(s) = \frac{H_p}{\left(1 + \frac{s}{s_0}\right)^{\alpha}} \tag{3.75}$$

where α is a real number and $0 < \alpha < 1$.

The introduction of the fractional feed-forward improves the robustness of the adaptation algorithm in the presence of disturbances, since these systems do not amplify these random signals. This configuration can be considered as in (Eq. 3.7) as the inverse of an improper fractional PD controller, which is currently used in control systems with good performance [51, 104].

3.3.3.2 Application to a DC/DC boost converter

Without loss of generality, this adaptive robust control method will be applied to a non-minimum phase system of a DC/DC Boost Converter Stabilization given by the schematic representation shown in (Fig. 3.27). From (Fig. 3.27), the mathematical model of the boost converter is [54]:

$$\begin{cases} \dfrac{di_L}{dt} = -\dfrac{R}{L} i_L - \dfrac{1}{L}(1-d)v_c + \dfrac{1}{L} v_i \\ \dfrac{dv_c}{dt} = \dfrac{1}{C}(1-d)i_L - \dfrac{1}{R_L C} v_c \end{cases} \tag{3.76}$$

where i_L is the inductor current; v_c is the output voltage; v_i is the input voltage source; control input d is the duty ratio ($0 \leq d \leq 1$); R, L and C are the circuit parameters; R_L is the load resistance.

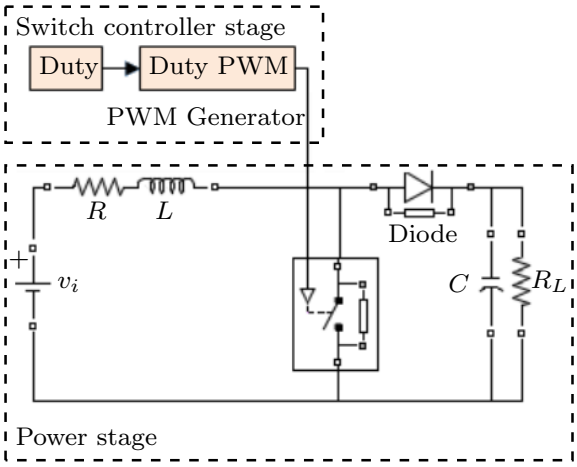

Figure 3.27 Schematic representation of the Boost Converter

When the inductor resistance is disregarded (i.e. $R = 0$) from model (Eq. 3.76), the steady-state relation between the voltage source and the output voltage is given by [54],

$$V_c = \frac{1}{(1-D)} V_i \tag{3.77}$$

where V_c is the output voltage and D is the duty ratio at the equilibrium point. This equation shows that the output voltage is always higher than the input voltage if the system is stable at the range of duty ratio [131].

From (Eq. 3.76) the boost converter is a bilinear system including the multiplication of input and system states [129]. And it is a non-minimum phase system because the zero dynamics of the system is unstable as to the output voltage [130].

This property makes the converter control problem very complicated and many works have been made by the researchers in the control theory field as well as power electronics for many years [131].

The linearized model of the power converter system at the desired equilibrium point,

$$\dot{x} = \begin{bmatrix} -\frac{R}{L} & -\frac{(1-d)}{L} \\ \frac{(1-d)}{C} & -\frac{1}{R_L C} \end{bmatrix} x + \begin{bmatrix} \frac{V_c}{L} \\ -\frac{I}{C} \end{bmatrix} u \tag{3.78}$$

where x is the system states $[i_L - I \;\; v_c - V_c]^T$ and the input u is $d - D$. The transfer function of (Eq. 3.78) shows that its zero is located at [131]:

$$z_1 = \frac{(V_c(1-D)/I - R)}{L} \tag{3.79}$$

Since the inductor resistance R is very small, the zero is at the right half plane. This implies the linearized system (Eq. 3.78) is also non-minimum phase. The system parameters of the boost converter are determined as in (Tab. 3.4) [131].

Table 3.4 Plant Parameters

Parameter	Value
Inductor	$L = 1mH$
Inductor Resistance	$R = 0.6$
Capacitor	$C = 1mF$
Voltage Source	$V_i = 12V$
Desired Output Voltage	$V_o = 24V$
Load Resistance (Disturbance)	$R_L = 50$
Nominal Equilibrium Point	
Output Voltage	$V_c = 24V$
Inductor Current	$I = 1.0111A$
Duty Ratio	$D = 0.5253$

Transfer function of the linearized model is [131]:

$$G(s) = \frac{Y(s)}{U(s)} = \frac{-1011s + (1.079 \times 10^7)}{s^2 + 620s + (2.374 \times 10^5)} \tag{3.80}$$

The designed PI controller, the parallel Feed-Forward and the Model reference are [131]:

$$C_{PI}(s) = \frac{0.001s + 0.03}{s} \tag{3.81}$$

$$H(s) = \frac{0.001}{0.001s + 1} \tag{3.82}$$

$$G_m(s) = \frac{300}{s + 300} \tag{3.83}$$

3.3.3.3 Design of the MRAC for the DC/DC boost converter

Using the MRAC structure given in (Fig. 3.9), the control law u chosen in this this work, is given by,

$$u = \theta_1 u_c - \theta_2 y \tag{3.84}$$

where; θ_1 and θ_2, are the adaptation parameters, and u_c is a unit step input. From (Eq. 3.80). we have,

$$Y(s) = \left(\frac{-1011s + 1.079 \times 10^7}{s^2 + 620s + 2.374 \times 10^5} \right) [\theta_1 U_c - \theta_2 Y(s)] \tag{3.85}$$

and

$$Y(s) = \frac{-1011s + 1.079 \times 10^7}{s^2 + (620 - 1011)s + 2.374 \times 10^5 + 1.079 \times 10^7\theta_2}\theta_1 U_c \tag{3.86}$$

The deviation between the desired response and the plant output, can be defined as:

$$e = y - y_m \tag{3.87}$$

Substituting (Eq. 3.86) in (Eq. 3.87), yields,

$$E(s) = \frac{-1011s + 1.079 \times 10^7}{s^2 + (620 - 1011)s + 2.374 \times 10^5 + 1.079 \times 10^7\theta_2}\theta_1 U_c - G_m U_c \tag{3.88}$$

If the MIT rule (Eq. 3.14) is used then,

$$\frac{\partial e}{\partial \theta_1} = \frac{-1011s + 1.079 \times 10^7}{s^2 + (620 - 1011)s + 2.374 \times 10^5 + 1.079 \times 10^7\theta_2}u_c \tag{3.89}$$

and

$$\frac{\partial e}{\partial \theta_2} = \frac{(-1011s + 1.079 \times 10^7)\theta_1}{s^2 + (620 - 1011)s + 2.374 \times 10^5 + 1.079 \times 10^7\theta_2}y \tag{3.90}$$

The reference model can be written as:

$$G_m = \frac{b_{0_m}}{a_{1_m}s + a_{2_m}} \tag{3.91}$$

But, we want the output y of the plant tracks the output y_m of the reference model, then,

$$s^2 + (620 - 1011)s + 2.374 \times 10^5 + 1.079 \times 10^7\theta_2 \approx a_{1_m}s + a_{2_m}$$

$$\frac{\partial e}{\partial \theta_1} = \frac{b_{0_m}}{a_{1_m}s + a_{2_m}}u_c \tag{3.92}$$

and

$$\frac{\partial e}{\partial \theta_2} = -\frac{b_{0_m}}{a_{1_m}s + a_{2_m}}y \tag{3.93}$$

Finally,

$$\frac{\partial e}{\partial \theta_1} = -\gamma\, e\frac{de}{d\theta_1} = -\gamma\left(\frac{b_{0_m}}{a_{1_m}s + a_{2_m}}u_c\right)e \tag{3.94}$$

and

$$\frac{\partial e}{\partial \theta_2} = -\gamma\, e\frac{de}{d\theta_2} = \gamma\left(\frac{b_{0_m}}{a_{1_m}s + a_{2_m}}y\right)e \tag{3.95}$$

Figure (Fig. 3.28), shows the SIMULINK model of the MRAC adaptation mechanism.

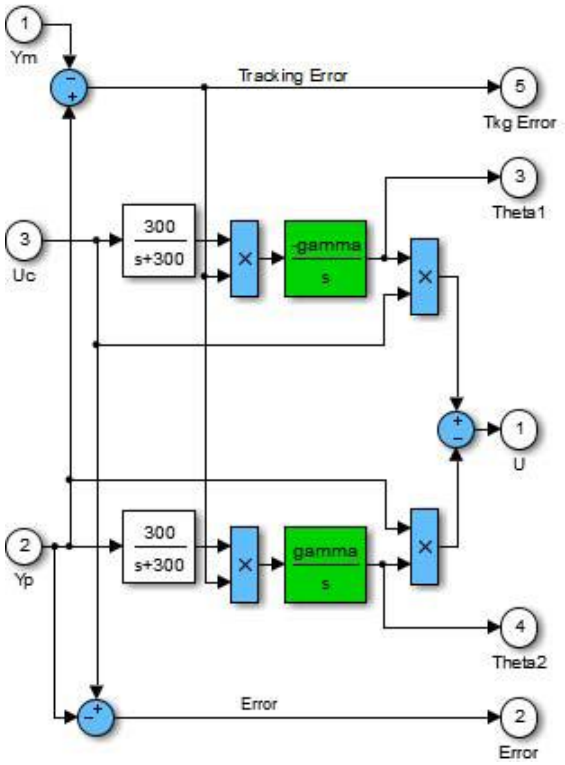

Figure 3.28 Block diagram of the adaptation mechanism

Furthermore, to improve the robustness of this improved adaptive control scheme, we will use the fractional order parameter adaptation law proposed in [66] instead of (Eq. 3.14), which is given by [67]:

$$\frac{d^{\beta}\theta}{dt^{\beta}} = -\gamma \left(\frac{\partial e}{\partial \theta}\right) e \tag{3.96}$$

where β is a real number such that $0 < \beta < 2$. For this work β is fixed to 0.55.

Reference model :

The fractional order form of the model (Eq. 3.83) is given as,

$$G_{m_f}(s) = \left(\frac{300}{s+300}\right)^{\mu} = \left(\frac{1}{\frac{s}{300}+1}\right)^{\mu} \tag{3.97}$$

In this work, the singularity function (Charef's method) presented in (Section 1.4.1.2), is used to convert the fractional order transfer function to rational one with $\mu = 0.85$ and $2\,dB$ as a tolerated approximation error, Charef's approximation gives us the following transfer

function which serves as the reference model for the adaptive control presented in this work.

$$G_{m_f}(s) \approx \frac{676.2s + 5.73 \times 10^6}{s^2 + 1.496 \times 10^4 s + 5.73 \times 10^6} \tag{3.98}$$

Fractional feed-forward :

The fractional order feed-forward of (Eq. 3.82) is considered as:

$$F_f(s) = \frac{0.001}{(0.001s + 1)^\alpha} = 0.001 \frac{1}{\left(\frac{s}{1000} + 1\right)^\alpha} \tag{3.99}$$

The fractional order pole power is chosen arbitrarily ($\alpha = 0.6$). Singularity function (Charef's method), gives us:

$$F_f(s) = 0.001 \frac{1}{\left(\frac{s}{1000} + 1\right)^{0.6}} \approx \frac{6.813s^2 + 2.471 \times 10^5 s + 1 \times 10^9}{s^3 + 7.96 \times 10^4 s^2 + 7.96 \times 10^8 s + 1 \times 10^{12}} \tag{3.100}$$

Fractional order PI :

In this work, the PI (Proportional-Integrator) controller of (Eq. 3.81) is considered in a fractional order form as,

$$C_{PI_f}(s) = 0.001 + \frac{0.03}{s^\gamma} \tag{3.101}$$

with $\gamma = 0.95$ the transfer function in integer order approximation is,

$$C_{PI_f}(s) = \frac{0.7379s^3 + 35.03s^2 + 241.6s + 21.24}{707.9s^3 + 8024s^2 + 900.3s + 1} \tag{3.102}$$

3.3.3.4 Application and simulation results

This section, presents the simulation and results obtained using the designed MRAC algorithm with fractional MIT rule, fractional reference model, fractional parallel Feed-forward, and fractional PI controller for the considered DC-DC Boost Converter with load variation.

The load was changed from $R_L = 15\Omega$ to 50Ω as depicted in the (Tab. 3.5). The overall simulation system under Matlab Simulink is presented in (Fig. 3.29).

Table 3.5 Cases considered for simulation

Cases	Value	Corresponded transfer function
1	$R_L = 15\,\Omega$	$G_1(s) = \frac{-1011s+(1.079\times10^7)}{s^2+666.7+(2.653\times10^5)}$
2	$R_L = 25\,\Omega$	$G_2(s) = \frac{-1011s+(1.079\times10^7)}{s^2+640+(2.653\times10^5)}$
3	$R_L = 35\,\Omega$	$G_3(s) = \frac{-1011s+(1.079\times10^7)}{s^2+628.6+(2.653\times10^5)}$
4	$R_L = 45\,\Omega$	$G_4(s) = \frac{-1011s+(1.079\times10^7)}{s^2+622.2+(2.653\times10^5)}$
5	$R_L = 50\,\Omega$ (Nominal value)	$G_5(s) = \frac{-1011s+(1.079\times10^7)}{s^2+620+(2.653\times10^5)}$

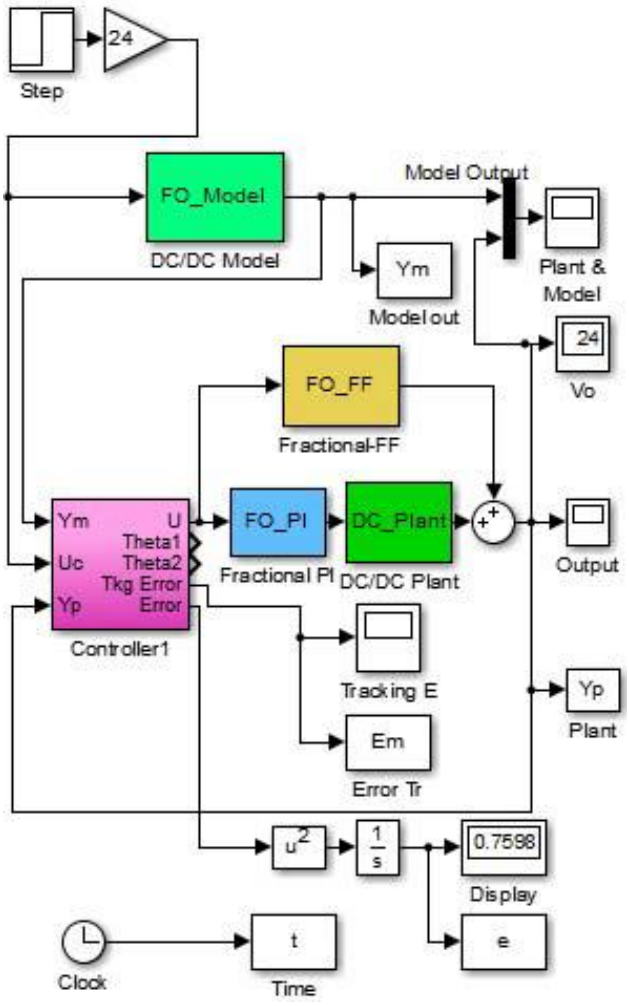

Figure 3.29 Simulation of the overall system

Figure (Fig. 3.30). and (Fig. 3.31) show the effectiveness of the proposed control strategy in improving the system performance in spite disturbances on the load values.

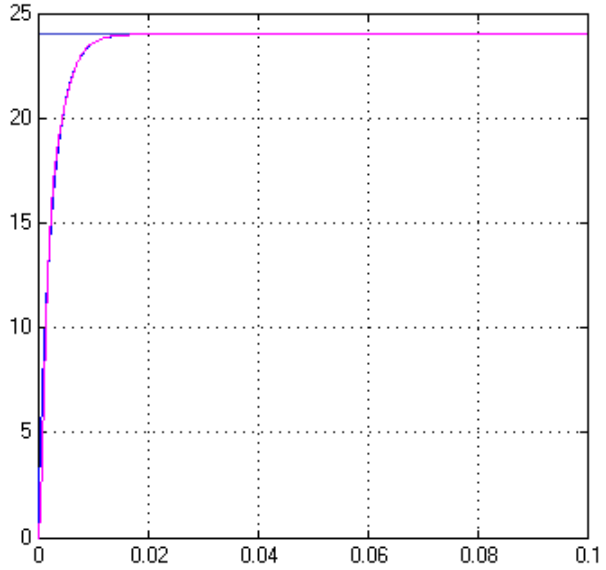

Figure 3.30 Model and plant responses for the cases given in (Tab. 3.5)

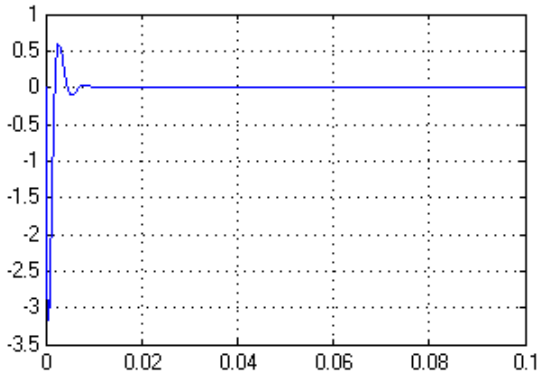

Figure 3.31 Tracking error between model and plant for the cases given in (Tab. 3.5)

Figure (Fig. 3.32) shows a comparison of the proposed fractional order MRAC control based on fractional parallel feed-forward configuration scheme with a classic MRAC based integer parallel feed-forward and a classic PI controller.

The load was changed from $RL = 50\,\Omega$ (nominal value) to $RL = 20\,\Omega$ at $t = 0.05$ seconds as variation parameters, then changed back to $RL = 50\,\Omega$ at $t = 0.1$ seconds.

From the simulation results shown in (Fig. 3.32), we can see that the plant response in fractional order MRAC is pretty good than in the integer case with improvement in the robustness of the control system.

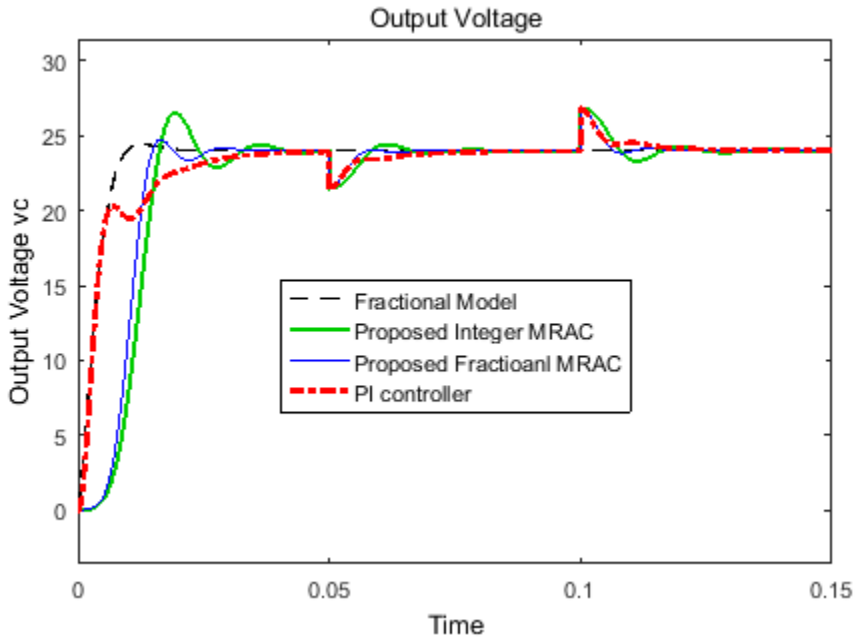

Figure 3.32 Comparison of fractional MRAC with integer MRAC; Thick line proposed classic MRAC (green), Thin line proposed fractional MRAC (blue), and PI controller thick dashed line (red)

Control of DC-DC Boost Converter requires adaptive control techniques since its load changes within time. In this work we proposed a factional-order robust adaptive control using the property of ASPR condition and a MRAC control scheme with a feed-forward action and a modified fractional order MIT control law. The simulation results demonstrated the efficiency of the proposed controller to stabilize the plant even in presence of disturbances. Further researches are focused on robust stability analysis and demonstration using classical theory.

3.4 Conclusion

The main part of this chapter was devoted to the Model Reference Adaptive Control MRAC, with the MIT control law. This method has the advantage of being easy to be implemented. It allows to propose various modifications of its algorithm based on the use of fractional order operators.

We have shown that the introduction of a fractional order reference model has a beneficial effect on the performance of the control process such as, time response, stability and robustness of the closed loop. Tests with random additive noises of substantial amplitudes both at the input and at the output of the controlled system have shown the improvement of the robustness of the control law.

We are also closely interested in the notion of robustness of the model reference adaptive control, using a classic robustification technique which is the addition of a parallel Feed-Forward to the adaptation loop.

The simulation results on a DC/DC boost converter process with a non-minimum phase model and a variable load, confirmed the superiority of the proposed algorithm compared to the classical scheme.

We know that many other approaches of adaptive control need to be re-studied from fractional-order point of view, in order to obtain better results.

It is clear that most of the results obtained in this part are based on numerical applications or simulations.

In the next chapter we perform experimental validation of some control strategy approaches developed in this work.

Chapter 4

NUMERICAL IMPLEMENTATION OF FRACTIONAL CONTROLLERS

In this chapter, numerical implementation of fractional order control and some tools to deal with Real Time Data Acquisition and Fractional Order Speed Control of a DC Motor (on both dSPACE controller board and a Low Cost microcontroller) are presented to validate some results discussed in the previous chapters.

4.1 Introduction

This chapter presents experimental setup and results of a DC motor fractional order control implemented in both DS1104 board and a low cost platform based Arduino. It is organized in two sections:

- The first section considers the fractional order controller implementation using MATLAB/SIMULINK with ControlDesk software and dSPACE 1104 Controller board as the first platform.

- The second section presents a Real-Time data acquisition and fractional order control using Simulink Support Package and Arduino board as a low-cost platform.

4.2 Implementation Using dSPACE Platform

This part depicts the experimental validation of some developed fractional order control algorithms (see Section 2.5) using dSPACE platform. The obtained Real-time experimental results will be compared with the simulation results.

4.2.1 Experimental Setup

The experimental platform (Fig. 4.1) consists of a DC Motor/Generator set (Fig. 4.2) with the characteristics shown in (Tab. 4.1), dSPACE 1104 Controller board and a Personal Computer with MATLAB/SIMULINK & ControlDesk software.

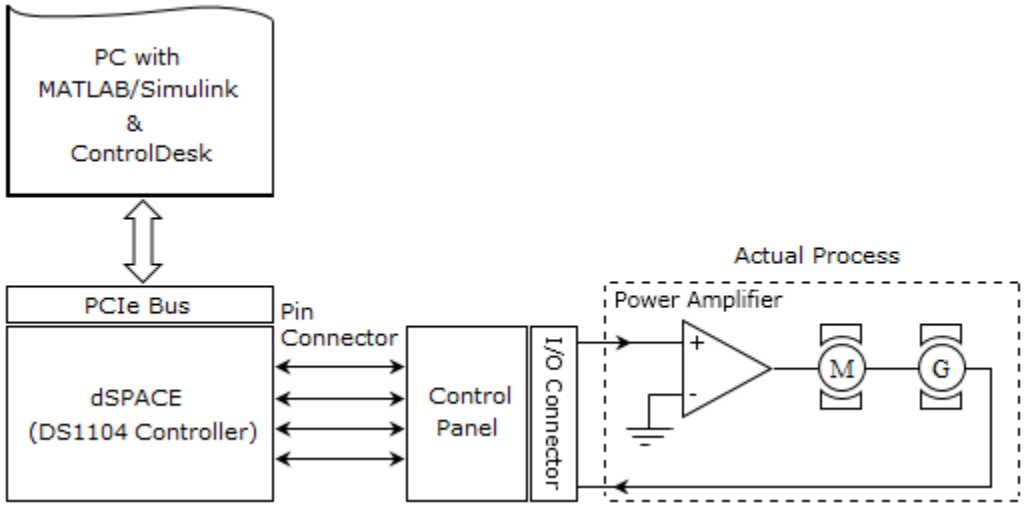

Figure 4.1 Experimental platform scheme

The speed sensor output unit (Encoder/Generator) provides information to the anti-aliasing filter (anti-repliement) via analog to digital (ADC) port of the dSPACE board. The fractional order control algorithm is implemented using Simulink model set. Real-Time Interface (RTI) data block is used to generate C code from the developed model, this C code is then converted to target specific code by Target Language Compiler (TLC) supported by DS1104 board. This code is then deployed onto the rapid prototype hardware system to run the Hardware In-the-Loop Simulation (HIL).

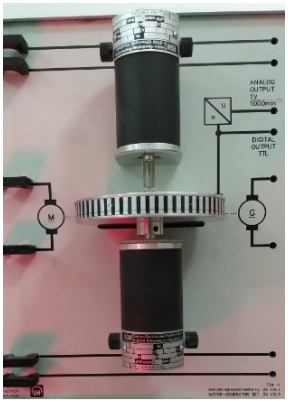

Figure 4.2 DC Motor/ Generator set used in this work

Table 4.1 DC Motor/Generator set characteristics

No	Characteristic	Motor
1	Power Consumption	≈10W
2	Input Voltage	24V
3	Max. Speed	3000 min^{-1}
No	**Characteristic**	**Generator**
1	Power Output	≈4W
2	Output Voltage	0 . . . 20 V DC
3	Speed (Analog)	1 V/1000 min^{-1}
4	Speed (Digital)	60 pulses/revolution, TTL level

The control signal u is converted to analog output and applied to the DC motor via a power amplifier system. The power amplifier output is limited to $\pm 10\,V$ which is the maximum voltage that can be applied to the DC motor system. ControlDesk software connects the user to the Real-time simulation, and allows to easily control, read and change parameters online in Simulink model. The overall experimental setup is shown in (Fig. 4.3).

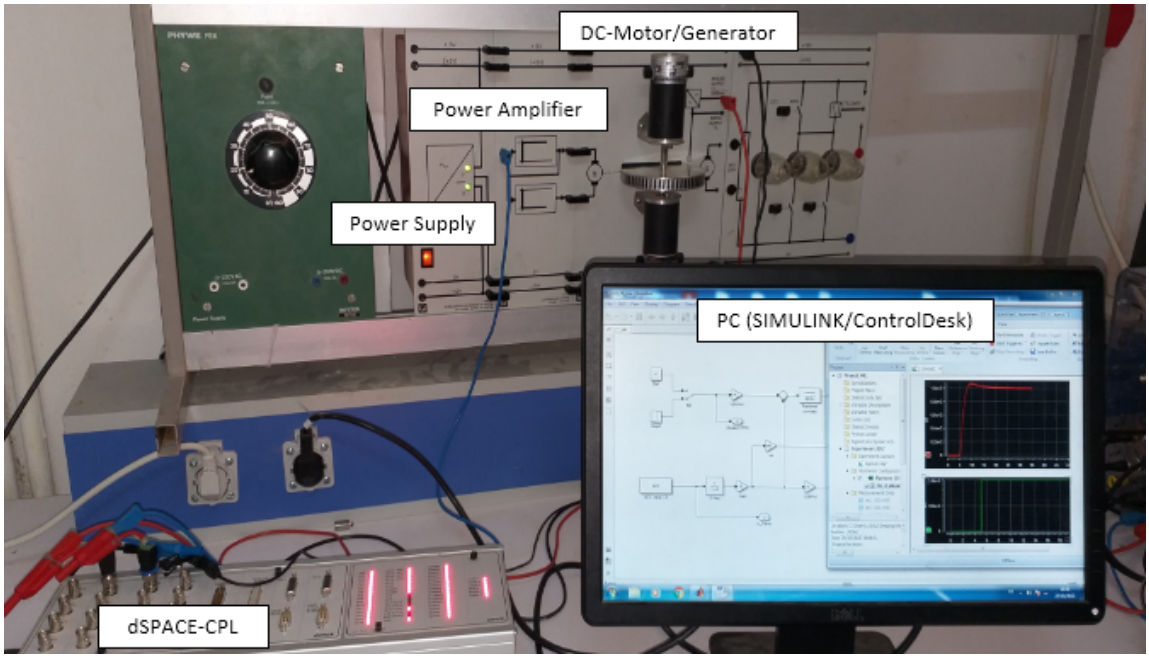

Figure 4.3 The overall experimental setup of DC motor-generator platform

4.2.2 dSPACE DS1104 Controller

The control board consists of three components: DS1104 controller board mounted within a personal computer, a breakout panel (Panel Connectors and LEDs) for connecting input/output signals to the DS1104 controller board and software tools (ControlDesk software) for operating the DS1104 controller board through the Simulink environment. The system is able to run complex control algorithms at high sampling rates.

The I/O chips (ADC, DAC, muxADC, muxDAC) are used as the communication ports for the I/O signals such as sensor output signal and the control signal. The control signal from the DAC port is used for controlling some of the state variables of the plant. All the ADC and DAC chips are bipolar with a voltage range of $\pm 10\,V$.

4.2.3 DC Motor Identification

For control purposes, the Motor/Generator set is modeled using Black-box identification technique (Fig. 4.4). This technique requires a prior model structure that fit system dynamics and estimate its parameters. There are many structures available to perform system identification such as *Transfer function*, with a given number of poles and zeros.

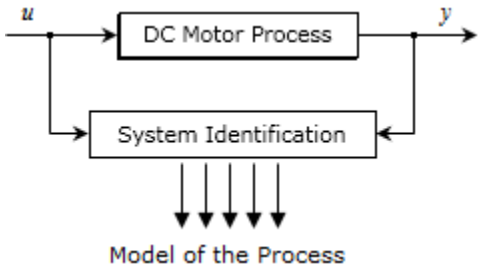

Figure 4.4 Schematic representation of system identification

4.2.3.1 System linearity

To determine the range in which the plant has linear behavior, different voltage step inputs are applied to the open-loop system and the corresponding motor RPM is recorded (Tab. 4.2). To check the linear behavior of the system in a chosen range of values, a figure (4.5) is prepared. The figure shows that the system has linear behavior in all chosen range of values.

Table 4.2 Voltage input & motor RPM data.

No	Voltage [V]	Motor RPM
1	1.71	250
2	2.37	490
3	3.50	860
4	4.50	1200
5	5.50	1570
6	7.50	2220
7	8.50	2550
8	10.0	3050

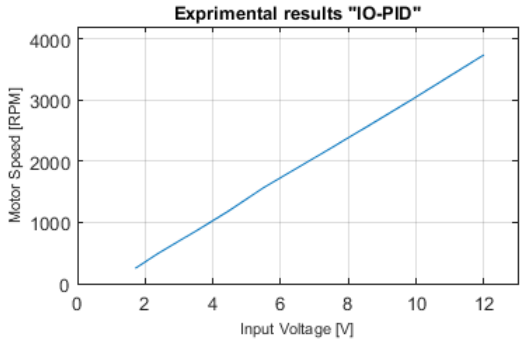

Figure 4.5 Input voltage vs. motor RPM

4.2.3.2 Consistency PRBS Sequence

To collect real-time data (input and output) from the system, a Simulink model (Fig. 4.7) is prepared. For a useful and consistency process data, the physical plant is excited by a PRBS (Pseudo-Random, Binary Signal) sequence, more details are given in (Appendix. (B.1)). Motor response to the PRBS sequence is presented in (Fig. 4.6).

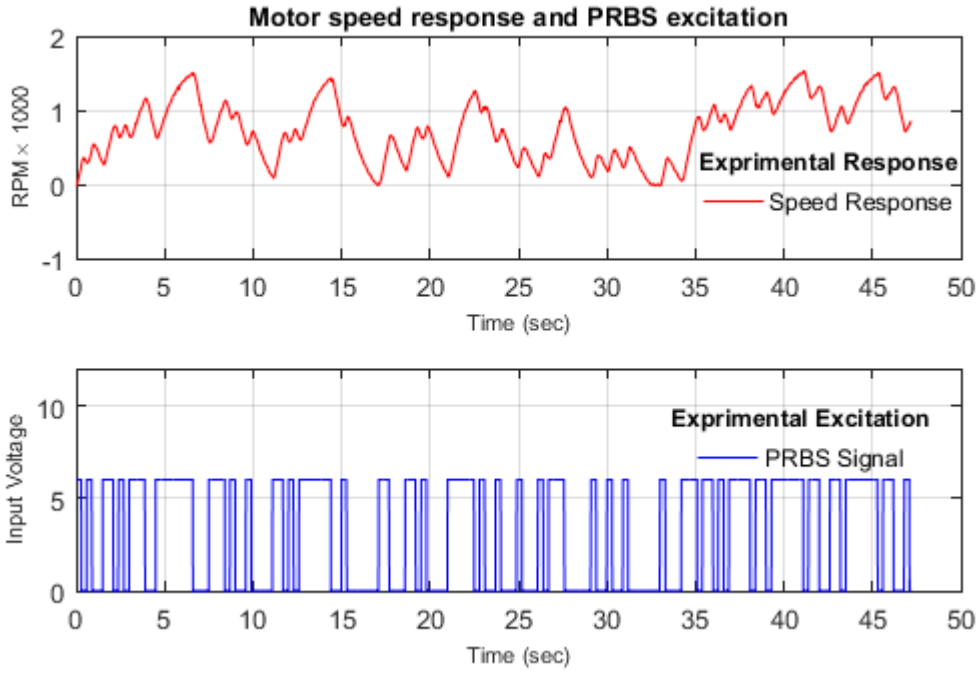

Figure 4.6 Identification data

4.2.3.3 Acquiring and Processing Data

Using the Simulink model (Fig. 4.7) and ControlDesk software, excitation input and the corresponding RPM speed can be recorded in real time. The collected data is converted into *iddata* objects for import into System Identification Toolbox.

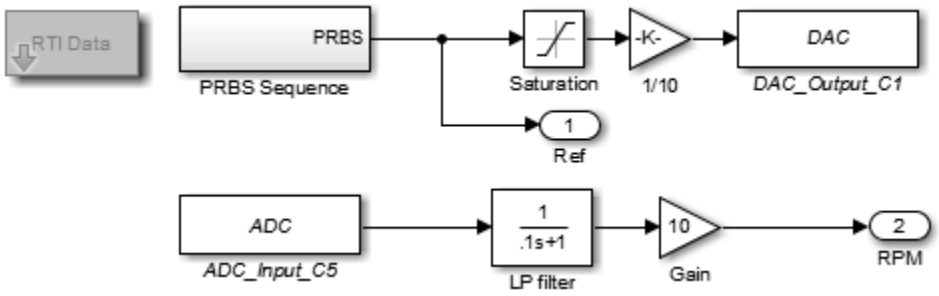

Figure 4.7 Open Loop Block for System Identification

Once the appropriate plant data are collected, we proceed to obtain the DC-motor model.

4.2.3.4 Plant Model Identification

Matlab command *ident* is used to launch the System Identification Tool. Figure (Fig. 4.8.b) shows six (6) models obtained using the System Identification Steps (Fig. 4.8.a).

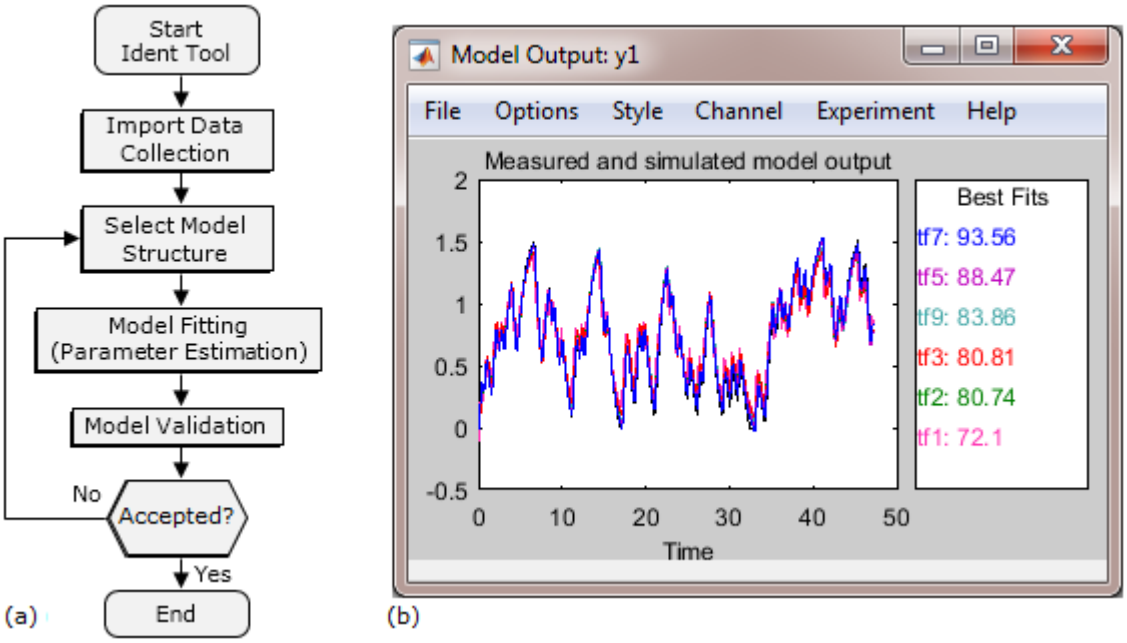

Figure 4.8 System Identification Process

The best model (Eq. 4.1) for the plant (Motor/Generator+Sensor+Power Amplifier) was obtained using Transfer Function Models approach, reaching 93.56% fit.

$$G(s) = \left(\frac{k_n}{s + 0.9013}\right) \tag{4.1}$$

where $k_n = 0.2507$ is the nominal value.

The figure (4.9) shows a comparison between simulated model and experimental response of DC motor. It is clear that identified model fits the real measured data.

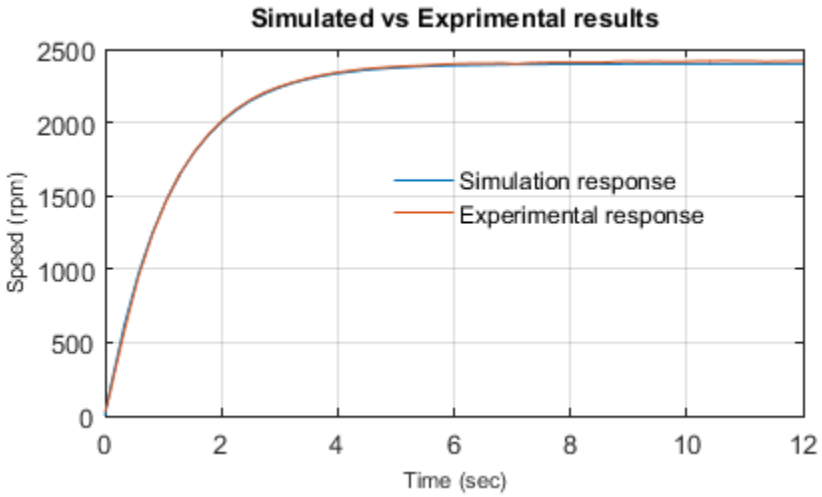

Figure 4.9 Comparing open-loop simulation and experimental results

4.2.4 Design of the Fractional Controller

For designing the speed fractional controller, the technique discussed in Section (2.5) is used. Thus, the specifications of the design are,

- Phase margin $\phi_m = 62°$,

- Unity gain crossover frequency $\omega_u = 0.7\,rad/s$.

To achieve these specifications in a frequency range $[\omega_l,\ \omega_h] = [0.07\,rad/s,\ 7\,rad/s]$ around ω_u, the open loop reference Bode's ideal function should be designed as (see Section 2.2.3),

$$L(s) = \frac{1}{(s/0.7)^{1.233}} \tag{4.2}$$

Using the Charef's method discussed in Section (1.4.1.2), $L(s)$ can be approximated by,

$$L(s) \approx L_a = \frac{49.269(s+0.02302)(s+0.1587)(s+1.094)(s+7.546)(s+52.03)}{(s+0.01467)(s+0.007)(s+0.1012)(s+0.6975)(s+4.809)(s+33.16)} \times \frac{1}{(s+228.6)} \tag{4.3}$$

Using equation (Eq. 2.27), the pole of $L_a(s)$ that is close to the pole of the original process $G_p(s)$ is, $L_D(s) = (s + 0.6975)$.

With the *MATLAB Control Toolbox*, the state feedback gain matrix K is obtained as, $K = [-0.2038]$. Then, the obtained fractional controller for the DC motor (Eq. 4.1) is,

$$C(s) = \frac{196.53(s+0.02302)(s+0.1587)(s+1.094)(s+7.546)(s+52.03)}{(s+0.01467)(s+0.007)(s+0.1012)(s+4.809)(s+33.16)(s+228.6)} \tag{4.4}$$

In the following section, the designed fractional controller will be simulated on MATLAB and compared to the experimental results.

4.2.5 Simulation Results

For simulation purposes, a Simulink model of control system is constructed as shown in (Fig. 4.10).

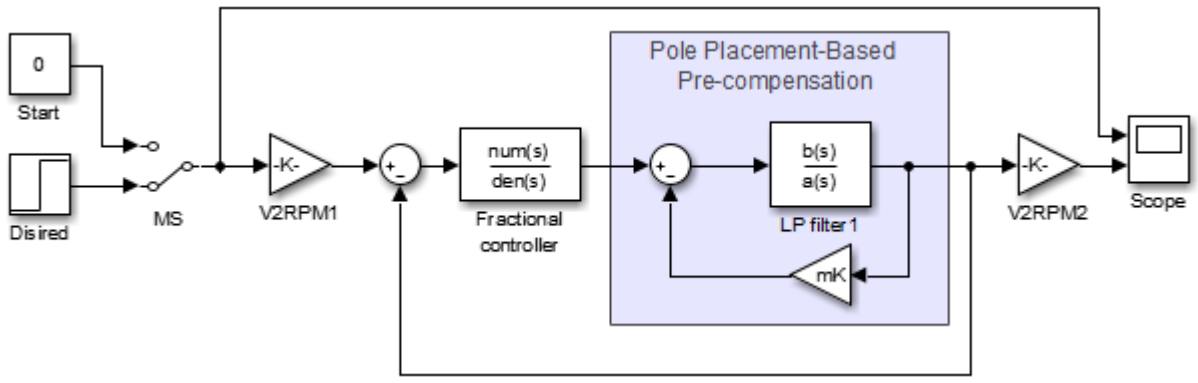

Figure 4.10 Closed-loop Simulink model for simulated DC motor

To check the controller design, a step input is given to the DC Motor. The simulation results of (Fig. 4.11) show that the designed controller satisfies the performance described in the Bode's ideal loop. Thus, the next step, is the controller implement in a real-time system.

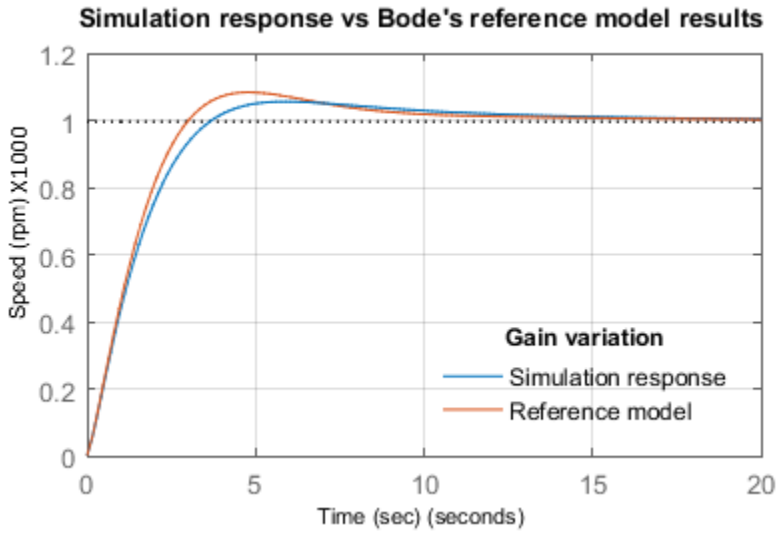

Figure 4.11 Simulated DC motor step response vs Reference model step response

4.2.6 Experimental Results

For dSPACE implementation, the DC-motor model is replaced with the real-motor of (Fig. 4.1). The closed-loop of the real-motor is shown in (Fig. 4.12).

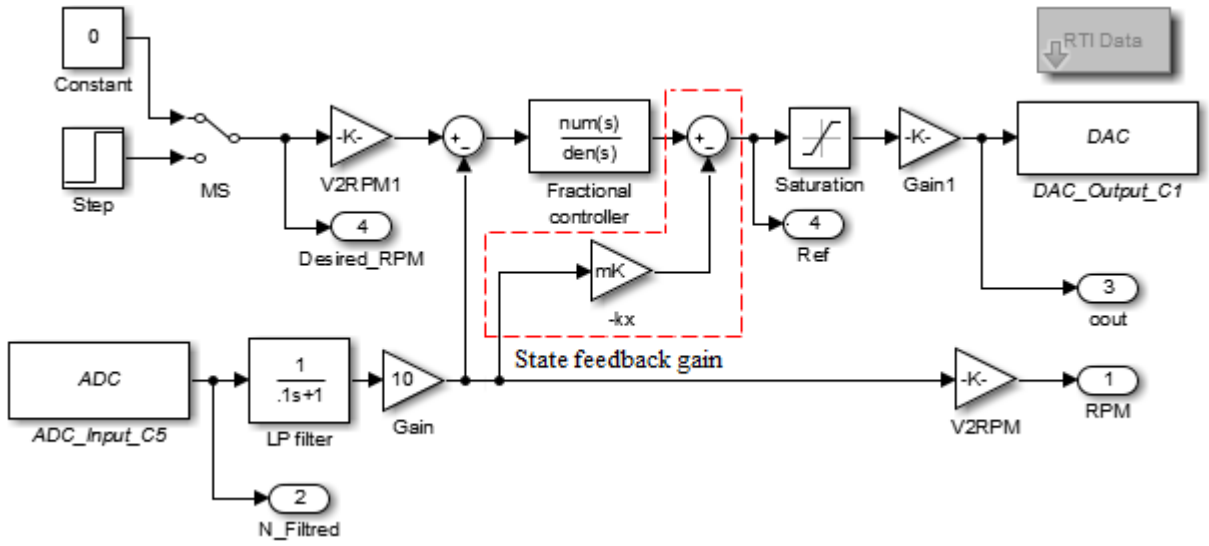

Figure 4.12 Simulink model for real-time implementation of DC motor control

Figure (4.13) shows comparison of the response simulation with real-time results for $k_n = 1.0$.

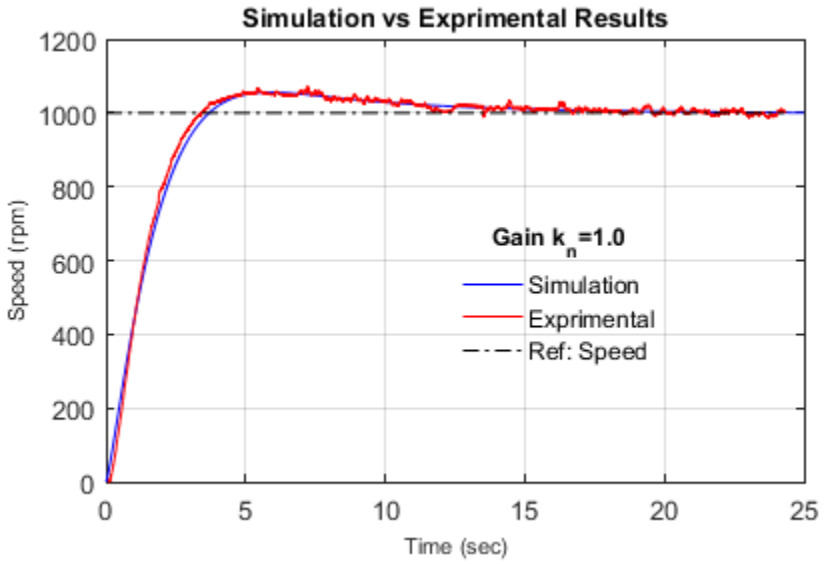

Figure 4.13 Real-time vs simulation results for a step of 1000 (rpm) with $k_n = 1.0$

Form (Fig. 4.13), we can see that the experimental response overlaps the simulation response, which validates the effectiveness of the designed fractional controller.

In order to check the robustness of the control system, a variation of $\pm 50\%$ in the nominal plant gain k_n was considered. The step responses of the simulation and experimental results are illustrated in (Fig. 4.14) and (Fig. 4.15) respectively.

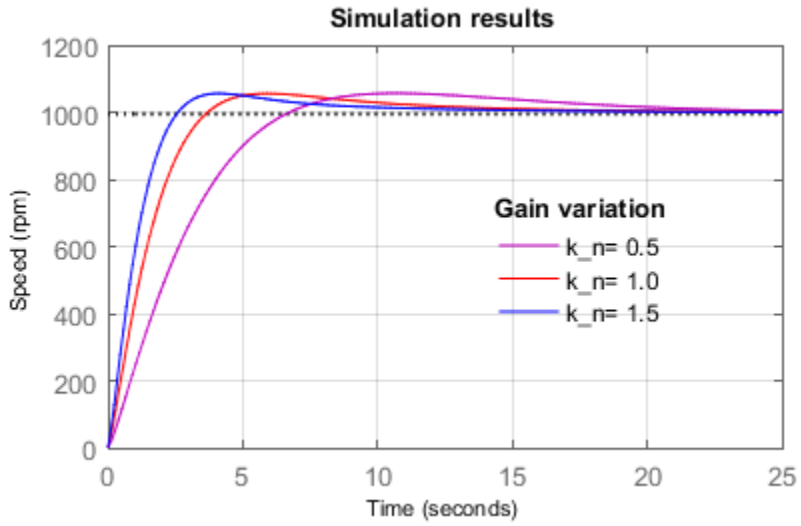

Figure 4.14 Robustness to gain variation (Simulation:results)

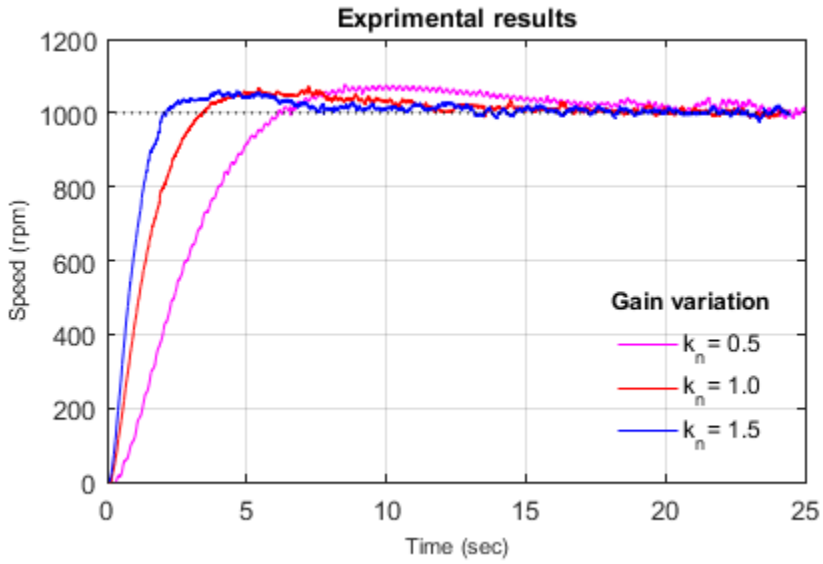

Figure 4.15 Robustness to gain variation (Experimental:results)

Figure (Fig. 4.11) and (Fig. 4.12), show that the experimental are close to simulation results and the control system is robust to gain variations with iso-damping property as expected.

This part presents a successful implementation of fractional order controller for a power amplifier actuated DC-motor speed control system in both simulation and experimental studies. For the simulation model, a mathematical first order model to study DC-motor dynamics behavior is generated from real data collection. The simulated DC-motor model is then validated experimentally using dSPACE controller board DS1104, ControlDesk software and MatLab/Simulink.

A PC-based fractional order controller for the DC-motor system using the proposed control structure (see Section 2.5) was then implemented through experimental test on real DC-motor speed control. Two types of DC-motor dynamics test are performed for the purpose of model validation namely normal step response test and robustness against gain change test. The results of model validation show that the behaviors of the model closely follow the behavior of a real plant.

Finally, we also demonstrated the capacity of dSPACE platform to accomplish real time fractional order control and we can conclude that this platform can be a powerful tool for the development of different fractional order control strategies.

4.3 Implementation Using Low-Cost Platform

MATLAB Simulink environment is a good choice for implementing complicated mathematical models of control. Arduino-Simulink interface is on the other hand a low-cost for data acquisition/communication with real time world.

In MATLAB suite, there exist several toolboxes and functions used for identification and data collecting, e.g.,

- *ident*: System Identification Toolbox.
- *idinput* : Generates input signals for identification.

The PRBS type is used to generate a Pseudo-Random, Binary Signal, see Appendix. (B.1) for more details.

Arduino board (a very quickly popular microcontroller) is an open hardware platform used along this project. All necessary tools including software, libraries and documentation to work with his board can be found on its webpage. Additional Arduino IO package needed to link both platforms (Simulink and Arduino) can also be downloaded from the file exchange area of the MathWorks web.

There are two different ways to communicate Arduino board with Matlab Simulink: (1) Running the Arduino IO package as a server on the Arduino board that listens for Matlab commands from the serial port, and after execute such commands, if asked, returns an answer. (2) Converting the Simulink model to code that runs directly on Arduino, and the Arduino board can be disconnected from host Computer. This work is based on the first method .

Motivated by the remarkable robustness, performance quality and the high computing power challenges in terms of real implementation of the fractional controllers. The aim of this work, is the control of FOPTD by a FOC using data acquisition-based Arduino board. A simple analytical rules are used for the analysis and design of the FOC. The good experimental results, compared with those obtained with theoretical simulation, confirm that the proposed interface can be used to support research and teaching feedback control systems via experimental investigations on a low-cost laboratory kit.

4.3.1 Experimental Platform

The experimental platform (homemade) used in this work is a DC motor-generator set that consists of two DC motors connected face to face via a shaft as shown in (Fig. 4.16). The first one is a 12 volts DC motor acts as the actuator for our plant and operates with a maximum output shaft speed of 4200 rpm. The second one is a 5 volts DC motor used as a tachometer to measure the speed of the motor. The first motor fed by a voltage-to-current PWM and converts it into angular speed, the second motor (generator), in turn, converts this angular speed back into a voltage. The generator acts as a tachometer (a device for measuring rotational speed). The set motor/generator together gives us a system that takes an input voltage and produces an output voltage.
A photo-interrupter sensor mounted below the encoder wheel can also be used as a negative feedback/speed sensor.

The configuration Voltage-in/Voltage-out is easy and ideally suited to DAC/ADC computer-based instrument such as Arduino board (a very quickly popular microcontroller).

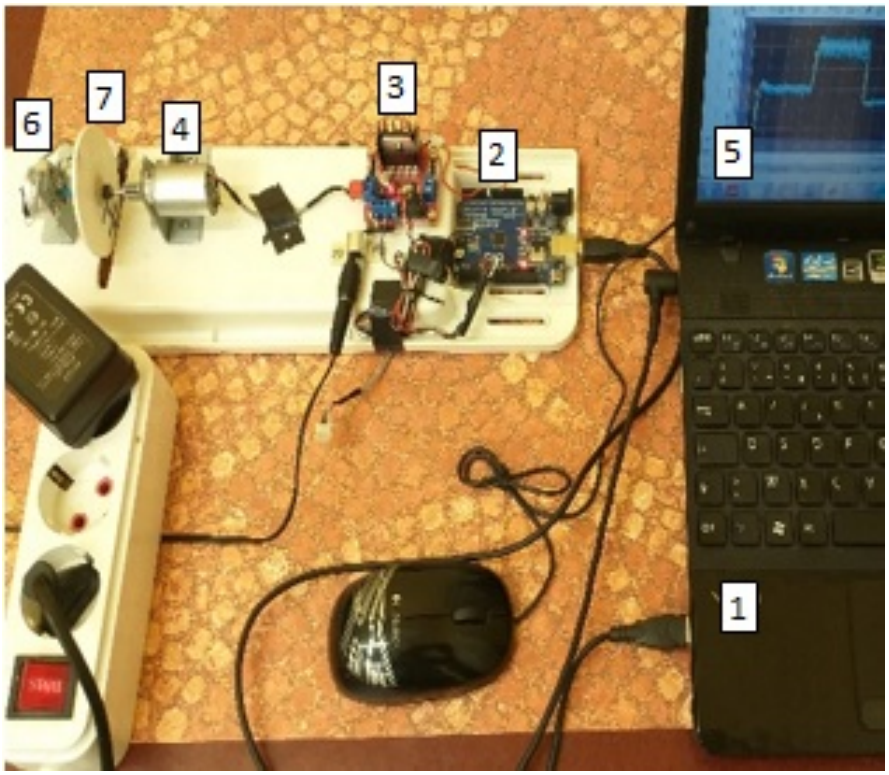

Figure 4.16 DC motor-generator platform

4.3.2 Experimental setup

Components used in our experimental system are: (1) A personal computer, (2) An Arduino Uno (Atmel board) used as Data Acquisition System (DAQ) to send/receive date to/from the computer, performs tachometer's calculations and processes the PWM signal generation, (3) A full-bridge motor driver L298N used for smooth operation of the DC motor, (4) A 12V DC motor acts as an actuator, (5) A MATLAB/Simulink software, (6) A DC motor (generator) used as a tachometer to measure rotational speed, (7) An incremental encoder only used to measure minimum and maximum speed of the motor also used to calculate the ratio voltage/angular speed constant.

The experimental setup is described in the block diagram of (Fig. 4.17). I/O configurations of the Arduino are given in (Tab. 4.3).

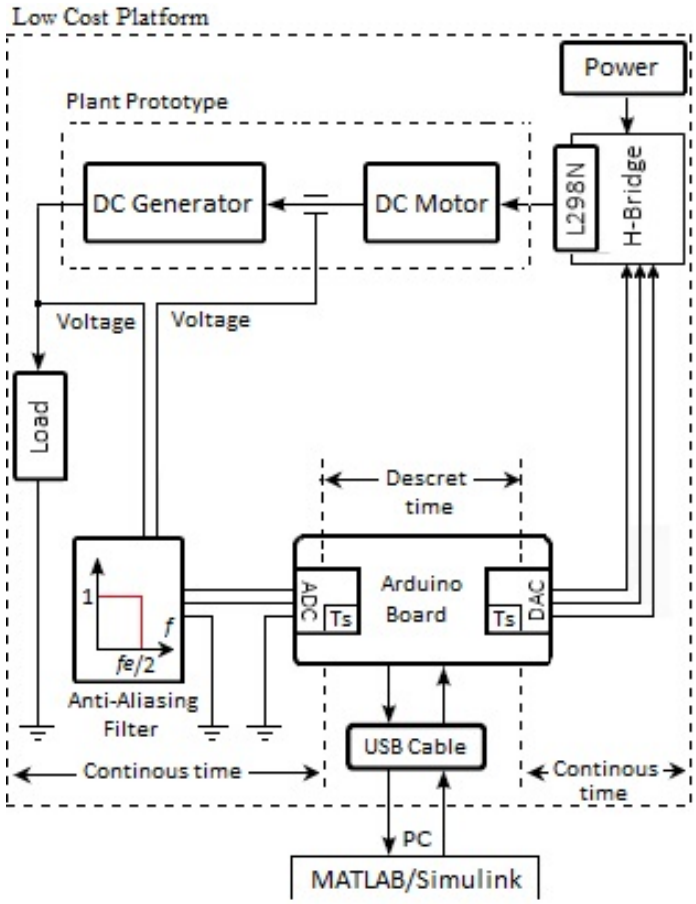

Figure 4.17 The proposed experimental setup

Table 4.3 Arduino I/O Configuration

No	Pin	Type	Description
1	2	Digital Input	Incremental encoder
2	5	Digital Output	PWM signal.
3	7	Digital Output	Forward direction.
4	9	Digital Output	Backward direction.
5	11	Digital Output	PWM signal.
6	12	Digital Output	Used for output relay.
7	A0	Analog Input	Measured generator voltage.

4.3.3 Plant Modelling and Identification

To simplify the considered plant, the dynamic characteristics of the generator can be ignored and considered simply as a speed sensor. Figure (Fig. 4.18) shows the simplified scheme of the plant.

The plant (to us unknown) is approximately modeled by a first order plus time delay as,

$$G(s) = \left(\frac{k_n}{\tau s + 1}\right) e^{-Ls} \tag{4.5}$$

To identify the parameters k_n, τ and L, the plant was excited by a PRBS (pseudo random binary signal) input signal.

To generate this PRBS sequence, the following command is used in Matlab,

$$idinput(1001,\text{'PRBS'}, [0\ 1/1], [0\ 5]);$$

By using the Matlab *ident* ToolBox for identification, the transfer function of the plant's model (voltage-voltage) of (Eq. 4.5) was identified experimentally to a FOPTD as,

$$G(s) = \frac{V_{out}(s)}{V_{in}(s)} = \left(\frac{0.4540}{0.591s + 1}\right) e^{-0.132s} \tag{4.6}$$

Figure (Fig. 4.18), presents the plant response excited by a PRBS signal.

From (Fig. 4.19) the plant transfer function voltage-speed can be given by,

$$\frac{\omega(t)}{V_{in}(t)} = \left(\frac{0.4540/K_{gen}}{0.591s + 1}\right) e^{-0.132s} \tag{4.7}$$

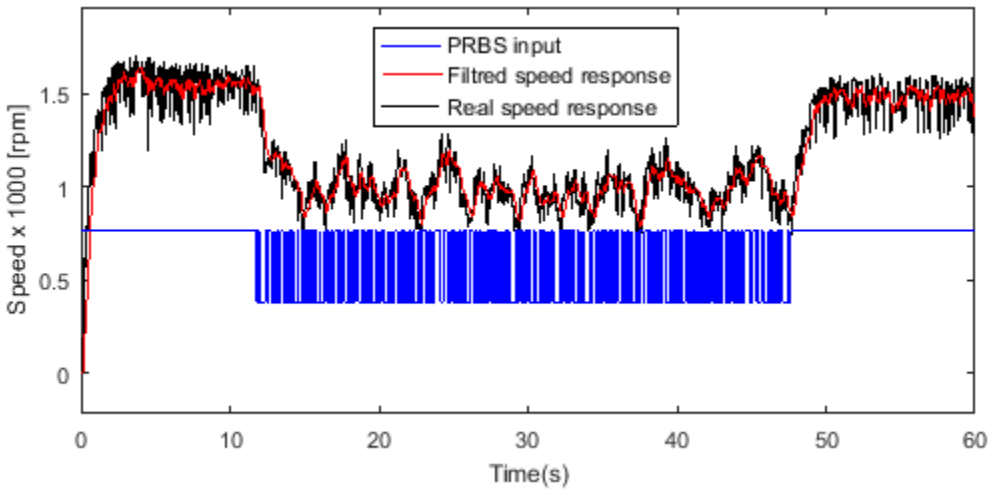

Figure 4.18 Real identification data

where K_{gen} is the voltage/angular speed ratio, this constant was found to be $K_{gen} \cong 1/1000$. Then, DC motor speed is the measured voltage from the generator multiplied by 1000.

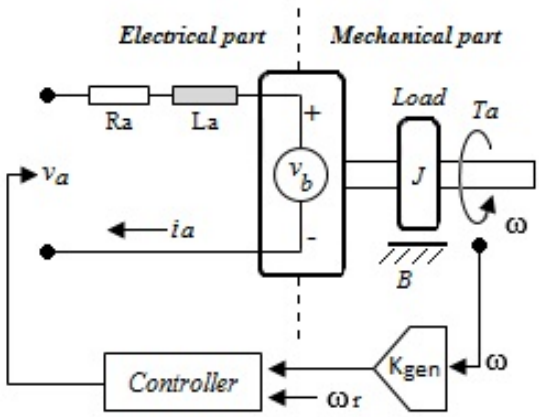

Figure 4.19 Simplified scheme of the plant

4.3.4 Design of the Fractional Controller

After identification of the plant, the next step is the designing of a fractional order controller for the speed of the DC motor control. To this end, we apply a simple analytical design approach based on gain and phase margins. The obtained fractional order controller is [15],

$$C(s) = k_p \left(\frac{Ts+1}{s^{\lambda}} \right) = k_p \left(\frac{1}{s^{\lambda}} + Ts^{1-\lambda} \right) \tag{4.8}$$

which is, in fact, a particular case of a $PI^{\lambda}D^{\mu}$ controller, with $\mu = 1 - \lambda$. The parameters k_p, T and λ are tuned as discussed in [15].

Given a desired gain and phase margin (A_m=10, ϕ_m=55°) for the specifications of the control loop, the fractional order controller was designed as follows,

$$C(s) = 3.5653 \left(\frac{0.591s + 1}{s^{1.38}} \right) \tag{4.9}$$

In order to have a realistic form of the fractional controller (Eq. 4.9), approximation method [20] is used to approximate the fractional integration operator to feasible filters.

Before the implementation and verification of the controller performances, a Simulink model (see Fig. 4.24) of the fractional controller was created then, its validation is achieved by means of pure software and hardware-in-the-loop (HIL) real-time simulations.

4.3.5 Experimental Results and Discussion

In this section, a part of the simulation and experimental results that were conducted in order to validate the fractional order controller are presented.

Hence, kits and tools used to set-up the platform of our application are shown in (Fig. 4.20).

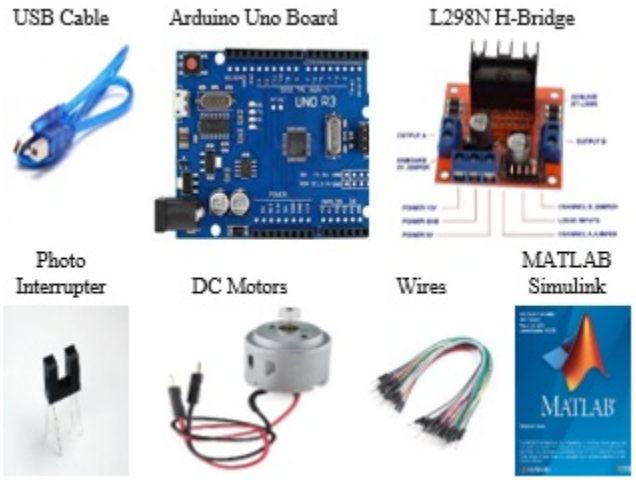

Figure 4.20 Tools Kit used in the application

Figure (Fig. 4.24), illustrates the Simulink model of the Hardware-In-the-Loop (HIL) real-time simulation with the designed fractional controller used in this experimental.

Figure (4.21) shows comparison step responses of the simulation vs experimental results.

In order to check the control system robustness, a variation of ±50% in the nominal plant gain k_n was introduced. The experimental and simulation step responses are shown in (Fig. 4.22). From (Fig. 4.21), and (Fig. 4.22) we can see that the experimental results are close to simulation results and the control system is robust to gain variations with iso-damping property as expected.

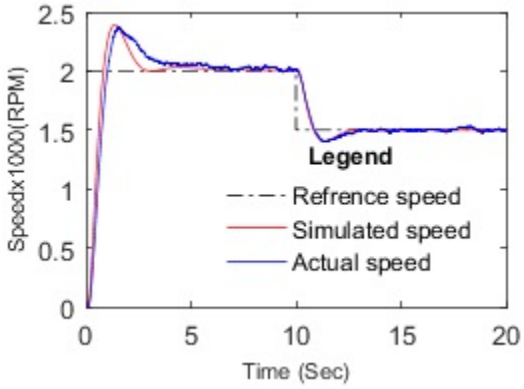

Figure 4.21 Simulation vs Experimental Results

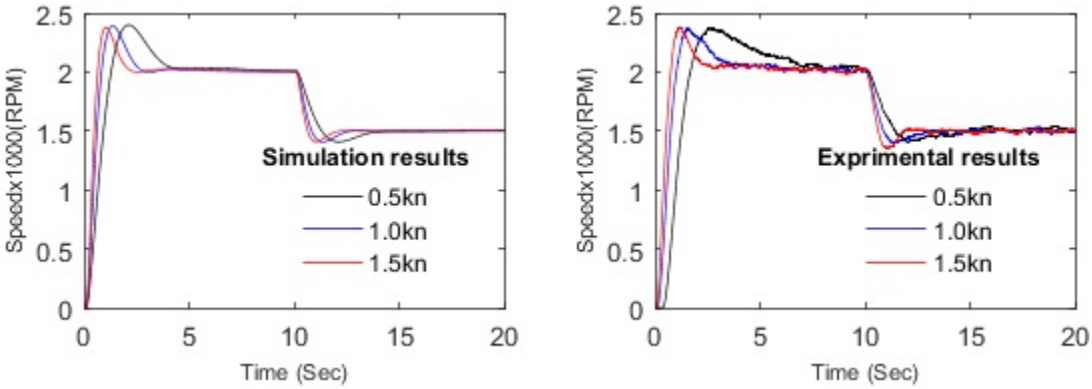

(a) Simulation results **(b)** Experimental results

Figure 4.22 Robustness to gain variation

4.3.5.1 Robustness to load disturbances test

To achieve this test, the plant is subject to electrical load disturbances during steady-state behavior which is set to RL=55Ω at t=20 seconds as a parameter variation, then set back to RL=0Ω at t=40 seconds. The results of this test are illustrated in (Fig. 4.23a) and (Fig. 4.23b). Figure (Fig. 4.23c) shows the error between the reference and the speed output.

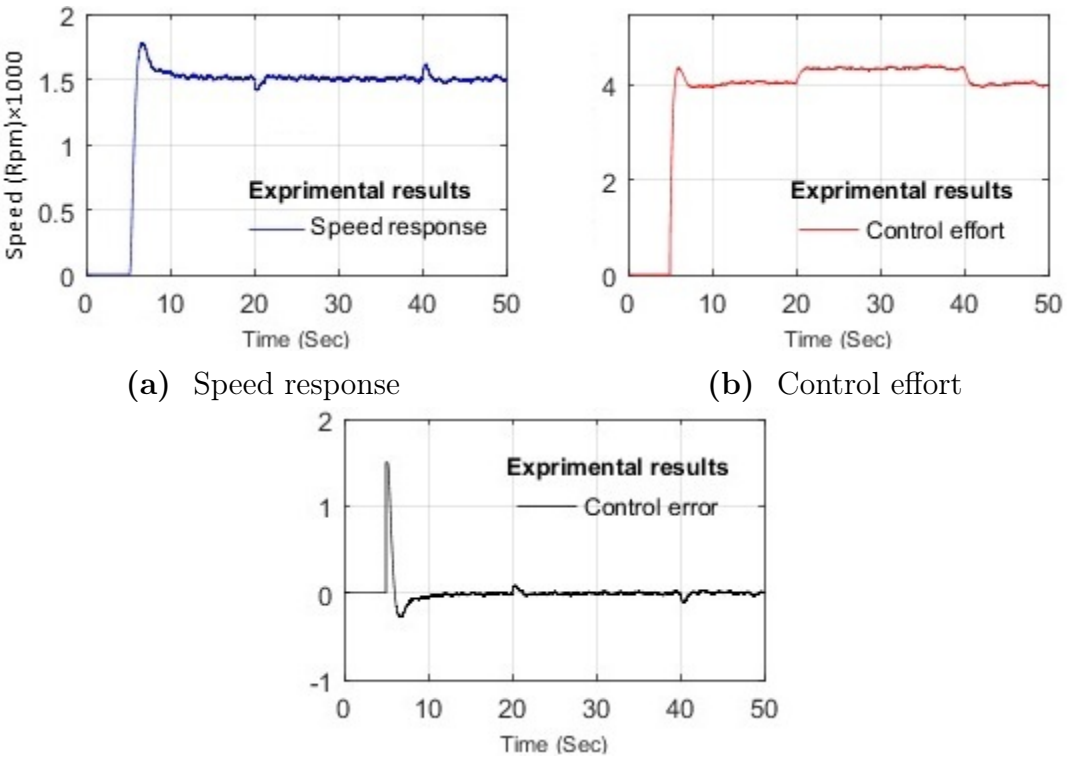

(a) Speed response **(b)** Control effort

(c) Error

Figure 4.23 DC motor response for the robustness to load disturbance tests

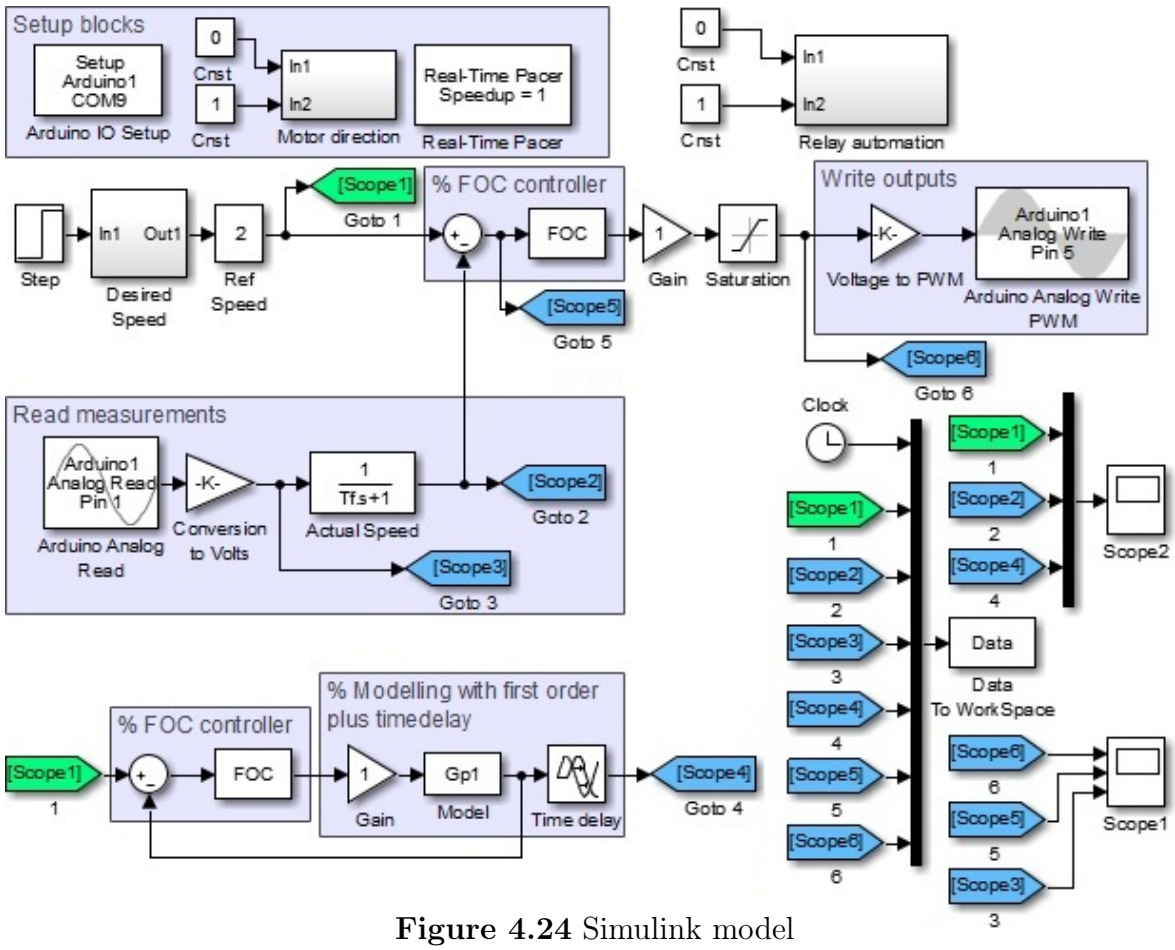

Figure 4.24 Simulink model

4.4 Conclusion

This part, presents a successful development of a low-cost platform containing the necessary tools to deal with Real Time Data Acquisition and control on Arduino board.

Important robustness tests have been done to validate the control system. The validation has been successfully done through an example of DC motor control. The results were obtained nearly close to those of the simulation which confirm and approve that the proposed Arduino-Simulink interface can be used to support research and teaching feedback control systems via experimental investigations on a low-cost laboratory tool.

CONCLUSION AND FUTURE WORK

In this work, various aspects of research on fractional order adaptive control are discussed in accordance with the problems stated at the beginning of the thesis. In this part, we formulate concluding remarks, summarize the contributions of this work and sketch future research directions.

Conclusion

This work focuses on the contribution to fractional order robust control, as well as robust adaptive control. Indeed, new techniques and strategies of control are proposed in this context, while showing their advantages by applying them to different processes.

We have first presented various aspects and fundamentals of fractional order systems that are necessary for theoretical development in fractional order control.
A big problem encountered as a part of fractional control is determining and tuning of controller parameters to achieve user-desired controller performances.

Next, we presented, in chapter 2, the first contributions of this work which lies in the following two aspects:

(1) A new simple and useful tuning technique of fractional order robust controllers. This technique can simply achieves user-specified gain and phase margins using the so-called Bode's ideal transfer function or fractional order integrator (FOI) as a reference model.

The basis of this method is to use a standard pole placement technique to align each pole of the plant transfer function with the nearest one given by the Rational Transfer Function Approximation of the FOI. The most innovative character of this method is its simplicity and its remarkable performances in terms of robustness towards the static gain variation. Simulations results show that the proposed method is simple, effective, can ensures the iso-damping property for the control system and can be investigated to cover processes that have complex-conjugate poles or unstable conditions.

(2) A simple technique based on a fractional PI controller where its coefficients are estimated online in the time domain using the Bode's ideal loop as a reference model. The order of the integration in PI^{λ} controller is tuned based on opminimizing performance indices such as Integral Square Error(ISE). We showed, through one example of simulation, that the robustness against the gain variations accomplished by the fractional order PI^{λ} controller is clearly better than that of integer order PI controller.

In the following chapters, we presented a second contribution concerning the robust adaptive control. The main part of the Chapter 3 was devoted to the Model Reference Adaptive Control MRAC, with the MIT control law. In this part a novel design scheme is proposed to tune fractional adaptive PI controller for a class of First Order Plus Time Delay (FOPTD) plants where. The fractional adaptive control is improved in the two following points,

- The initial parameters of the adaptive algorithm can be fixed in offline first, then an online tuning is performed to achieve the robustness of the controlled plant,
- The second point is the new fractional order Model Reference tuning form which is introduced using the plant model.

Through an illustrative example, simulation results show the effectiveness of the proposed scheme.

In Chapter 4, two different platform types are developed containing the necessary tools to deal with Real Time Data Acquisition and Control for the purpose of fractional order control validation namely, dSPACE Controller DS1104 and a low-cost platform on Arduino

board using MATLAB/Simulink with ControlDesk software and MATLAB/Simulink Support Package, respectively. Important robustness tests have been done to validate the implemented platforms. The validation has been successfully done through an example of DC motor control.

In addition to the above contributions, further research directions and many improved results where presented during this thesis. Most of the new results listed above were published in conferences and journals, in particular (see Appendix C).

Future Research

We now formulate concluding remarks pertaining to the results discussed in this thesis in accordance with the problems stated at the beginning of the thesis. The most important remarks can be summarized as follows,

- The tuning of the fractional order (λ) of the technique presented in (Section 2.6) can be optimized using optimization algorithms such as particle swarm optimization (PSO).
- The new tuning technique presented in (Section 2.5) can be extended to the fractional order adaptive control technique.
- Most techniques presented in this work are intended to be studied and analyzed for stability performance using Lyapunov theorem namely,
  - Fractional Robust Controller Design Using Bode's Ideal Transfer Function detailed in (Section 2.5),
  - Design of PI$^{\lambda}$ using Bode's integrals based online estimation algorithm presented in (Section 2.6).
- The implementation of fractional controller in a Low-Cost Platform presented in Chapter 4 can be extended to a real and stand alone application instead of software and hardware-in-the-loop (HIL) real-time simulations.

REFERENCES

[1] M. Abedini et al. "Model reference adaptive control in fractional order systems using discrete-time approximation methods". In: *Communications in Nonlinear Science and Numerical Simulation* 25.1-3 (2015), pp. 27–40.

[2] M.A. Al-Alaoui. "Novel IIR differentiator from the Simpson integration rule". In: *IEEE Transactions on Circuits and Systems I: Fundamental Theory and Applications* 41.2 (1994), pp. 186–187.

[3] T.J. Anastasio. "The fractional-order dynamics of brainstem vestibulo-oculomotor neurons". In: *Biological cybernetics* 72.1 (1994), pp. 69–79.

[4] M. Aoun et al. "Numerical simulations of fractional systems". In: *ASME 2003 International Design Engineering Technical Conferences and Computers and Information in Engineering Conference*. American Society of Mechanical Engineers Digital Collection. 2003, pp. 745–752.

[5] K. Assaleh and W.M. Ahmad. "Modeling of speech signals using fractional calculus". In: *2007 9th International Symposium on Signal Processing and Its Applications*. IEEE. 2007, pp. 1–4.

[6] K.J Åström and T. Hägglund. "PID controllers: theory, design and tuning". In: *Research Triangle Park, Instrument Society of America* (1995).

[7] K.J. Åström and B. Wittenmark. *Adaptive control. Mineola*. 2008.

[8] R. Bagley, D. Swinney, and K. Griffin. "Fractional calculus-A new approach to modeling unsteady aerodynamic forces". In: *29th Aerospace Sciences Meeting*. 1991, p. 748.

[9] I. Bar-Kana. "On parallel feedforward and simplified adaptive control". In: *Adaptive Systems in Control and Signal Processing 1986*. Elsevier, 1987, pp. 99–104.

[10] I. Bar-Kana. "Positive realness in discrete-time adaptive control systems". In: *1986 American Control Conference*. IEEE. 1986, pp. 1440–1443.

[11] R.S. Barbosa, J.T. Machado, and I.M. Ferreira. "Tuning of PID controllers based on Bode's ideal transfer function". In: *Nonlinear dynamics* 38.1-4 (2004), pp. 305–321.

[12] Y. Bensafia and S. Ladaci. "Adaptive control with fractional order reference model". In: *Int. J. of Sciences and Techniques of Automatic control & computer engineering, IJ-STA* 5.2 (2011), pp. 1614–1623.

[13] H.W. Bode et al. "Network analysis and feedback amplifier design". In: *INC. Princeton New York* (1945).

[14] M. Bošković et al. "Analysis of electrical circuits including fractional order elements". In: *2017 6th Mediterranean Conference on Embedded Computing (MECO)*. IEEE. 2017, pp. 1–6.

[15] B. Boudjehem, D. Boudjehem, and H. Tebbikh. "Analytical Design Method for Fractional Order Controller Using Fractional Reference Model". In: *New Trends in Nanotechnology and Fractional Calculus Applications*. Springer, 2010, pp. 295–303.

[16] D. Cafagna. "Fractional calculus: A mathematical tool from the past for present engineers [Past and present]". In: *IEEE Industrial Electronics Magazine* 1.2 (2007), pp. 35–40.

[17] G. Carlson and C. Halijak. "Approximation of fractional capacitors (1/s)ˆ(1/n) by a regular Newton process". In: *IEEE Transactions on Circuit Theory* 11.2 (1964), pp. 210–213.

[18] A. Charef, A. Djouambi, and H. Sun. "Fractional order feedback control systems". In: *Proceedings of the 4th JIEEEC, Jordanie* (2001).

[19] A. Charef and D. Idiou. "Design of analog variable fractional order differentiator and integrator". In: *Nonlinear Dynamics* 69.4 (2012), pp. 1577–1588.

[20] A. Charef et al. "Fractal system as represented by singularity function". In: *IEEE Transactions on automatic Control* 37.9 (1992), pp. 1465–1470.

[21] A. Charef et al. "Fractional order adaptive controller for stabilised systems via high-gain feedback". In: *IET Control Theory & Applications* 7.6 (2013), pp. 822–828.

[22] Y.Q. Chen, C. Hu, and K.L. Moore. "Relay feedback tuning of robust PID controllers with iso-damping property". In: *42nd IEEE International Conference on Decision and Control (IEEE Cat. No. 03CH37475)*. Vol. 3. IEEE. 2003, pp. 2180–2185.

[23] Y.Q. Chen and K.L. Moore. "Discretization schemes for fractional-order differentiators and integrators". In: *IEEE Transactions on Circuits and Systems I: Fundamental Theory and Applications* 49.3 (2002), pp. 363–367.

[24] Y.Q. Chen, I Petráš, and D. Xue. "Fractional order control-a tutorial". In: *2009 American control conference*. IEEE. 2009, pp. 1397–1411.

[25] Y.Q. Chen, R. Sun, and A. Zhou. "An overview of fractional order signal processing (FOSP) techniques". In: *ASME 2007 International Design Engineering Technical*

Conferences and Computers and Information in Engineering Conference. American Society of Mechanical Engineers Digital Collection. 2007, pp. 1205–1222.

[26] Y.Q. Chen and B.M. Vinagre. "A new IIR-type digital fractional order differentiator". In: *Signal processing* 83.11 (2003), pp. 2359–2365.

[27] Y.Q. Chen, B.M. Vinagre, and I. Podlubny. "Continued fraction expansion approaches to discretizing fractional order derivatives—an expository review". In: *Nonlinear Dynamics* 38.1-4 (2004), pp. 155–170.

[28] Y.Q. Chen, D. Xue, and H. Dou. "Fractional calculus and biomimetic control". In: *2004 IEEE International Conference on Robotics and Biomimetics*. IEEE. 2004, pp. 901–906.

[29] Y.Q. Chen et al. "A robust tuning method for fractional order PI controllers". In: *IFAC Proceedings Volumes* 39.11 (2006), pp. 22–27.

[30] C. Copot, C.I. Muresan, and R. De Keyser. "Speed and position control of a DC motor using fractional order PI-PD control". In: *3rd International Conference on Fractional Signals and Systems (FSS-2013)*. 2013.

[31] G. Cottone and M. Di Paola. "On the use of fractional calculus for the probabilistic characterization of random variables". In: *Probabilistic Engineering Mechanics* 24.3 (2009), pp. 321–330.

[32] S. Das and A. Gupta. "Generalized frequency domain robust tuning of a family of fractional order PI/PID controllers to handle higher order process dynamics". In: *Advanced Materials Research*. Vol. 403. Trans Tech Publ. 2012, pp. 4859–4866.

[33] Y. Ding and H. Ye. "A fractional-order differential equation model of HIV infection of CD4+ T-cells". In: *Mathematical and Computer Modelling* 50.3-4 (2009), pp. 386–392.

[34] A. Djouambi, V.A. Besançon, and A. Charef. "Fractional system identification using recursive algorithms approach". In: *2007 European Control Conference (ECC)*. IEEE. 2007, pp. 1436–1441.

[35] A. Djouambi, A. Charef, and T. Bouktir. "Fractal Robustness and Parameter Tuning $PI^{\lambda}D^{\mu}$ Controllers". In: *Proceedings of the 5th WSEAS Int. Conf. on Signal, Speech and Image Processing, Corfu, Greece*. 2005.

[36] A. Djouambi, A. Charef, and A. Voda. "Fractional order controller based on bode's ideal transfer function". In: *Control and Intelligent Systems* 38.2 (2010), p. 67.

[37] A. Djouambi, A. Charef, and A. Voda. "Numerical simulation and identification of fractional systems using digital adjustable fractional order integrator". In: *2013 European Control Conference (ECC)*. IEEE. 2013, pp. 2615–2620.

[38] A. Djouambi, A. Voda, and A. Charef. "Recursive prediction error identification of fractional order models". In: *Communications in Nonlinear Science and Numerical Simulation* 17.6 (2012), pp. 2517–2524.

[39] D.M. Domínguez, M. Marín, and M. Camacho. "Macrophage ion currents are fit by a fractional model and therefore are a time series with memory". In: *European Biophysics Journal* 38.4 (2009), pp. 457–464.

[40] F.B.M. Duarte and J.T. Machado. "Pseudoinverse trajectory control of redundant manipulators: a fractional calculus perspective". In: *Proceedings 2002 IEEE International Conference on Robotics and Automation (Cat. No. 02CH37292)*. Vol. 3. IEEE. 2002, pp. 2406–2411.

[41] N. Engheia. "On the role of fractional calculus in electromagnetic theory". In: *IEEE Antennas and Propagation Magazine* 39.4 (1997), pp. 35–46.

[42] N. Engheta. "Fractional curl operator in electromagnetics". In: *Microwave and Optical Technology Letters* 17.2 (1998), pp. 86–91.

[43] M. Faryad and Q.A. Naqvi. "Fractional rectangular waveguide". In: *Progress In Electromagnetics Research* 75 (2007), pp. 383–396.

[44] M. Ganji and F. Gharari. "An application of discrete fractional calculus in statistics". In: *Investigación Operacional* 38.3 (2018), pp. 272–280.

[45] M.L. Hadjili and L. Abida. "Commande adaptative à modèle de référence d'ordre fractionnaire". In: *Proc. CMSE* 94 (1994).

[46] S.E. Hamamci. "An Algorithm for Stabilization of Fractional-Order Time Delay Systems Using Fractional-Order PID Controllers". In: *IEEE Transactions on Automatic Control* 52.10 (2007), pp. 1964–1969.

[47] T.T. Hartley. *Fractional system identification: an approach using continuous order-distributions*. Vol. 99. 209640. NASA Glenn Research Center, 1999.

[48] T.T. Hartley and C.F. Lorenzo. "Dynamics and control of initialized fractional-order systems". In: *Nonlinear Dynamics* 29.1-4 (2002), pp. 201–233.

[49] R. Hilfer. *Applications of fractional calculus in physics*. Vol. 35. 12. World scientific Singapore, 2000.

[50] I. Horowitz. "Application of quantitative feedback theory (QFT) to flight control problems". In: *29th IEEE Conference on Decision and Control*. IEEE. 1990, pp. 2593–2598.

[51] R. Hotzel and M. Fliess. "Systémes linéaires fractionnaires avec et sans retard: Stabilité, commande, exemples". In: *Proc. Actes d'AGIS* 97 (1997), pp. 53–58.

[52] M. Ichise, Y. Nagayanagi, and T. Kojima. "An analog simulation of non-integer order transfer functions for analysis of electrode processes". In: *Journal of Electroanalytical Chemistry and Interfacial Electrochemistry* 33.2 (1971), pp. 253–265.

[53] The MathWorks Inc. *PRBS Input Signals*. 2020. URL: https://www.mathworks.com/help/slcontrol/ug/prbs-input-signals.html (visited on 10/28/2020).

[54] G.J. Jeong, I.H. Kim, and Y.I.k. Son. "Application of simple adaptive control to a dc/dc boost converter with load variation". In: *2009 ICCAS-SICE*. IEEE. 2009, pp. 1747–1751.

[55] W. Jifeng and L. Yuankai. "Frequency domain analysis and applications for fractional-order control systems". In: *Journal of physics: Conference series*. Vol. 13. 1. IOP Publishing. 2005, p. 268.

[56] B. Keziz, A. Djouambi, and S. Ladaci. "A new fractional order controller tuning method based on Bode's ideal transfer function". In: *International Journal of Dynamics and Control* (2020), pp. 1–11.

[57] B. Keziz, S. Ladaci, and A. Djouambi. "Design of a MRAC-Based Fractional order $PI^{\lambda}D^{\mu}$ Regulator for DC Motor Speed Control". In: *2018 International Conference on Electrical Sciences and Technologies in Maghreb (CISTEM)*. IEEE. 2018, pp. 1–6.

[58] A. Kiani-B et al. "A chaotic secure communication scheme using fractional chaotic systems based on an extended fractional Kalman filter". In: *Communications in Nonlinear Science and Numerical Simulation* 14.3 (2009), pp. 863–879.

[59] B.T. Krishna and K. Reddy. "Design of digital differentiators and integrators of order 1/2". In: *World Journal of Modelling and Simulation* 4.3 (2008), pp. 182–187.

[60] D. Kumar and D. Baleanu. "Fractional Calculus and its Applications in Physics". In: *Frontiers in Physics* 7 (2019), p. 81.

[61] S. Ladaci and Y. Bensafia. "Indirect fractional order pole assignment based adaptive control". In: *Engineering Science and Technology, an International Journal* 19.1 (2016), pp. 518–530.

[62] S. Ladaci and A. Charef. "Commande Adaptative à modèle de référence d'ordre Fractionnaire d'un bras artificiel". In: *Revue Sciences et Communication, ENSET Oran Algeria* 1 (2002), pp. 53–55.

[63] S. Ladaci and A. Charef. "Commande adaptative robuste avec feedforward d'ordre fractionnaire". In: *Proc. CMGE* 4 ().

[64] S. Ladaci and A. Charef. "Fractional adaptive control. A survey". In: *Classification and application of fractals: New research* (2011), pp. 261–275.

[65] S. Ladaci and A. Charef. "Fractional order model reference adaptive control of a robot arm". In: *Revue Communication Sciences and Technologie* 1 (2002), pp. 20–52.

[66] S. Ladaci and A. Charef. "On fractional adaptive control". In: *Nonlinear Dynamics* 43.4 (2006), pp. 365–378.

[67] S. Ladaci, A. Charef, and J. Loiseau. "Robust fractional adaptive control based on the strictly positive realness condition". In: *International Journal of Applied Mathematics and Computer Science* 19.1 (2009), pp. 69–76.

[68] S. Ladaci, J.J. Loiseau, and A. Charef. "Adaptive internal model control with fractional order parameter". In: *International Journal of Adaptive Control and Signal Processing* 24.11 (2010), pp. 944–960.

[69] S. Ladaci, J.J. Loiseau, and A. Charef. "Fractional order adaptive high-gain controllers for a class of linear systems". In: *Communications in Nonlinear Science and Numerical Simulation* 13.4 (2008), pp. 707–714.

[70] S. Ladaci et al. "Commande adaptative robuste avec feedforward". In: *Proc. CNIE* 2 (2004).

[71] I.D. Landau. "From robust control to adaptive control". In: *Control Engineering Practice* 7.9 (1999), pp. 1113–1124.

[72] P. Lanusse, J. Sabatier, and A. Oustaloup. "Extension of PID to fractional orders controllers: a frequency-domain tutorial presentation". In: *IFAC Proceedings Volumes* 47.3 (2014), pp. 7436–7442.

[73] M.P. Lazarević, S.A. Batalov, and T.S. Latinović. "Fractional PID controller tuned by genetic algorithms for a three DOF's robot system driven by DC motors". In: *IFAC Proceedings Volumes* 46.1 (2013), pp. 385–390.

[74] Y. Li and H.F. Chen. "Robust adaptive pole placement for linear time-varying systems". In: *IEEE transactions on automatic control* 41.5 (1996), pp. 714–719.

[75] C. Lubich. "Discretized fractional calculus". In: *SIAM Journal on Mathematical Analysis* 17.3 (1986), pp. 704–719.

[76] M. M'saad and I.D. Landau. "Adaptive control: an overview". In: *Advanced Control of Chemical Processes 1991*. Elsevier, 1992, pp. 1–9.

[77] B. Maâmar and M. Rachid. "IMC-PID-fractional-order-filter controllers design for integer order systems". In: *ISA transactions* 53.5 (2014), pp. 1620–1628.

[78] J. Machado. "Analysis and design of fractional-order digital control systems". In: *SAMS* 27 (1997), pp. 107–122.

[79] R.L. Magin. *Fractional Calculus in Bioengineering*. Vol. 2. 6. Begell House Redding, 2006.

[80] R.L. Magin. "Fractional calculus models of complex dynamics in biological tissues". In: *Computers & Mathematics with Applications* 59.5 (2010), pp. 1586–1593.

[81] G. Maione and P. Lino. "New tuning rules for fractional PI$^{\alpha}$ controllers". In: *Nonlinear dynamics* 49.1-2 (2007), pp. 251–257.

[82] H. Malek, Y. Luo, and Y.Q. Chen. "Tuning Fractional Order Proportional Integral Controllers for Time Delayed Systems with a Fractional Pole". In: *ASME 2011 International Design Engineering Technical Conferences and Computers and Information in Engineering Conference*. American Society of Mechanical Engineers Digital Collection, 2011, pp. 311–321.

[83] S. Manabe. "The non-integer integral and its application to control systems". In: *Journal of Institute of Electrical Engineers of Japan* 80.860 (1960), pp. 589–597.

[84] M. Manfred and Z. Evanghelos. *Robust process control*. 1989.

[85] B. Mathieu et al. "Fractional differentiation for edge detection". In: *Signal Processing* 83.11 (2003), pp. 2421–2432.

[86] Denis Matignon. "Generalized fractional differential and difference equations: stability properties and modelling issues". In: *Mathematical Theory of Networks and Systems symposium*. 1998, pp. 503–506.

[87] K. Matsuda and H. Fujii. "H (infinity) optimized wave-absorbing control-Analytical and experimental results". In: *Journal of Guidance, Control, and Dynamics* 16.6 (1993), pp. 1146–1153.

[88] F.C. Meral, T.J. Royston, and R. Magin. "Fractional calculus in viscoelasticity: an experimental study". In: *Communications in Nonlinear Science and Numerical Simulation* 15.4 (2010), pp. 939–945.

[89] K.S. Miller and B. Ross. "An Introduction to the Fractional Calculus and Fractional Differential Equations, Willey, New York". In: *NY. Zbl0789* 26002 (1993).

[90] C.A. Monje et al. "Auto-tuning of fractional lead-lag compensators". In: *IFAC Proceedings Volumes* 38.1 (2005), pp. 319–324.

[91] C.A. Monje et al. *Fractional-Order Systems and Controls: Fundamentals and Applications*. Springer Science & Business Media, 2010.

[92] C.A. Monje et al. "Tuning and auto-tuning of fractional order controllers for industry applications". In: *Control engineering practice* 16.7 (2008), pp. 798–812.

[93] X. Moreau, C. Ramus-Serment, and A. Oustaloup. "Fractional differentiation in passive vibration control". In: *Nonlinear Dynamics* 29.1-4 (2002), pp. 343–362.

[94] K. Najim, D. Hodouin, and A. Desbiens. "Adaptive control: state of the art and an application to a grinding process". In: *Powder Technology* 82.1 (1995), pp. 59–68.

[95] Q.A. Naqvi and M. Abbas. "Complex and higher order fractional curl operator in electromagnetics". In: *Optics Communications* 241.4-6 (2004), pp. 349–355.

[96] A. Neçaibia and S. Ladaci. "Self-tuning fractional order PI λ D μ controller based on extremum seeking approach". In: *International Journal of Automation and Control 3* 8.2 (2014), pp. 99–121.

[97] A. Neçaibia et al. "Fractional order extremum seeking control". In: *2nd Mediterranean Conference on Control and Automation*. IEEE. 2014, pp. 459–462.

[98] K.B. Oldham. "Fractional differential equations in electrochemistry". In: *Advances in Engineering software* 41.1 (2010), pp. 9–12.

[99] K.B. Oldham. "Semiintegral electroanalysis. Analog implementation". In: *Analytical Chemistry* 45.1 (1973), pp. 39–47.

[100] K.B. Oldham and J. Spanier. *The Fractional Calculus, vol. 111 of Mathematics in science and engineering*. Academic Press, New York, London, 1974.

[101] M.D. Ortigueira, J.T. Machado, and J. Da Costa. "Which differintegration?" In: *IEE Proceedings-Vision, Image and Signal Processing* 152.6 (2005), pp. 846–850.

[102] A. Oustaloup. "La Commande CRONE: Commande Robuste d'ordre Non Entier. 1991". In: *Hermés, Paris* (1990).

[103] A. Oustaloup. *La dérivation non entière théorie, synthèse, applications. série Automatique*. Éditions Hermés, 1995.

[104] A. Oustaloup and P. Coiffet. *Systémes asservis linéaires d'ordre fractionnaire: théorie et pratique: par Alain Oustaloup*. Masson, 1983.

[105] A. Oustaloup, O. Cois, and L. Le Lay. *Représentation et identification par modéle non entier*. Lavoisier, 2005.

[106] A. Oustaloup and B. Mathieu. *La commande CRONE: du scalaire au multivariable*. Hermés, science, 1999.

[107] A. Oustaloup et al. "Frequency-band complex noninteger differentiator: characterization and synthesis". In: *IEEE Transactions on Circuits and Systems I: Fundamental Theory and Applications* 47.1 (2000), pp. 25–39.

[108] A. Oustaloup et al. "The crone aproach: Theoretical developments and major applications". In: *IFAC Proceedings Volumes* 39.11 (2006), pp. 324–354.

[109] F. Padula, R. Vilanova, and A. Visioli. "H∞ Model Matching PID Design for Fractional FOPDT Systems". In: *2012 American Control Conference (ACC)*. IEEE, 2012, pp. 5513–5518.

[110] I. Petráš. "Fractional-order feedback control of a DC motor". In: *Journal of electrical engineering* 60.3 (2009), pp. 117–128.

[111] I. Petráš. "Tuning and implementation methods for fractional-order controllers". In: *Fractional Calculus and Applied Analysis* 15.2 (2012), pp. 282–303.

[112] I. Petráš and B. Vinagre. "Practical application of digital fractional-order controller to temperature control". In: *Acta Montanistica Slovaca* 7.2 (2002), pp. 131–137.

[113] I. Podlubny. *Fractional differential equations, vol. 198 of Mathematics in Science and Engineering*. 1999.

[114] I. Podlubny. *Fractional-order Systems and Fractional-order Controllers, The Academy of Sciences Institute of Experimental Physics*. Tech. rep. UEF-03-94, Kosice, Slovak Republic, 1994.

[115] I. Podlubny. "Fractional-order systems and PI$^{\lambda}$D$^{\mu}$-controllers". In: *IEEE Transactions on automatic control* 44.1 (1999), pp. 208–214.

[116] I. Podlubny, L. Dorcak, and I. Kostial. "On fractional derivatives, fractional-order dynamic systems and PI$^{\lambda}$D$^{\mu}$-controllers". In: *Proceedings of the 36th IEEE Conference on Decision and Control*. Vol. 5. IEEE. 1997, pp. 4985–4990.

[117] I. Podlubny et al. "Analogue realizations of fractional-order controllers". In: *Nonlinear dynamics* 29.1-4 (2002), pp. 281–296.

[118] L. Qiu and D.E. Miller. "Robust Stabilization for $\mathcal{L}_p$ Gap Perturbations". In: *Robust Control Theory*. Springer, 1995, pp. 55–80.

[119] C. Quintano and E. Cuesta. "Improving satellite image classification by using fractional type convolution filtering". In: *International Journal of Applied Earth Observation and Geoinformation* 12.4 (2010), pp. 298–301.

[120] R. Ranganayakulu et al. "A comparative study of fractional order PI$^{\lambda}$/PI$^{\lambda}$D$^{\mu}$ tuning rules for stable first order plus time delay processes". In: *Resource-Efficient Technologies* 2 (2016), S136–S152.

[121] D.E. Rivera, M. Morari, and S. Skogestad. "Internal model control: PID controller design". In: *Industrial & engineering chemistry process design and development* 25.1 (1986), pp. 252–265.

[122] B. Ross. *Fractional calculus and its applications: proceedings of the international conference held at the University of New Haven, June 1974*. Vol. 457. Springer, 2006.

[123] S.G. Samko, A.A. Kilbas, and O.I. Marichev. *Fractional integrals and derivatives*. Vol. 1. Gordon and Breach Science Publishers, Yverdon Yverdon-les-Bains, Switzerland, 1993.

[124] H.S. Sánchez et al. "Tuning rules for robust FOPID controllers based on multi-objective optimization with FOPDT models". In: *ISA transactions* 66 (2017), pp. 344–361.

[125] H. Schiessel, C. Friedrich, and A. Blumen. "Applications to problems in polymer physics and rheology". In: *Applications of fractional calculus in physics*. World Scientific, 2000, pp. 331–376.

[126] B. Şenol and U. Demiroğlu. "Analytical Design of PI Controllers for First Order plus Time Delay Systems". In: *International Scientific and Vocational Studies Journal* 2.2 (2018), pp. 40–47.

[127] N.A. Shah, D. Vieru, and C. Fetecau. "Effects of the fractional order and magnetic field on the blood flow in cylindrical domains". In: *Journal of Magnetism and Magnetic Materials* 409 (2016), pp. 10–19.

[128] X. Shen. "Applications of Fractional Calculus In Chemical Engineering". PhD thesis. Université d'Ottawa/University of Ottawa, 2018.

[129] H. Sira-Ramirez. "Sliding motions in bilinear switched networks". In: *IEEE transactions on circuits and systems* 34.8 (1987), pp. 919–933.

[130] H. Sira-Ramírez. "On the generalized PI sliding mode control of DC-to-DC power converters: a tutorial". In: *International journal of control* 76.9-10 (2003), pp. 1018–1033.

[131] T.L. Skvarenina. "DC-DC Converters". In: *The Power Electronics Handbook*. CRC Press, 2001, pp. 117–146.

[132] A.C. Sparavigna and P. Milligan. "Using fractional differentiation in astronomy, Instrumentation and Methods for Astrophysics (astro-ph. IM)". In: *arXiv preprint arXiv: 0910.4243* (2009).

[133] M. Sugi et al. "Simulation of fractal immittance by analog circuits: an approach to the optimized circuits". In: *IEICE Transactions on Fundamentals of Electronics, Communications and Computer Sciences* 82.8 (1999), pp. 1627–1635.

[134] H.H. Sun and A. Charef. "Fractal system—A time domain approach". In: *Annals of biomedical Engineering* 18.6 (1990), pp. 597–621.

[135] A. Tepljakov. *Fractional-order modeling and control of dynamic systems*. Springer, 2017.

[136] A. Tepljakov et al. "Design and implementation of fractional-order PID controllers for a fluid tank system". In: *2013 American Control Conference*. IEEE. 2013, pp. 1777–1782.

[137] A. Tepljakov et al. "FOPID controllers and their industrial applications: a survey of recent results". In: *IFAC-PapersOnLine* 51.4 (2018), pp. 25–30.

[138] C.C. Tseng. "Design of fractional order digital FIR differentiators". In: *IEEE Signal Processing Letters* 8.3 (2001), pp. 77–79.

[139] C.C. Tseng, S.C. Pei, and S.C. Hsia. "Computation of fractional derivatives using Fourier transform and digital FIR differentiator". In: *Signal Processing* 80.1 (2000), pp. 151–159.

[140] D. Valerio and J.S. da Costa. "A review of tuning methods for fractional PIDs". In: *4th IFAC Workshop on Fractional Differentiation and its Applications, FDA*. Vol. 10. 5. 2010.

[141] D. Valério. "Fractional robust system control". In: *Universidade Técnica de Lisboa* (2005).

[142] D. Valério and J. da Costa. "Tuning rules for fractional PIDs". In: *Advances in Fractional Calculus*. Springer, 2007, pp. 463–476.

[143] B.M. Vinagre. "Modelado y control de sistemas caracterizados por ecuaciones íntegro-diferenciales de orden fraccional". PhD thesis. UNED. Universidad Nacional de Educación a Distancia (España), 2001.

[144] B.M. Vinagre and Y.Q. Chen. "Lecture notes on fractional calculus applications in automatic control and robotics". In: *The 41st IEEE CDC2002 Tutorial Workshop*. Vol. 2. 2002, pp. 1–310.

[145] B.M. Vinagre et al. "On fractional PID controllers: A frequency domain approach". In: *IFAC Proceedings Volumes* 33.4 (2000), pp. 51–56.

[146] B.M. Vinagre et al. "On realization of fractional-order controllers". In: *Proc. of the Conference Internationale Francophone d'Automatique*. 2000, pp. 5–8.

[147] B.M. Vinagre et al. "Some Approximations of Fractional Order Operators Used in Control Theory and Applications". In: *Fractional calculus and applied analysis* 3.3 (2000), pp. 231–248.

[148] B.M. Vinagre et al. "Two digital realizations of fractional controllers: Application to temperature control of a solid". In: *2001 European Control Conference (ECC)*. IEEE. 2001, pp. 1764–1767.

[149] B.M. Vinagre et al. "Using fractional order adjustment rules and fractional order reference models in model-reference adaptive control". In: *Nonlinear Dynamics* 29.1-4 (2002), pp. 269–279.

[150] Y. Wei et al. "On fractional order composite model reference adaptive control". In: *International Journal of Systems Science* 47.11 (2016), pp. 2521–2531.

[151] B.J. West. "Fractional Calculus and Memory in Biophysical Series Time". In: *Fractals in Biology and Medicine* (2012), p. 221.

[152] Y. Wu et al. "Characteristic modeling and control of servo systems with backlash and friction". In: *Mathematical Problems in Engineering* 2014 (2014).

[153] J. Xu and L. Qiao. "Robust adaptive PID control of robot manipulator with bounded disturbances". In: *Mathematical Problems in Engineering* 2013 (2013).

[154] V. Zaborovsky and R. Meylanov. "Informational network traffic model based on fractional calculus". In: *2001 International Conferences on Info-Tech and Info-Net. Proceedings (Cat. No. 01EX479)*. Vol. 1. IEEE. 2001, pp. 58–63.

[155] M. Zamani et al. "Design of a fractional order PID controller for an AVR using particle swarm optimization". In: *Control Engineering Practice* 17.12 (2009), pp. 1380–1387.

[156] C. Zhao, D. Xue, and Y.Q. Chen. "A fractional order PID tuning algorithm for a class of fractional order plants". In: *IEEE International Conference Mechatronics and Automation, 2005*. Vol. 1. IEEE. 2005, pp. 216–221.

[157] D.J. Zhuang, F. Yu, and Y. Lin. "Evaluation of a vehicle directional control with a fractional order PD$^{\mu}$ controller". In: *International Journal of Automotive Technology* 9.6 (2008), pp. 679–685.

APPENDIX

This Part provides supplementary information to the main work discussed in this thesis. Mathematics for fractional calculus are explained in the Appendix A. Preliminaries for Implementation are presented in Appendix B. Papers published or submitted in conferences and journals are listed in the Appendix C.

Appendix A

Mathematics for Fractional Calculus

A.1 Gamma function

The Gamma function is defined by the following equation, which is useful as factorial is not defined for all real numbers,

$$\Gamma(x) = \int_0^\infty t^{x-1} e^{-t} dt, \quad \Re(Z) > 0 \tag{A.1}$$

Some properties of gamma function,

- $\Gamma(1) = 1$
- $\Gamma(x) = (x-1)!$
- $\Gamma(x+1) = x\Gamma(x)$
- $\Gamma(\frac{1}{2}) = \sqrt{\pi}$
- $\Gamma(\frac{3}{2}) = \frac{1}{2}\sqrt{\pi}$
- $\Gamma(x) = \lim_{n\to\infty} \frac{n!}{(x)_{n+1}} n^x$
- $\Gamma(x) = \lim_{n\to\infty} \frac{n! n^x}{x(x+1)(x+2)...(x+n)}, \quad (x \neq 0, -1, -2, \ldots)$

The gamma function for values between -5 to 5 is plotted in (Fig. A.1). One can remarked that gamma function is not defined for zero number and negative integer.

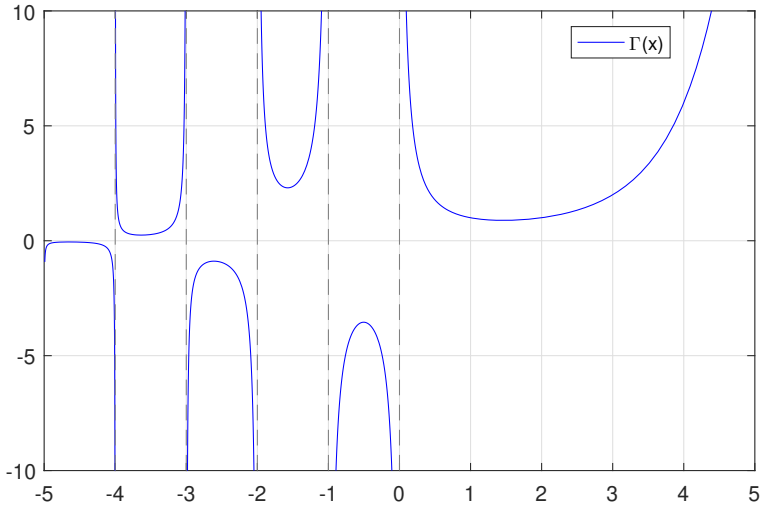

Figure A.1 Gamma function plot

A.2 Mittag-Leffler function

The Mittage Leffler one parameter function plays important role in solving ordinary integer order differential equations and its two parameter function solving fractional order differential equations. For one of the function, Mittage Leffler function is plotted in (Fig. A.2). The Mittag-Leffler function is defined by,

$$E_\alpha(z) = \sum_{k=0}^{\infty} \frac{z^k}{\Gamma(\alpha k + 1)}; \qquad \alpha > 0 \tag{A.2}$$

- The inverse Laplace of fractional order system comes in Mittag-Leffler function,
- It is generalized form of the exponential function,
- $E_1(z) = e^z$.

The two parameter Mittage Leffler function which is uesed for solving fractional order differential equation, was introduced by Agrawal. It is defined as,

$$E_{\alpha,\beta}(z) = \sum_{k=0}^{\infty} \frac{z^k}{\Gamma(\alpha k + \beta)}; \qquad \alpha, \beta > 0 \tag{A.3}$$

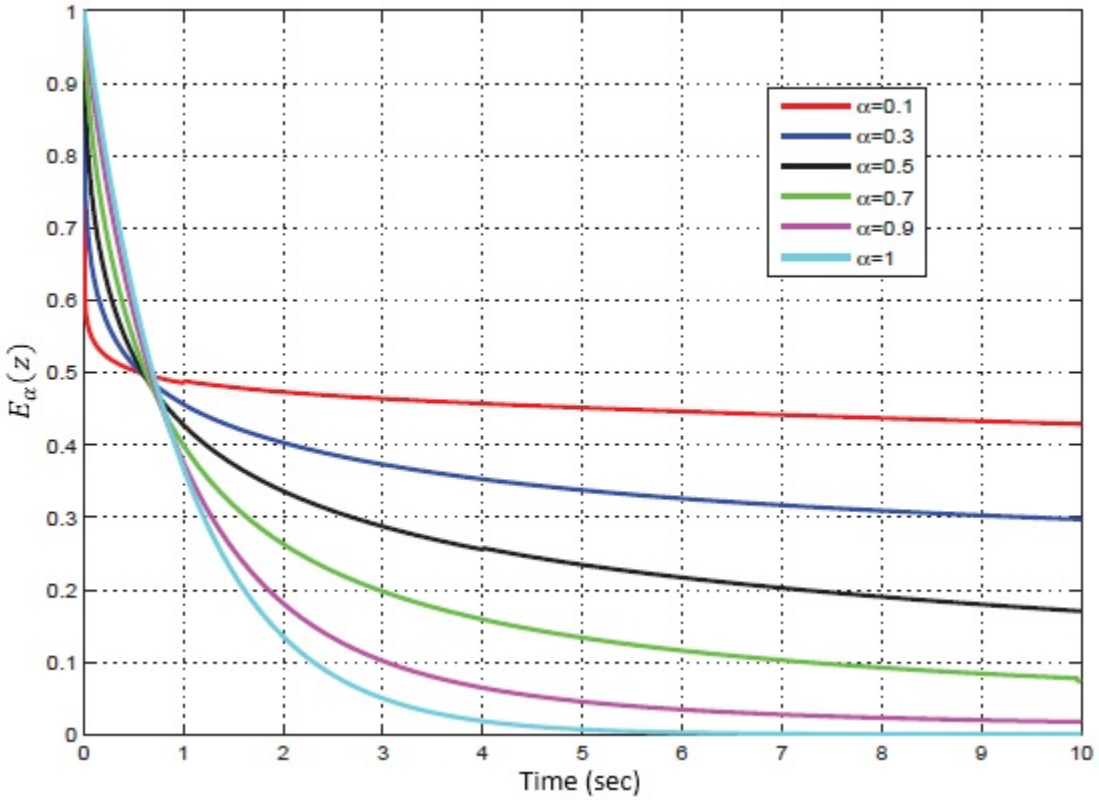

Figure A.2 Example of Mittage Leffer function $(-t^{\alpha})$

Special Case

$$E_{1,1}(z) = \sum_{k=0}^{\infty} \frac{z^k}{\Gamma(k+1)} = \sum_{k=0}^{\infty} \frac{z^k}{k!} = e^z \tag{A.4}$$

$$E_{1,2}(z) = \sum_{k=0}^{\infty} \frac{z^k}{\Gamma(k+2)} = \sum_{k=0}^{\infty} \frac{z^k}{(k+1)!} = \frac{e^z - 1}{z} \tag{A.5}$$

$$E_{1,m}(z) = \frac{1}{z^{m-1}} \left\{ e^z - \sum_{k=0}^{m-2} \frac{z^k}{k!} \right\} \tag{A.6}$$

Appendix B

Tools for Modelling and Identification

B.1 Preparing a PRBS Signal

Pseudo Random Binary Sequence (PRBS) is a periodic signal with a maximum period length of 2^n–1, where n is the PRBS order. To create a PRBS input signal, the following parameters (based on system dynamics) should be specified [53],

1- Signal amplitude: is set such that the system is properly excited,

2- The frequency range of the generated PRBS signal is $[F_min, F_max]$,

3- If the plant is a discrete-time system, then,

* The sample time of the PRBS is equal to the sample time of the system.
* The Order is,

$$Order = Ceil\left(\frac{\log\left(\frac{2\pi}{T_s.F_{min}}\right)}{\log(2)}\right)$$

4- If the plant is a continuous-time system, then,

* The sample time of the PRBS is,

$$T_s = \frac{2\pi}{5.F_{max}}$$

* The Order is,

$$Order = Floor\left(\frac{\log\left(\frac{2\pi}{T_s.F_{min}}\right)}{\log(2)}\right)$$

Appendix C

Publications

Parts of this thesis have been published in the following journal articles:

C.1 Journal Papers

J1 Keziz, B., Djouambi, A. & Ladaci, S. A new fractional order controller tuning method based on Bode's ideal transfer function. Int. J. Dynam. Control (2020).

C.2 Conference Papers

C1 Bouziane Keziz, Abdelbaki Djouambi, and Samir Ladaci. "Fractional-order model reference adaptive controller design using a modified MIT rule and a feed-forward action for a DC-DC boost converter stabilization". In 5^{th} International Conference on Electrical Engineering-Boumerdes (ICEE-B). IEEE. (2017), pp. 1–6.

C2 Bouziane Keziz, Abdelbaki Djouambi, and Samir Ladaci. "Online Fractional-Order PI$^{\alpha}$ Controller Tuning Scheme". In 6^{th} International Conference on Control Engineering & Information Technology (CEIT). IEEE. (2018), pp. 1–6.

C3 Bouziane Keziz, Samir Ladaci, and Abdelbaki Djouambi. "Design of a MRAC-Based Fractional order PI$^{\lambda}$D$^{\mu}$ Regulator for DC Motor Speed Control". In International Conference on Electrical Sciences and Technologies in Maghreb (CISTEM).IEEE. (2018), pp. 1–6.

C4 Bouziane Keziz, Samir Ladaci, and Abdelbaki Djouambi. "Recursive Parameter Estimation Algorithm for a Fractional Order PI$^{\lambda}$ Controller Design Using MRAC Config-

uration". In 1^{th} International Conference on Sustainable Renewable Energy Systems and Applications (ICSRESA). IEEE. (2019).

C5 Bouziane Keziz, Samir Ladaci, and Abdelbaki Djouambi. "A Low-Cost Platform for Real Time Data Acquisition and Fractional Control with Application to a DC motor". In 8^{th} International Conference on Defense Systems: Architectures & Technologies (DAT'2020). IEEE. (2020).

C.3 Workshops

W1 Keziz, B., Djouambi, A. & Ladaci, S. "A Low Cost Platform for Real time data Acquisition and Control". Int. Training Days of Science and Engineering ITDSE (2019), Institute of Science and applied techniques, Ain M'lila, Algeria.